

ROADMAP • OPEN ACCESS

## Roadmap on thermoelectricity

To cite this article: Cristina Artini *et al* 2023 *Nanotechnology* **34** 292001

View the [article online](#) for updates and enhancements.

### You may also like

- [Lasing mode manipulation in a Benz-shaped GaN cavity via the Joule effect of individual Ni wires](#)  
Feifei Qin, Xin Ji, Ying Yang et al.
- [Warped product of Hamiltonians and extensions of Hamiltonian systems](#)  
Claudia Maria Chanu, Luca Degiovanni and Giovanni Rastelli
- [An overview of physics teacher professional development activities organized within the Italian PLS-Physics plan over the past five years](#)  
Marisa Michelini, Massimiliano Malgieri, Olindo Corradini et al.



**EDINBURGH INSTRUMENTS**

WORLD LEADING MOLECULAR SPECTROSCOPY SOLUTIONS

edinst.com

The advertisement features a red background with the Edinburgh Instruments logo on the left, which consists of a circular pattern of white dots. In the center and right, several pieces of laboratory equipment are displayed, including a spectrometer labeled 'FSS', a microscope-like device, and a larger unit labeled 'FLS 1000'. The text 'WORLD LEADING MOLECULAR SPECTROSCOPY SOLUTIONS' is written in white, bold, uppercase letters. The website 'edinst.com' is shown in a white box in the bottom right corner.

## Roadmap

# Roadmap on thermoelectricity

**Cristina Artini**<sup>1,2,24,\*</sup> , **Giovanni Pennelli**<sup>3,24,\*</sup>, **Patrizio Graziosi**<sup>4,5</sup>, **Zhen Li**<sup>5</sup> , **Neophytos Neophytou**<sup>5</sup>, **Claudio Melis**<sup>6</sup> , **Luciano Colombo**<sup>6</sup> , **Eleonora Isotta**<sup>7,8</sup> , **Ketan Lohani**<sup>7</sup> , **Paolo Scardi**<sup>7</sup>, **Alberto Castellero**<sup>9,15</sup> , **Marcello Baricco**<sup>9</sup> , **Mauro Palumbo**<sup>9</sup>, **Silvia Casassa**<sup>9</sup>, **Lorenzo Maschio**<sup>9</sup>, **Marcella Pani**<sup>1,10</sup> , **Giovanna Latronico**<sup>11</sup> , **Paolo Mele**<sup>11</sup> , **Francesca Di Benedetto**<sup>12</sup>, **Gaetano Contento**<sup>12</sup>, **Maria Federica De Riccardis**<sup>12</sup>, **Raffaele Fucci**<sup>12</sup>, **Barbara Palazzo**<sup>12</sup>, **Antonella Rizzo**<sup>12</sup>, **Valeria Demontis**<sup>13</sup>, **Domenico Prete**<sup>13</sup>, **Muhammad Isram**<sup>14</sup>, **Francesco Rossella**<sup>14</sup> , **Alberto Ferrario**<sup>15</sup> , **Alvise Miozzo**<sup>15</sup>, **Stefano Boldrini**<sup>15</sup> , **Elisabetta Dimaggio**<sup>3</sup>, **Marcello Franzini**<sup>16</sup>, **Simone Galliano**<sup>17</sup>, **Claudia Barolo**<sup>16</sup>, **Saeed Mardi**<sup>18,19</sup>, **Andrea Reale**<sup>18</sup>, **Bruno Lorenzi**<sup>20</sup>, **Dario Narducci**<sup>20</sup> , **Vanira Trifiletti**<sup>21</sup> , **Silvia Milita**<sup>22</sup>, **Alessandro Bellucci**<sup>23</sup> and **Daniele M Trucchi**<sup>23</sup>

<sup>1</sup> DCCI, Department of Chemistry and Industrial Chemistry, University of Genova, Via Dodecaneso 31, I-16146 Genova, Italy

<sup>2</sup> Institute of Condensed Matter Chemistry and Technologies for Energy, National Research Council, CNR-ICMATE, Via De Marini 6, I-16149 Genova, Italy

<sup>3</sup> Dipartimento di Ingegneria dell'Informazione, University of Pisa, Via Caruso 16, I-56122 Pisa, Italy

<sup>4</sup> CNR—ISMN, v. Gobetti 101, I-40129, Bologna, Italy

<sup>5</sup> University of Warwick, School of Engineering, Coventry, CV4 7AL, United Kingdom

<sup>6</sup> Department of Physics, University of Cagliari, Cittadella Universitaria, I-09042 Monserrato (CA), Italy

<sup>7</sup> Department of Civil, Environmental and Mechanical Engineering, University of Trento, Italy

<sup>8</sup> Department of Chemical Engineering and Materials Science, Michigan State University, United States of America

<sup>9</sup> Department of Chemistry, NIS, INSTM, University of Turin, Italy

<sup>10</sup> CNR-SPIN Genova, Corso Perrone 24, I-16152 Genova, Italy

<sup>11</sup> Shibaura Institute of Technology, Omiya Campus, 307 Fukasaku, Minuma-ku, Saitama City, Saitama 337-8570, Japan

<sup>12</sup> ENEA—Italian National Agency for New Technologies, Energy and the Sustainable Economic Development, SSPT-PROMAS-MATAS Brindisi Research Centre S.S. 7 - Km I-706 72100 Brindisi, Italy

<sup>13</sup> Scuola Normale Superiore and Istituto Nanoscienze—CNR, Piazza San Silvestro 12, I-56127, Pisa, Italy

<sup>14</sup> Dipartimento di Scienze Fisiche Informatiche e Matematiche, University of Modena and Reggio Emilia, via G. Campi 213/A, I-41125, Modena, Italy

<sup>15</sup> CNR—ICMATE, Corso Stati Uniti 4, I-35127 Padova, Italy

<sup>16</sup> Department of Chemistry, NIS Interdepartmental Centre and INSTM Reference Centre, Università degli Studi di Torino, Via Gioacchino Quarello 15A, Torino I-10135, Italy

<sup>17</sup> Department of Agricultural, Forest and Food Science, INSTM Reference Centre, Università degli Studi di Torino, Largo Paolo Braccini 2, Grugliasco I-10095, Italy

<sup>18</sup> CHOSE - Centre for Hybrid and Organic Solar Energy and Department of Electronic Engineering, University of Rome Tor Vergata, I-00133 Rome, Italy

<sup>19</sup> Laboratory of Organic Electronics (LOE) Department of Science and Technology, University of Linköping, Bredgatan 34, Norrköping 581 83, Sweden

<sup>20</sup> Department of Materials Science—University of Milano Bicocca, Via R. Cozzi 55, I-20125—Milano, Italy

<sup>21</sup> Department of Materials Science and Solar Energy Research Center (MIB-SOLAR), University of Milano-Bicocca, Via Cozzi 55, I-20125 Milan, Italy

<sup>22</sup> Institute for Microelectronics and Microsystems (CNR-IMM), Via Piero Gobetti 101, I-40129 Bologna, Italy

<sup>23</sup> Istituto di Struttura della Materia (ISM-CNR), DiaTHEMA Lab, Montelibretti Unit, Via Salaria km 29.300, 00015 Monterotondo (RM), Italy

E-mail: [artini@chimica.unige.it](mailto:artini@chimica.unige.it), [giovanni.pennelli@unipi.it](mailto:giovanni.pennelli@unipi.it), [Patrizio.Graziosi@gmail.com](mailto:Patrizio.Graziosi@gmail.com), [Zhen.Li.2@warick.ac.uk](mailto:Zhen.Li.2@warick.ac.uk), [N.Neophytou@warwick.ac.uk](mailto:N.Neophytou@warwick.ac.uk), [claudio.melis@dsf.unica.it](mailto:claudio.melis@dsf.unica.it), [luciano.colombo@dsf.unica.it](mailto:luciano.colombo@dsf.unica.it), [isotta@msu.edu](mailto:isotta@msu.edu), [ketan.lohani@unitn.it](mailto:ketan.lohani@unitn.it), [paolo.scardi@unitn.it](mailto:paolo.scardi@unitn.it), [alberto.castellero@unito.it](mailto:alberto.castellero@unito.it), [marcello.baricco@unito.it](mailto:marcello.baricco@unito.it), [mauro.palumbo@unito.it](mailto:mauro.palumbo@unito.it), [silvia.casassa@unitn.it](mailto:silvia.casassa@unitn.it), [lorenzo.maschio@unito.it](mailto:lorenzo.maschio@unito.it), [marcella.pani@unige.it](mailto:marcella.pani@unige.it) (M.P.) [i048025@shibaura-it.ac.jp](mailto:i048025@shibaura-it.ac.jp) (G.L.) [pmele@shibaura-it.ac.jp](mailto:pmele@shibaura-it.ac.jp) (P.M.) [francesca.dibenedetto@enea.it](mailto:francesca.dibenedetto@enea.it), [gaetano.contento@enea.it](mailto:gaetano.contento@enea.it), [federica.dericcadi@enea.it](mailto:federica.dericcadi@enea.it), [raffaele.fucci@enea.it](mailto:raffaele.fucci@enea.it), [barbara.palazzo@enea.it](mailto:barbara.palazzo@enea.it), [antonella.rizzo@enea.it](mailto:antonella.rizzo@enea.it), [valeria.demontis@sns.it](mailto:valeria.demontis@sns.it), [domenic.prete@sns.it](mailto:domenic.prete@sns.it), [muhammad.isram@unimore.it](mailto:muhammad.isram@unimore.it), [francesco.rossella@unimore.it](mailto:francesco.rossella@unimore.it), [alberto.ferrario@cnr.it](mailto:alberto.ferrario@cnr.it), [alvise.miozzo@cnr.it](mailto:alvise.miozzo@cnr.it), [stefano.boldrini@cnr.it](mailto:stefano.boldrini@cnr.it), [elisabetta.dimaggio@unipi.it](mailto:elisabetta.dimaggio@unipi.it), [marcello.franzini@unito.it](mailto:marcello.franzini@unito.it) (M.F.) [simone.galliano@unito.it](mailto:simone.galliano@unito.it), [claudia.barolo@unito.it](mailto:claudia.barolo@unito.it) (C.B.) [saeed.mardi@liu.se](mailto:saeed.mardi@liu.se), [reale@uniroma2.it](mailto:reale@uniroma2.it), [bruno.lorenzi@unimib.it](mailto:bruno.lorenzi@unimib.it), [dario.narducci@unimib.it](mailto:dario.narducci@unimib.it), [vanira.trifiletti@unimib.it](mailto:vanira.trifiletti@unimib.it), [milita@bo.imm.cnr.it](mailto:milita@bo.imm.cnr.it), [alessandro.bellucci@cnr.it](mailto:alessandro.bellucci@cnr.it) and [danielemaria.trucchi@cnr.it](mailto:danielemaria.trucchi@cnr.it)

Received 25 October 2022, revised 1 February 2023

Accepted for publication 5 April 2023

Published 9 May 2023



CrossMark

## Abstract

The increasing energy demand and the ever more pressing need for clean technologies of energy conversion pose one of the most urgent and complicated issues of our age. Thermoelectricity, namely the direct conversion of waste heat into electricity, is a promising technique based on a long-standing physical phenomenon, which still has not fully developed its potential, mainly due to the low efficiency of the process. In order to improve the thermoelectric performance, a huge effort is being made by physicists, materials scientists and engineers, with the primary aims of better understanding the fundamental issues ruling the improvement of the thermoelectric figure of merit, and finally building the most efficient thermoelectric devices. In this Roadmap an overview is given about the most recent experimental and computational results obtained within the Italian research community on the optimization of composition and morphology of some thermoelectric materials, as well as on the design of thermoelectric and hybrid thermoelectric/photovoltaic devices.

Keywords: thermoelectricity, thermoelectric materials, thermoelectric devices, heat transport, electronic transport, modelling

(Some figures may appear in colour only in the online journal)

## Contents

1. Modelling of electronic transport in complex band structure thermoelectric materials	4
2. Atomistic simulations for heat transport in thermoelectric materials	7
3. Disordered multinary chalcogenides for sustainable thermoelectric generation	10
4. Experimental and computational investigations of skutterudites and half Heusler alloys for thermoelectric conversion at medium and high temperature	13
5. Filled skutterudites and Heusler phases as candidate materials for thermoelectric thin films	16
6. Transparent thermoelectric thin film materials for energy harvesting at low temperature	19
7. Nanoscale thermoelectricity with III–V compound semiconductors	21

<sup>24</sup> Guest editors of the Roadmap.

\* Author to whom any correspondence should be addressed.



Original content from this work may be used under the terms of the [Creative Commons Attribution 4.0 licence](https://creativecommons.org/licenses/by/4.0/). Any further distribution of this work must maintain attribution to the author(s) and the title of the work, journal citation and DOI.

---

8. Challenges and advances in the fabrication and characterization of large temperature gradient cascade thermoelectric modules	24
9. Nanostructured silicon devices for thermoelectric applications	26
10. Solution processable organic thermoelectric materials and devices	29
11. Towards an effective thermoelectric hybridization of photovoltaics	31
12. Advances and challenges in low-dimensional halide perovskite thermoelectrics	33
13. Thermoelectrics for hybrid solid-state power generators	35

## 1. Modelling of electronic transport in complex band structure thermoelectric materials

Patrizio Graziosi<sup>1,2</sup>, Zhen Li<sup>2</sup>, Neophytos Neophytou<sup>2</sup>

<sup>1</sup>CNR – ISMN, v. Gobetti 101, 40129, Bologna, Italy

<sup>2</sup>University of Warwick, School of Engineering, Coventry, CV4 7AL, United Kingdom

Email: [Patrizio.Graziosi@gmail.com](mailto:Patrizio.Graziosi@gmail.com), [Zhen.Li.2@warick.ac.uk](mailto:Zhen.Li.2@warick.ac.uk), [N.Neophytou@warwick.ac.uk](mailto:N.Neophytou@warwick.ac.uk)

**Status.** The thermoelectric (TE) figure of merit, which quantifies the energy conversion efficiency, is  $ZT = \sigma S^2 T / \kappa$ , with  $\sigma$  the electrical conductivity,  $S$  the Seebeck coefficient,  $T$  the temperature,  $\kappa$  the thermal conductivity [1]. The power factor  $PF = \sigma S^2$  is determined by charge transport, where  $\sigma$  and  $S$  are defined from the solution of the Boltzmann Transport equation (BTE) [2]:

$$\sigma = R^{(0)}, S = \frac{k_B R^{(1)}}{q_0 R^{(0)}}, \text{ where } R^{(\alpha)} = q_0^2 \int_{E_0}^{\infty} dE \left( -\frac{\partial f_0}{\partial E} \right) \Xi_{(E, E_F, T)} \left( \frac{E - E_F}{k_B T} \right)^\alpha \quad (1)$$

$\Xi_{ij(E, E_F, T)} = \sum_{\mathbf{k}(E, n)} v_i(\mathbf{k}, n, E) v_j(\mathbf{k}, n, E) \tau_i(\mathbf{k}, n, E, E_F, T) g(\mathbf{k}, n, E)$  is the transport distribution function (TDF) which contains all the material information;  $\mathbf{k}$ ,  $n$ ,  $E$ , are the charge carrier momentum, band index, and energy, respectively,  $E_F$ ,  $T$  are the Fermi level and temperature;  $v_i$  and  $g$  are the carrier velocity, relaxation time and density of states;  $i$  and  $j$  are the cartesian coordinate indexes.

The drastic  $ZT$  improvements in the last two decades were allowed by: (i) the introduction of nanostructuring, and (ii) the progress in the synthesis of a myriad of new materials [1]. The introduction of nanoscale features and structure discontinuities can scatter phonons and drastically reduce  $\kappa$ , without significantly affecting  $\sigma$ . Some of the lowest thermal conductivities demonstrated were below  $\kappa \sim 1 \text{ W mK}^{-1}$ , which lead to the sudden  $ZT$  increase in the last 20 years. Despite the success of nanostructuring, it is evident that with such low  $\kappa$  values, further  $ZT$  improvements must be provided by the PF [3]. The materials with the best PF have *complex bandstructures*, with many bands and multiple valleys per band, preferably anisotropic [1], as example we show the valence band of NbCoSn in figures 1(a)–(c). The combination of complex bandstructure materials in their nanostructured form, is the main direction for the thermoelectric technology. The optimal bandstructure features, however, cannot be known *a priori* for a specific material class, nor can be easily extracted from experiment, thus advanced computational tools are needed to accurately guide the identification and optimization of this process.

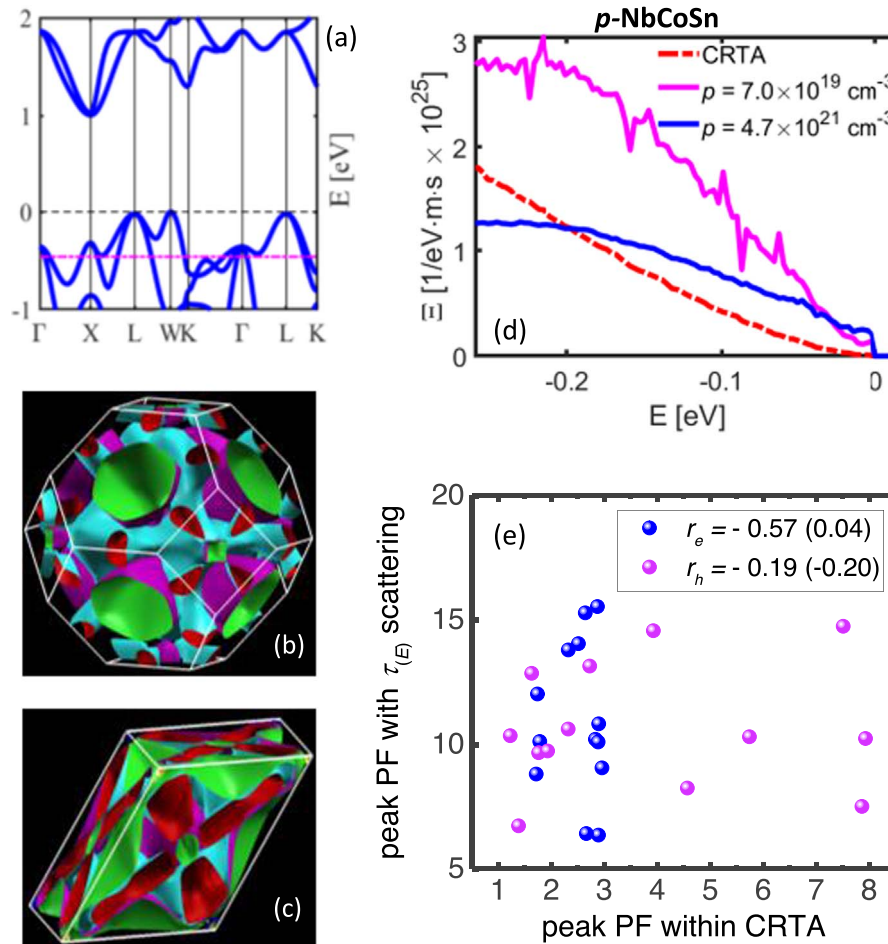
Typically, the band structure of the material is computed via density functional theory (DFT) and used within the BTE. The big unknown in this process are the scattering times,  $\tau_s(E, \mathbf{k}, n)$ , which are generally energy, momentum, and band dependent, and require the coupling of electrons with phonons. The scattering times are the main focus of the current development of simulation tools.

**Current and future challenges.** Since to accurately obtain  $\tau_s(E, \mathbf{k}, n)$  is computationally challenging [7], the common approach is to use a constant relaxation time approximation (CRTA), often  $\tau_s = 10 \text{ fs}$  [8]. CRTA is currently used across materials, temperatures, doping conditions, etc, even in high-throughput screening studies [9]. This ultimately smears out many bandstructure details [5], as depicted in figure 1(d) for hole transport TDF of NbCoSn, and introduces an arbitrary error [6], with uncorrelated (or even negatively correlated) outcomes compared to performing the calculations properly, as shown in figure 1(e). However, in absence of proper tools, the CRTA can at least provide some first order indications for  $S$ .

The fact that the electronic structures are complex, the scattering processes are not well understood,  $\sigma$  and  $S$  are adversely interdependent, and the scattering physics is crucial in determining the performance, makes the need for accurate, flexible, and computationally robust tools imperative. Some codes exist, which go beyond the CRTA [8] or constant electron-phonon interaction [10], and are based on the accurate quantum mechanical evaluation of the electron-phonon matrix elements, generally along high symmetry lines, to evaluate the electron-phonon scattering rates, like EPW [7] or PERTURBO [11]. However, these methods are computationally extremely expensive [12], while cheaper codes are under study, where the electron-phonon interaction with non-polar phonons is parametrized in an acoustic phonon deformation potential, and other scattering mechanisms can be included, like AMSET [12] AMMCR [13], and others [14].

We have recently developed a full-band code, *ElecTra* [15], which solves the BTE by considering the complete carrier energy, momentum, and band index dependence of the momentum relaxation rate [2, 16, 17]. A textbook implementation of the deformation potential theory [17] enables to extend this approach also to inelastic intra- and inter-band processes with non-polar optical phonons. *ElecTra* can consider the details of the electronic structure via the construction of constant energy surfaces, the effects of an extended zone scheme in the evaluation of the exchange vector in anisotropic scattering mechanisms (Polar Optical Phonons, POP, and Ionized Impurity Scattering, IIS) [5], as well as a full direct evaluation of bipolar transport and its effects in narrow gap materials [15, 18, 19]. Importantly, *ElecTra* is *compatible with any DFT code* which can save the electronic structure in the ‘.bxsf’ format [4], which is the case of many DFT codes. This code has been thoroughly validated with well-known semiconductors as well as existing codes [15, 20].

We also mention that other computational approaches exist, which find use in specific cases. One notable example is a recent approach based on the Kubo’s linear response theory and in principle applicable to random potentials and confined nanostructures [21]. This approach found interesting application in the description of magnon drag in ferromagnetic thin films [22], with the possibility to explain an exceptionally high observed Seebeck coefficient in some thin films Heusler alloys [23].



**Figure 1.** (a) NbCoSn bandstructure, projections along high symmetry lines, highlighting the complex bandstructure features. The magenta line shows the energy level at which the constant energy surfaces of figures (b) and (c) are taken at. (b) and (c) Constant energy surfaces, obtained with the XCrystden code [4], of the NbCoSn valence band at the energy cut shown by the magenta line in (a). The surfaces are represented, respectively, on the Brillouin Zone (BZ) and the reciprocal unit cell ( $uc^*$ ), which *ElecTra* uses - see the main text for details on the *ElecTra* code. It illustrates the complexity of the electronic structure with highly anisotropic surfaces compenetrating each other. (d) TDF,  $\Xi$ , for the valence band of NbCoSn under the CRTA, dash-dot red line, and when involved scattering physics are considered, for two carrier densities. It exemplifies how the CRTA smears out many details of the electronic structure, also indicating a different zone for the ‘steepest’ increase, where the Fermi level should be placed for maximum PF [5]. (e) Correlation between the peak PF computed under CRTA and with involved scattering physics, for 14 half-Heuslers, with the scattering parameters as in [6]. The absence of correlation between the materials’ peak PF, i.e. materials ranking, points to the relevance of accurate scattering physics considerations. In the legend, the Pearson correlation coefficients are reported for  $n$ -type ( $r_e$ ) and  $p$ -type ( $r_h$ ), in parenthesis we show those values but excluding the most significant outliers. Some of the data presented in (a) and (d) are from [P Graziosi, C Kumarasinghe, and N Neophytou, *J. Appl. Phys.* **126**, 155701 (2019)], with the permission of AIP Publishing.

#### Advances in science and technology to meet challenges.

With the CRTA being quantitatively weak, and methods such as EPW being computationally extremely expensive, methods that use scattering parameters such as deformation potentials can provide the middle ground in terms of accuracy and computational cost. However, a complete Deformation Potentials Extraction Method is lacking. Such method would be able to provide deformation potentials for non-polar phonon scattering (including separating the intra- and inter-valley scattering processes), as well as polar phonon scattering rates including short- and long-range scattering rates. We are in the process of developing such a method, likely adaptable to all existing codes which utilize deformation potentials. Below we outline the main steps for this method. Details can be found in reference [20], where an example for Si mobility calculations entirely from first

principles is successfully described. The computational efficiency of the method is expected to be by at least  $20\times$  compared to fully *ab initio* methods, as in the case of Si, still with no penalties on the accuracy.

This approach is based on the quantum mechanical calculation of the electron-phonon matrix element performed by EPW, along relevant symmetry lines [20]. Few points are used for subsequent fit which enables the evaluation of the relevant deformation potential values for acoustic and optical phonons. This approach is much cheaper than a full EPW evaluation of the mobility.

Conceptually, the steps are as follows:

1. Use DFT to extract the electronic structure of the material and detect the valleys that form the bandstructure. This step is usually computationally cheap.

2. Use DFPT (Density Functional Perturbation Theory) to extract the phonon modes, on a coarse grid, as this is a computationally expensive step.
3. Use EPW to compute the electron-phonon matrix elements using as a starting point for the electronics states, the valley extrema.
4. Evaluation of the deformation potentials from the short-range part of the matrix elements, as described in reference [20]. The critical points are to disentangle the inter-valley processes, and to perform proper symmetry averages, mostly important for acoustic phonons.
5. Perform charge transport calculation using the deformation potentials (i.e. using *ElecTra*) as inputs to determine the scattering rates.

Being able to perform accurate and robust calculations is not only essential to understand individual TE material operation, but can also allow the development of general indications for the discovery of new TE materials [6], such as material descriptors or transport parameters, experimentally extractable, which would allow forecasting of promising directions. Another critical task involves the evaluation of the role of the structural defects, like grain boundaries, nanoinclusions, spatial inhomogeneities [3]. For these, it is also important to have accurate scattering models, which however, are currently missing. Real-space transport methods such as quantum mechanical Non-Equilibrium Green Functions (NEGF) approaches [2] and semi-classical Monte Carlo methods [2, 3] have recently being developed and can lead to important insight in transport under nanostructuring.

*Concluding remarks.* We have highlighted how the complexity of the bandstructure of advanced thermoelectric materials offer promises, but also require additional understanding. Especially the research on such wide materials playground can be boosted by accurate and efficient predictive modelling techniques. For this, it is crucial to implement proper approaches to the carrier scattering, to consider all the details of the complex electronic structures because strong and/or arbitrary approximations on the side of the scattering physics might affect, even reverse, any materials ranking and hence the choice of the research direction.

We have summarized the current approaches to the full-band simulation of the thermoelectric properties capable of including the physics complexities of the scattering processes. The main computational challenge is currently the evaluation of the electron-phonon scattering in a transport-oriented perspective. To overcome the bottleneck of extremely expensive calculations, cheaper approaches based on the deformation potential theory are implemented. On this ground, protocols to accurately bridge the twos are under development.

*Acknowledgments.* This work has received funding from the Marie Skłodowska-Curie Actions under the Grant agreement ID: 788465 (GENESIS - Generic semiclassical transport simulator for new generation thermoelectric materials) and from the European Research Council (ERC) under the European Union's Horizon 2020 Research and Innovation Programme (Grant Agreement No. 678763).

## 2. Atomistic simulations for heat transport in thermoelectric materials

Claudio Melis and Luciano Colombo

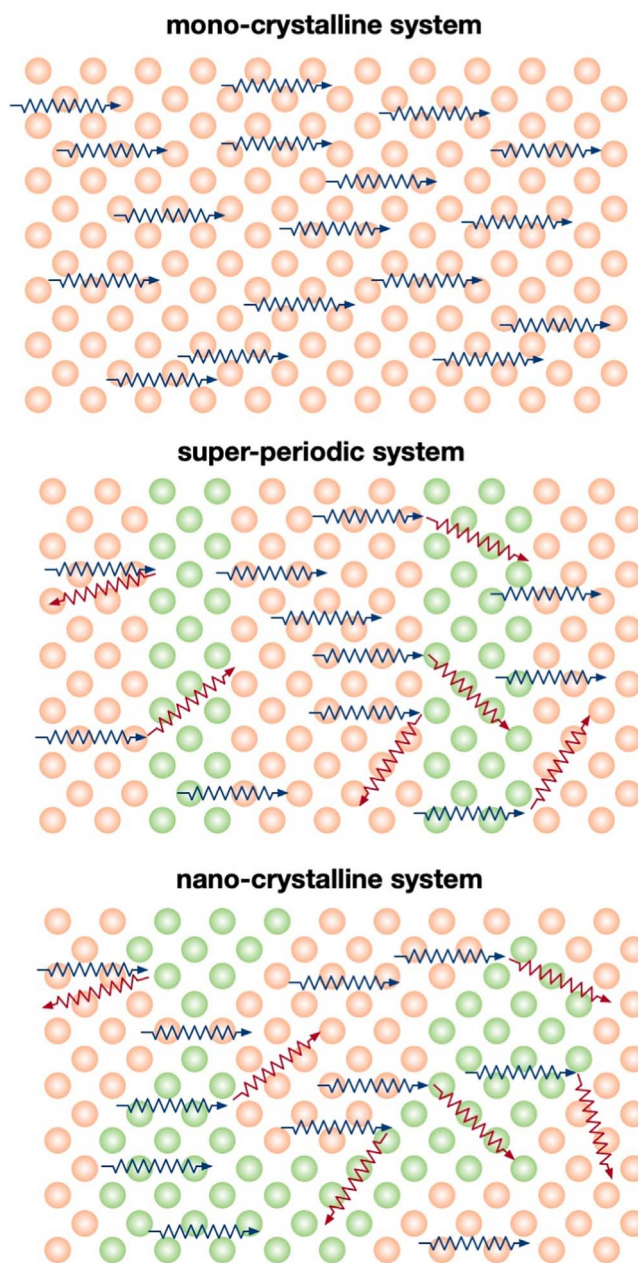
Department of Physics, University of Cagliari, Cittadella Universitaria, 09042 Monserrato (CA), Italy

Email: [claudio.melis@dsf.unica.it](mailto:claudio.melis@dsf.unica.it), [luciano.colombo@dsf.unica.it](mailto:luciano.colombo@dsf.unica.it)

**Status.** The renewed interest in thermoelectric (nano) materials following the publication of the two seminal papers by Hicks and Dresselhaus [24, 25] has triggered a parallel increase of interest in understanding and controlling thermal transport at the atomic scale. More specifically, in [24, 25]. It has been suggested that, among many possible strategies aimed at increasing the thermoelectric figure of merit  $ZT$ , the tailored insertion of a suitable interface population within a thermoelectric material could act as an efficient source of scattering for phonons (which are the microscopic heat carriers), thus dramatically affecting the lattice thermal conductivity and, hence, potentially increasing  $ZT$  (see figure 2). Another fundamental idea proposed by Slack [26] was the ‘Phonon Glass Electron Crystal’ paradigm describing an ideal architecture of novel thermoelectric materials with independent electrical and thermal transport properties.

Following these two paradigms, many experimental, as well as theoretical works, investigated thermal transport at the nanoscale by explicitly focusing on potential strategies to efficiently scatter phonons in nanomaterials and, possibly, decouple electrical and thermal transport. In this scenario, the role of atomistic simulations has quickly emerged as an important tool, mainly addressed to a twofold task: (i) to understand the fundamentals of phonon-mediated heat transport and, thanks to the corresponding predictive modelling, (ii) to design *in silico* novel nano(materials) with suppressed thermal conductivity for thermoelectric applications. More specifically, among different theoretical/computational approaches, two rather different atomistic simulation techniques have been mainly used so far [27], namely the Boltzmann Transport Equation (BTE) and molecular dynamics (MD) simulations.

The phenomenological BTE equation, formulated in 1929 by Peierls, describes the response of a phonon population to an external temperature gradient by explicitly considering all possible scattering processes [28]. In particular, the *ab initio* solution of BTE provides either intrinsic phonon features (i.e. their frequencies and group velocities) and phonon scattering rates (provided by any possible mechanism, including anharmonicity, defect or boundary scattering, and isotope scattering) by density functional perturbation theory calculations. This approach has been successfully applied to characterize thermal transport in bulk 3D materials as well as low dimensional materials [29, 30]. The ‘*ab initio*’ BTE technique guarantees high robustness and accuracy, in addition to the fact that it formally describes all quantum effects [27, 28].



**Figure 2.** Pictorial representation of the increased phonon scattering regime occurring in super-periodic (middle panel) or nano-crystalline (bottom panel) samples with respect to mono-crystalline (top panel) ones, caused by a population of interfaces (found at the boundary between regions populated by orange and green atoms). Drifting heat carriers under the action of a temperature gradient (set from the left to the right) are shown by blue zig-zag lines, while scattered ones are shown in red color. In order to illustrate the concept more effectively, the scattering phenomena associated to anharmonic phonon-phonon interactions have been omitted.

The alternative approach is based on MD, mainly used with empirical force fields, both in non-equilibrium (NEMD) [31, 32] and equilibrium approaches (EMD) [33]. MD simulations allow to efficiently describe relatively large systems and complex nanostructures by a reduced computational cost. NEMD and EMD have been successfully applied to study thermal transport in bulk semiconductors, low dimensional materials as well as organic materials [27].



Interesting enough, MD is not based on the phonon language and, at variance with BTE, it does not assume any constitutive law for the evolution of a nonequilibrium phonon population under an imposed thermal bias; rather, it allows a direct calculation of thermal conductivity through the Fourier heat transport equation. Although this is a more phenomenological approach, it is under many respects more versatile, being able to treat any system even if lacking translational invariance along one or more directions.

*Current and future challenges.* Despite the great impact that both BTE and MD simulations had in the last 10 years on the atomistic characterization of nanoscale thermal transport, there are still several challenges that need to be fully addressed in order to make them fully predictive tools to design novel thermoelectric devices.

Concerning *ab initio* BTE, the main current issue is related to their high computational cost related to the explicit inclusion of anharmonic effects above the third order. Although *ab initio* methods are largely used for the atomistic characterization of many thermal transport problems, there are nevertheless conditions and/or systems that are exceedingly heavy for present-day computational capabilities [27]. This makes *ab initio* BTE not suitable for the description of realistic disordered and nanostructured materials currently explored for thermoelectric applications. On the other hand, whenever a complex chemistry must be considered (as, for instance, in the case of perovskite thermoelectrics) this approach is the only viable way.

MD simulations, because of their comparatively low computational cost, can in principle describe comparatively very large systems (containing up to  $O(10^6)$  atoms) with dimensions up to the micrometer regime, thus approaching the experimental complexity of real nanostructured or disordered samples. On the other side, the main issue here is the overall accuracy of the force field, especially in describing harmonic and anharmonic properties. As a matter of fact, many works [34, 35] have stressed the limitations of current model potentials to describe thermal transport in different materials, often due to the approximate analytical functional form to describe intra- and intermolecular interactions [34, 35].

Another severe issue affecting both BTE- and MD-based atomistic techniques is the fact that both can only describe lattice thermal conductivity without considering any explicit electronic effect on thermal transport, limiting their applicability to low-doped semiconductors or insulators.

Finally, it is important to mention that even though BTE and MD provide a thorough description of nano-/micro-scale features ruling over the heat transport issues, a solid multi-scale theoretical background is still missing on anomalous thermal transport phenomena, including (but not limited to) non-diffusive regime, phonon hydrodynamics, second sound, and the dual-phase-lag model regime.

*Advances in science and technology to meet challenges.* Even though, as described in the previous section, both BTE

and MD show some limitations, there are nevertheless many possible promising advances that can be followed to improve their performances.

Concerning the applicability of *ab initio* BTE to disordered materials, a recent work by Simoncelli *et al* [36], proposes a novel approach based on the Wigner phase space formulation of quantum mechanics able to describe the interplay between the quantum Bose-Einstein statistics of atomic vibrations, anharmonicity, and disorder. This formulation has the potential to accurately describe thermal transport in disordered systems even above the crystal melting temperature. The present technique has been successfully applied to many systems including CsPb3 perovskites [36].

Concerning the accuracy of model potentials in MD simulations, a solution to this severe MD limitation is the use of a novel class of model potentials developed through machine learning techniques on an extended data set of DFT calculations. Machine-learning potentials are constructed by mapping the local environment of single atoms in the system onto a set of specific descriptors that allow for efficiently training force fields by reproducing first-principles energies, stresses and forces with controlled uncertainties [37]. This procedure will allow for the generation of accurate model potentials for a wide variety of nanomaterials, reaching the accuracy of quantum mechanical computations at a substantially reduced computational cost. Machine-learning potentials have been already used to efficiently study thermal transport in many materials including 3- and 2D inorganic crystalline and disordered materials [38].

As mentioned above, another severe issue is the actual lack of description of the electronic component of thermal transport. To this aim, the most straightforward solution is the use of the Weidemann–Franz law to roughly estimate the electronic contribution to thermal conductivity. However, it has been shown that for many systems (e.g. graphene or gold thin films [39, 40]) the use of such approximations gives rise to large uncertainties. A more accurate methodology consists of the employment of the semi-classical Boltzmann transport theory to study its electronic transport properties including the electronic contribution to thermal conductivity. This procedure has shown an accurate description of the electronic thermal conductivity partially overcoming the limits of the Weidemann–Franz law [41].

*Concluding remarks.* In conclusion, atomistic simulations represent nowadays an effective tool to understand, predict and ultimately control the physical mechanisms of heat conduction at the nanoscale, indeed a key challenge faced by modern technologists. In particular, as far as thermoelectric applications are concerned, atomistic simulations represent a valuable tool for the *in silico* design of novel nano(materials) to efficiently scatter phonons and finally decouple electrical and thermal transport.

Since, depending on the level of accuracy, each specific simulation technique works at a different time-/size-scale, what appears fundamental for the field is the combination of

different methodologies in a multi-method and multi-scale approach. The use of such a multiple approach would, in fact, lead to a complete understanding of the problem finally making atomistic simulation a reliable and predictive tool for designing novel thermoelectric devices.

*Acknowledgments.* This work was financed by Ministero dell'Università e Ricerca (MUR) under the Piano Operativo Nazionale 2014–2020 asse I, action I.2'Mobilità dei Ricercatori' (PON 2014–2020, AIM), through project AIM1809115-1.

### 3. Disordered multinary chalcogenides for sustainable thermoelectric generation

Eleonora Isotta<sup>1,2,3</sup>, Ketan Lohani<sup>1</sup>, Paolo Scardi<sup>1,4</sup>

<sup>1</sup>Department of Civil, Environmental and Mechanical Engineering, University of Trento, Italy

<sup>2</sup>Department of Chemical Engineering and Materials Science, Michigan State University, USA

<sup>3</sup>Guest editor of the Roadmap.

<sup>4</sup>Author to whom any correspondence should be addressed.

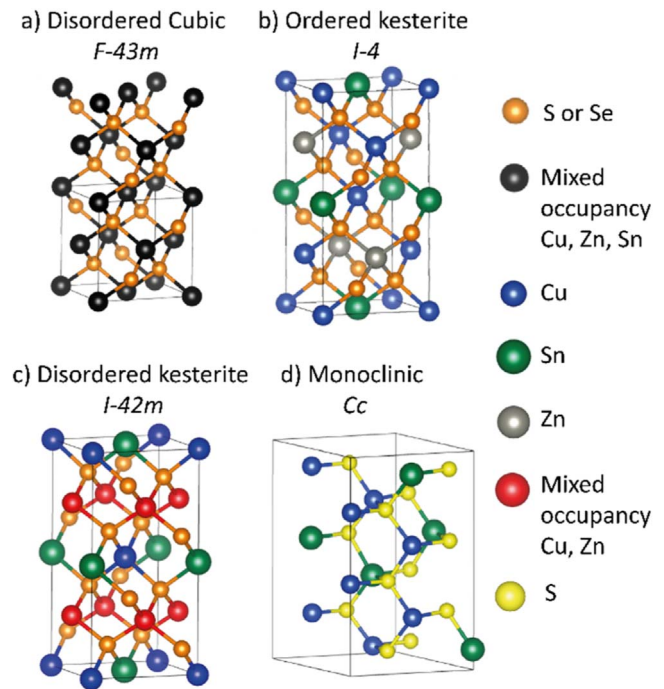
E-mail: [isottael@msu.edu](mailto:isottael@msu.edu), [ketan.lohani@unitn.it](mailto:ketan.lohani@unitn.it), [paolo.scardi@unitn.it](mailto:paolo.scardi@unitn.it)

**Status.** Nanostructures and atomic disorder are of interest for thermoelectric (TE) applications, where they can be employed to suppress the thermal conductivity ( $\kappa$ ). In particular, complex and disordered crystalline phases were proposed as a critical strategy to achieve the so-called Phonon-Glass-Electron-Crystal (PGEC) behaviour [42]. In materials with PGEC characteristics, phonons have short mean free paths, like in an amorphous solid, whereas charge carriers possess high mobility, resulting in an optimal combination of material parameters for high TE performance.

In the quest for developing sustainable and low-cost TE, we have investigated the earth-abundant *p*-type semiconductors  $\text{Cu}_2\text{ZnSnS}_4$  (CZTS),  $\text{Cu}_2\text{SnS}_3$  (CTS), and  $\text{Cu}_2\text{ZnSnSe}_4$  (CZTSe). Their multinary nature makes them particularly prone to polymorphism and disorder, thus representing an interesting testbed for studying the role of structural complexity on TE properties. Furthermore, we employ syntheses based on reactive high-energy milling, which enables to stabilize at low-mid temperatures an additional polymorph, namely a cubic arrangement with full cation disorder. In these systems, we have observed that different types of disorder give rise to various consequences on both thermal and electronic properties, generally leading to improved TE behavior. From material study, the investigation has been then extended to thin film thermoelectric generators (TEGs), with the aim of developing real functioning devices based on cost-effective, non-toxic, and sustainable materials.

**Current and future challenges.** Given the importance of scalability for market implementations, materials are synthesised via reactive milling. Scalable mechanochemical processes were also recently used by other groups for preparing CZTS and CTS thermoelectric materials [43]. These non-equilibrium processes favour a cubic zinc-blende structure with full cation disorder [44] (figure 3(a)). Upon exposure to high temperatures, cubic phases transition to the reported stable structures, namely tetragonal for CZTS and CZTSe, and monoclinic for CTS (figures 3(b)–(d)).

These are not devoid of structural disorder. For example, tetragonal CZTS and CZTSe have been reported to face a reversible transition from ordered kesterite (figure 3(b)) to disordered kesterite (figure 3(c)) [45, 46]. This involves an in-



**Figure 3.** Crystal structures adopted by the multinary chalcogenides of CZTS (a)–(c), CTS (a), (d) and CZTSe (a)–(c).

plane randomization of Cu and Zn cations. In tetragonal CZTS, a sharp increase in the Seebeck coefficient was observed around the transition temperature and found originating from more converged and heavier electronic bands achieved with the transition [47].

Interesting TE properties have been observed for the fully disordered phases. Cubic CZTS was shown promoting the localization of some Sn lone pair electrons, leading to ‘rattling’ Sn ions. These, on one end remarkably suppress  $\kappa$  via low frequency optical phonons, on the other form localized acceptor states, beneficial for the electronic properties [48]. Overall, this leads to modest *zT* values, quantified as 0.05 and 0.25 at 500 K for disordered CZTS and CZTSe, respectively, while the ordered polymorphs show values below 0.01 (CZTS) and 0.15 (CZTSe) at the same temperature. Aside from the low performance, which in part stems from the fact that the carrier density was not optimized, we deem interesting the mechanisms behind the property-improvement upon the introduction of different types of disorder.

An ongoing investigation revealed that cubic CZTS presents topological insulator features arising from disorder, appointing the phase to the Topological Anderson Insulator (TAI) class [49]. A non-trivial topology could favour TEs as nanostructuring, commonly introduced to suppress  $\kappa$ , could turn out beneficial for electrical conduction too, as the improved fraction of high carrier-mobility surfaces would offer preferential paths for carriers [50].

Due to its low formation energy, disordered CTS can be stabilized by high-energy milling followed by sintering. In disordered CTS, Cu–S bonds form a three-dimensional conductive network and Sn–S bonds are relatively weak due to structural disorder. These bonds are relatively soft, contributing to

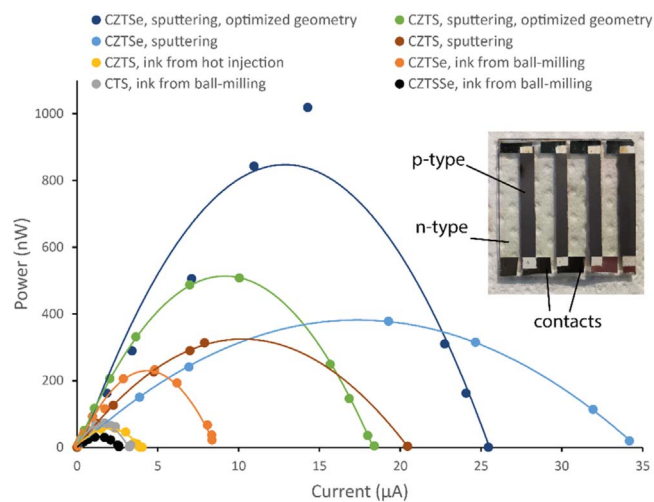
the suppression of  $\kappa$  to the ultra-low range. Moreover, structural disorder introduces potential energy fluctuations in the CTS lattice, contributing energy levels within the forbidden gap; this involves a reduction of bandgap, significantly increasing the TE performance [43, 44].

Interestingly, nanostructured CTS samples prepared via milling followed by spark plasma sintering revealed the conductive nature of its surfaces, enabling synergistically optimized electronic and thermal transport [51]. Disordered CTS polymorph presents a 10-fold higher  $zT$  ( $\sim 0.5$ ), than the ordered ( $\sim 0.05$ ) polymorph, around 723 K [44]. Even in this case, results refer to samples prior carrier-density optimization. Overall, structural disorder emerges as a favourable way to improve the TE performance, especially in the medium temperature range, where the TE technology can attain a large interest.

#### Advances in science and technology to meet challenges.

One of the major challenges in TEs is developing devices based on low-cost, abundant, and non-toxic materials. Traditional TE research has been somewhat focused either on finding new sustainable materials with good performance, or on developing TE generators and coolers (TEGs and TECs), mostly based on relatively established materials, like  $\text{Bi}_2\text{Te}_3$ ,  $\text{Sb}_2\text{Te}_3$ ,  $\text{PbTe}$ , and skutterudites. More recently, effort has been spent in joining these research areas and developing functioning devices based on more abundant materials [52]. Steps in this direction are exemplified by the high-performance  $\text{Mg}_3(\text{Sb},\text{Bi})_2$  and  $\text{MgAgSb}$ -based devices [53–55]. Along this line, our ongoing research is aimed at providing valid sustainable alternatives employing low-cost chalcogenides, in particular pushing for S-based compounds as considerably cheaper and non-toxic. Due to the possible applied interest of micro configuration, appealing for wearables, medical appliances, and micro-devices for the internet of things, we have chosen to develop thin film devices.

Thin film TEGs in planar configuration based on  $p$ -type CZTS, CZTSe (both carrier-density optimized) and CTS and  $n$ -type Al-doped zinc oxide (AZO) have been assembled with a sequential deposition of materials and silver contacts. A typical device is illustrated in the inset of figure 4. Different procedures have been explored for the preparation of thin films: from facile and inexpensive depositions of inks made with hot injection or mechanical-alloying [56], to more advanced sputtering and thermal deposition techniques [57]. As shown in figure 4, the devices present a spread of TE power generation capabilities, with CZTSe-based TEGs presenting the highest values. In terms of power densities per unit planar area, some of these thin-film devices, significantly outperform several other literature attempts based on more sustainable materials [57, 58], showing a peak value of  $280 \text{ nW cm}^{-2}$ . A recent development of  $\text{Mg}_2\text{Sn}_{0.8}\text{Ge}_{0.2}$ -Bi thin film TEGs managed to achieve an even more competitive power per unit planar area of  $430 \text{ nW cm}^{-2}$  [59]. Although CZTSe/AZO [57] and  $\text{Mg}_2\text{Sn}_{0.8}\text{Ge}_{0.2}$ /Bi [59] still partially



**Figure 4.** Thermoelectric generation performance of several thin film devices based on  $p$ -type CZTS, CTS and CZTSe, and  $n$ -type AZO, measured with cold and hot side temperatures of around  $50^\circ\text{C}$  and  $200^\circ\text{C}$  respectively. The insets illustrate a typical device. Data from [58, 59].

employ non-abundant (Se, Bi), or expensive (Ge) elements, these results represent important steps towards devices fully based on earth-abundant and inexpensive compositions. In this regard, it is interesting to notice the more modest power density of  $\sim 150 \text{ nW cm}^{-2}$  obtained with low-cost and non-toxic CZTS/AZO devices [57]. Despite materials make up only part of the cost of a final device, which includes a very significant portion arising from contacts, heat exchangers and manufacturing costs [52], the earth-abundance of the CZTS/AZO composition leads to an up to 80% material cost abatement with respect to traditional TEs [57]. Overall, this leads to power densities per unit material cost comparable to some recent  $\text{Bi}_2\text{Te}_3$ -based devices [60, 61], suggesting them as interesting candidates for further development. We believe that increasing the efforts in developing TE devices based on sustainable materials could substantially improve the applicability of TEs to everyday life technologies.

**Concluding remarks.** This section presents different examples illustrating how complexity and disorder concepts can lead to improved thermoelectric properties. In the pressing search for sustainable thermoelectrics, these concepts have been applied to earth abundant multinary CZTS, CTS and CZTSe to enhance their transport properties. Cation disorder from bottom-up milling syntheses demonstrated to increase a material's thermoelectric performance in several fundamental ways: from suppressing  $\kappa$  through rattling and anharmonicity, to enhancing the electronic properties via bandgap suppression, band degeneracy and conductive surface states. Thin film TEGs have been developed from these materials through facile and scalable production processes. These show a significantly improved performance with respect to several other literature devices based on earth-abundant compounds,

and a marked material cost reduction compared to traditional TEs. Future efforts will focus on how to exploit disorder-related strategies to accelerate the development of high-performance and sustainable devices for commercial applications.

*Acknowledgments.* The authors would like to acknowledge the help of Dr Binayak Mukherjee, Dr Narges Ataollahi, Dr Ubaidah Syafiq, Himanshu Nautiyal, and Dr Mirco D’Incau of the University of Trento, as well as of Dr Carlo Fanciulli of the CNR-ICMATE, Lecco unit.

#### 4. Experimental and computational investigations of skutterudites and half Heusler alloys for thermoelectric conversion at medium and high temperature

Alberto Castellero<sup>1,2</sup>, Marcello Baricco<sup>1</sup>, Mauro Palumbo<sup>1</sup>, Silvia Casassa<sup>1</sup>, and Lorenzo Maschio<sup>1</sup>

<sup>1</sup>Dipartimento di Chimica, NIS, INSTM, Università degli Studi di Torino, Turin, Italy

<sup>2</sup>CNR—ICMATE, Corso Stati Uniti 4, I-35127 Padova, Italy

Email: [alberto.castellero@unito.it](mailto:alberto.castellero@unito.it); [marcello.baricco@unito.it](mailto:marcello.baricco@unito.it); [mauro.palumbo@unito.it](mailto:mauro.palumbo@unito.it); [silvia.casassa@unito.it](mailto:silvia.casassa@unito.it); [lorenzo.maschio@unito.it](mailto:lorenzo.maschio@unito.it)

**Status.** Among inorganic thermoelectric materials [62], skutterudites and half Heusler alloys are the most promising materials for waste heat harvesting in medium and high temperatures due to following reasons [63].

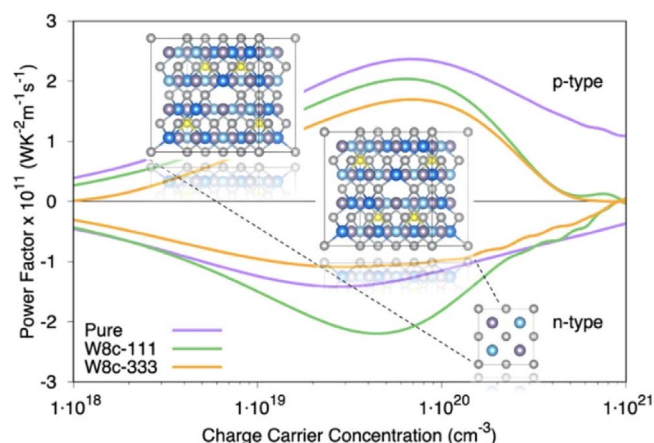
- Starting materials abundant, cheap and non-toxic, with respect to other reference materials, like tellurides and SiGe semiconductors [64].
- Good thermoelectric properties ( $ZT \geq 1$ ) for n- and p-type legs [63].
- Thermo-mechanical compatibility between n- and p-type legs [63], since small compositional changes allow to cross the n/p boundary [65].

Examples of large scale productions of skutterudites [66] and half Heusler alloys [67] have been reported in the literature, suggesting an upcoming commercialization of these materials.

In terms of thermoelectric behaviour, both skutterudites and half Heusler alloys show remarkable low thermal conductivity, that can be achieved through different mechanisms for decoupling the electron and phonon scattering.

In skutterudites, the main feature is the presence of two icosahedral cages in the crystallographic cell, that can be filled by large atoms, such as lanthanides. The filler atoms act as harmonic oscillators, that scatter heat carrying acoustic phonon modes, reducing the lattice thermal conductivity of about one order of magnitude with respect to unfilled counterparts [68]. Values of the lattice thermal conductivity near the glass limit can be approached combining multiple filler species with different vibration frequencies, leading to a broad-frequency phonon scattering [69].

In half Heusler alloys, different scattering mechanisms dominate phonon transport in various temperature ranges [70]. Near room temperature, the lattice thermal conductivity depends mainly on low energy phonons, so that the phonon boundary scattering is the prominent mechanism, as shown by the dependence of the phonon mean free path on the average grain diameter. Increasing the temperature to the range where  $ZT$  reaches a maximum, the phonons occupy higher frequency states. Thus, nanostructuring is not effective in scattering high energy phonons with short mean path, so the

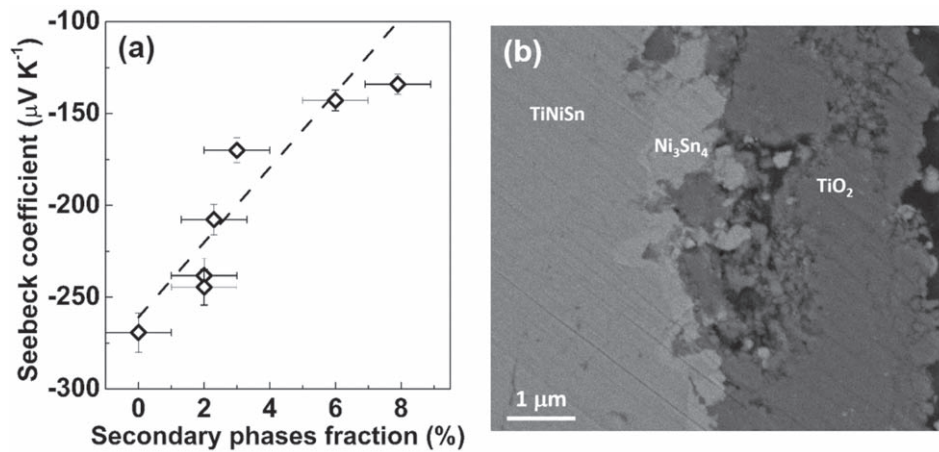


**Figure 5.** Power factor of TiNiSn half Heusler compound as function of the charge carrier concentration, considering different structures, with and without point defects, conserving the original stoichiometry. Reprinted with permission from [73], <https://pubs.acs.org/doi/full/10.1021/acs.jpcc.0c03243>. Copyright © 2022 American Chemical Society.

dominant scattering mechanism is based on mass fluctuations, tailored through a point defect strategy.

Since typical semiconducting half Heusler compounds XYZ (where X and Y are early and late transition metals, respectively, Z is a main group element) are characterized by 18 valence electrons, there are about 70000 candidates as the result of all the possible combinations of the constituting elements. Thus, in the last years, attempts to predict the stability of new half Heusler alloys were performed by means of high throughput DFT calculations and machine learning [71].

**Current and future challenges.** One of the main challenges is the use of predictive tools to identify new compositions with promising thermoelectric properties. This approach needs to validate the tools through model systems that are well known from the experimental point of view. In this framework, TiNiSn half Heusler alloy represents a model system, unravelling the complexity of this family of materials, and is the base constituent for high  $ZT$  and Hf-free half Heusler alloys [72] to be used in high performing and cost affordable devices. DFT calculations of the band gap estimate values exceeding 0.4 eV, depending on the functional used, that are well above the experimental value (0.12 eV). It was found that the calculated band gap values tends to the experimental ones only when point defects are considered [73]. Typically they are composition conserving anti-site defects, with low formation energy [73], and excess Ni (with respect to the 1:1:1 stoichiometry), that occupies the vacant 4d Wyckoff positions in the half Heusler crystal structure [74]. The sensitivity of the electronic structure to such defects strongly affects thermoelectric properties, suggesting that high throughput DFT calculations and machine learning is suitable only for preliminary screenings. For instance, figure 5 shows the trend of the power factor as a function of the charge carrier concentration for different half Heusler



**Figure 6.** (a) Dependence of the Seebeck coefficient as a function of the secondary phase fraction in TiNiSn at 700 K. The dashed line is a guide to the eye. (b) Back scattered electrons micrograph showing the surface oxidation of TiNiSn upon thermal cycling, with formation of  $\text{TiO}_2$  and  $\text{Ni}_3\text{Sn}_4$  on the TiNiSn substrate.

structures, with and without point defects, conserving the stoichiometry of the compound TiNiSn.

In view of mass and standardized productions, it is necessary to establish scalable processing routes that guarantee reproducibility among different batches. Both skutterudites and TiNiSn-based half Heusler alloys are difficult to be processed by casting, because of peritectic reactions that lead to porous [75] and inhomogeneous [76] ingots. Currently, long annealing time are needed to homogenize the microstructure and to solubilize the filler in the cage of skutterudites. Not fully homogenized or off-stoichiometry samples of TiNiSn can contain different amounts of residual secondary phases [76], that affect the thermoelectric properties of the material. An example is given in figure 6(a), where the effect of different amounts of secondary phases on the Seebeck coefficient of TiNiSn-based samples is shown. In skutterudites, the presence of secondary phases can change the amount of filler solubilized in the structure [77], altering transport properties.

Since intermetallic compounds exhibit the optimal thermoelectric performance at medium/high temperatures (i.e. 700–900 K), these materials are expected to be subjected to potentially critical working conditions upon service. TiNiSn-based half Heusler alloys tend to oxidize [76], as shown in figure 6(b), while in skutterudites volatile elements, such as Sb, can sublime, modifying the composition [78].

Finally, thermoelectric modules based on skutterudites and half Heusler alloys have been assembled only at the prototype level and are not commercialized yet. As a general issue, the current assembling of thermoelectric modules is limited to planar geometries, and it is usually performed by manual or semimanual procedures. Thus, a big challenge is to overcome this limitation by developing reliable and scalable manufacturing routes to produce thermoelectric modules.

*Advances in science and technology to meet challenges.* To compute reliable and accurate thermoelectric properties, the following steps are necessary:

- Definition of point defects that are usually present in the structure, affecting electronic and transport properties. In this approach, the use of adequate supercells is required in calculations, in order to consider realistic defect concentrations.
- Simulation of grain boundary interfaces to correctly compute the transport properties of polycrystalline materials.
- First-principle estimation of the lattice thermal conductivity by computing: (i) the phonon-phonon interaction and (ii) the electron-phonon coupling. In thermoelectric materials, which exhibit carrier concentration in the range of  $10^{19}$  to  $10^{21}$   $\text{cm}^{-3}$ , the latter contribution appears to be particularly important.

In the processing of skutterudites and half Heusler, rapid solidification can be successfully employed as an intermediate step between melt alloying and powder consolidation. It was demonstrated that rapid solidification of TiNiSn induces undercooling of the liquid, favouring the nucleation of the half Heusler phase with respect to the primary phase  $\text{TiNi}_2\text{Sn}$ , leading to an almost single phase material that can be directly sintered, avoiding long annealing steps [76, 79]. In skutterudites, rapid solidification produces a nanostructured mixture of non-equilibrium phases, that can be homogenized through an annealing step that is significantly shorter than the one needed for cast ingots, due to the increased grain boundary diffusivity [78].

Alternatively, severe plastic deformation (SPD) has been proposed for processing both skutterudites and half Heusler alloys, leading to improved thermoelectric properties due to reduced lattice thermal conductivity, as consequence of the ultrafine microstructure in combination with high density of point and linear defects [80]. Processing by SPD leads also to significant strengthening of the materials.

Concerning the assembling of the modules, an alternative approach to the current technologies would be the use of additive manufacturing. In this way, the layer-by-layer deposition would allow to assembly in customizable ways

the sequence of conductive layer, the n/p legs, diffusion barrier and conductive layer, overcoming the current limitation of planar geometries and leading to more standardized procedures [81]. From the materials perspective, additive manufacturing implies high solidification rates, that have been demonstrated to be beneficial in terms of phase formation (TiNiSn) and homogenization (skutterudites). Preliminary results obtained following this approach are limited to the deposition of the thermoelectric materials [81]. Thus, additive manufacturing of thermoelectric modules is still an open field.

Finally, the development of protective coatings is pivotal to ensure long durability of devices operating at medium/high temperature ranges.

*Concluding remarks.* Skutterudites and half Heusler alloys are promising materials for the harvesting of waste heat in medium/high temperature ranges, due to their good thermoelectric and thermomechanical properties, and to the possibility of large scale production using abundant, cheap and non-toxic elements. Transport properties of these materials are successfully manipulated by controlling

structural and microstructural features. A better understanding and an improvement of the thermoelectric behaviour can be achieved by combining computational and experimental tools. The experimental results can serve as validation of the new computational procedures developed to describe phenomena in an ever more accurate and realistic way. Modelling can provide atomic-level information about measured properties and characteristics, thus obtaining assumptions about structure-property relationships. Finally, accurate theoretical predictions can possibly orient the synthesis of new materials. In this context, a computational tool must be able to simulate various defects, considering the thermal effects, and to provide an accurate estimate of all quantities that define the thermoelectric figure of merit.

On the experimental counterpart, the absence of commercial modules based on these materials suggests that advances are needed in developing more flexible and reliable processing routes for assembling modules. In this view, additive manufacturing appears to be a suitable candidate for innovation.



## 5. Filled skutterudites and Heusler phases as candidate materials for thermoelectric thin films

Cristina Artini<sup>1,2</sup>, Marcella Pani<sup>1,3</sup>, Giovanna Latronico<sup>4,5</sup>, Paolo Mele<sup>4</sup>

<sup>1</sup>DCCI, Department of Chemistry and Industrial Chemistry, University of Genova, Via Dodecaneso 31, 16146 Genova, Italy

<sup>2</sup>Institute of Condensed Matter Chemistry and Technologies for Energy, National Research Council, CNR-ICMATE, Via De Marini 6, 16149 Genova, Italy

<sup>3</sup>CNR-SPIN Genova, Corso Perrone 24, 16152 Genova, Italy

<sup>4</sup>Shibaura Institute of Technology, Omiya Campus, 307 Fukasaku, Minuma-ku, Saitama City, Saitama 337-8570, Japan

<sup>5</sup>International Research Fellow of Japan Society for the Promotion of Science (JSPS), Japan

Email: [artini@chimica.unige.it](mailto:artini@chimica.unige.it) (C.A.); [marcella.pani@unige.it](mailto:marcella.pani@unige.it) (M.P.); [i048025@shibaura-it.ac.jp](mailto:i048025@shibaura-it.ac.jp) (G.L.); [pmele@shibaura-it.ac.jp](mailto:pmele@shibaura-it.ac.jp) (P.M.)

**Status.** Among the many materials currently studied by reason of their thermoelectric features, filled skutterudites ( $Y_yM_4Sb_{12}$ ,  $Y \equiv$  rare earth or alkaline earth,  $M \equiv$  transition element,  $0 < y \leq 1$ ) [82] and Heusler phases ( $X_2YZ$ ,  $X, Y \equiv$  transition element or rare earth,  $Z \equiv$  element of the III, IV or V group) [83] present some common characters, which justify a joint analysis of their structural, electronic and transport properties, as well as of their possible use in thermoelectric devices [84]. Both in fact can be deemed as Zintl phases; their electronic properties can be ruled by proper doping to achieve the semiconducting regime, and their phonon thermal conductivity ( $k_{ph}$ ) can be lowered by adding scattering centres in the form of foreign atoms; finally, both  $p$ - and  $n$ -conducting legs can be obtained from the same parent compound, which significantly reduces the coefficient of thermal expansion mismatch. Actually, while Heusler phases are experiencing a wide interest from the materials science community, with a continuously growing number of papers on the topic, filled skutterudites had their peak of success about a decade ago. Nevertheless, the optimization of these materials is largely attempted in many laboratories. The insertion of different lanthanide ions in Co/Ni- [85], Fe/Ni- [86] and Fe/Co- [87] based skutterudites, as well as the partial substitution of Sb by an aliovalent ion [87, 88], can be considered in this perspective; the partial substitution of Sn by Sb in the Heusler phase  $Fe_2TiSn$  pursues the same goals [89, 90].

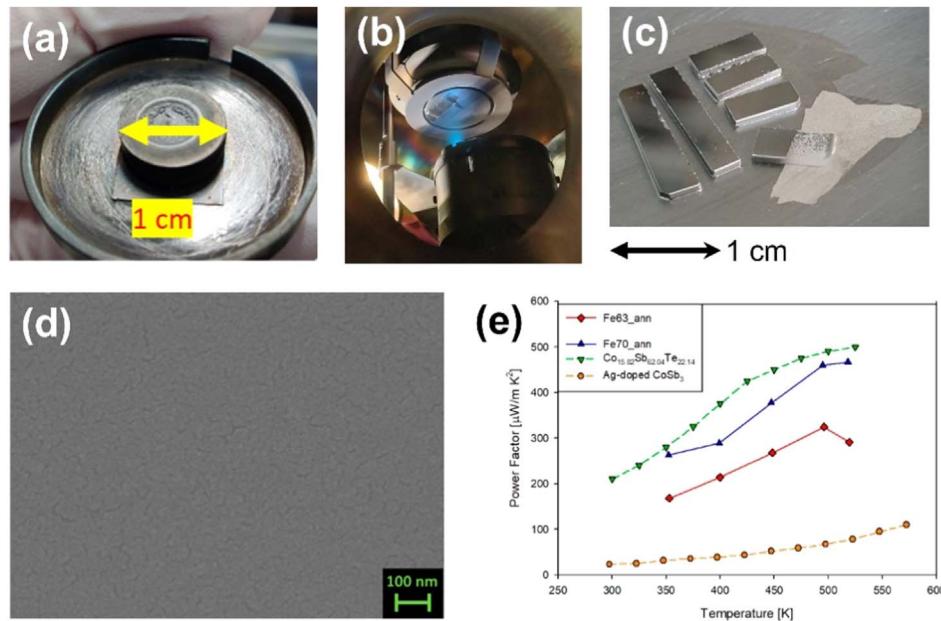
Within this framework, the deposition of thermoelectric thin films based on filled skutterudites and Heusler phases represents the attempt to combine the easy tunability of the thermoelectric properties of these materials and the reduced dimensionality of films, and to take advantage of the flexibility and robustness of thin film-based thermoelectric devices. Moreover, the out-of-plane application of the thermal gradient allows to exploit the whole length of the film and to maximize the output power. From the basic science viewpoint, in fact,

low dimensionality and the presence of interfaces make films ideal sources of additional scattering centres; from the technological side, it is highly desirable to build devices able to harvest heat from curved or irregularly shaped surfaces [91, 92]. Nonetheless, despite the evident benefits, the deposition of thin films poses some experimental concerns; the present research group recently undertook the deposition by pulsed laser deposition (PLD) of  $Sm_y(Fe_xNi_{1-x})_4Sb_{12}$  skutterudite thin films [93] and tried that of the  $Fe_2Ti(Sn_{1-x}Sb_x)$  Heusler phase.

**Current and future challenges.** To fully exploit the advantages of skutterudites and Heusler phases as thin films, two main research issues have to be faced, namely the optimization of materials and of the film deposition.

The most remarkable hallmark of filled skutterudites resides in the possibility to partly fill the cage in the  $2a$  crystallographic position, allowing to significantly lower  $k_{ph}$  thanks to the rattling movement of the guest ion(s). Many attempts have been done to use various fillers with the aim to perturb the transmission of different phonon frequencies [94, 95]. The most effective way seems to be multifilling: filling  $RE_yFe_xNi_{1-x}Sb_{12}$  by (Gd,Sm) instead of only Sm, for example, lowers thermal conductivity by  $\sim 1 \text{ Wm}^{-1} \text{ K}^{-1}$  at 700 K for  $x = 0.8$  [95]. In addition, current efforts mainly consist in the insertion of additional scattering centres, e.g. by preparing dense samples: densification favours in fact the introduction of defects, like point defects and dislocations, and reduces the domains average size. The synthesis at extremely high pressure, up to 2 GPa, addresses this need [96], and even the application of severe plastic deformations goes in this direction [97]. The optimization of Heusler phases in view of thermoelectric applications also relies on the engineering of defects aimed at the reduction of  $k_{ph}$ : while in fact many of them exhibit a high power factor, the high  $k_{ph}$  is the main drawback to the development of such materials for the employment in thermoelectric devices. To this purpose, strategies such as nanostructuring, introduction of vacancies and/or doping ions into the lattice, and creation of nanodomains with different stoichiometries, are currently pursued [98]. Besides, the study of Heusler phases thin films is particularly exciting, since high thermoelectric performances were recently discovered in some of them: metastable thin films of  $Fe_2V_{0.8}W_{0.2}Al$ , for example, were claimed to show a ZT approaching the astonishing value of 6 [99].

In addition to these issues, also the most effective deposition technique and deposition parameters must be chosen. PLD represents a widespread technique thanks to its adaptability to the processing of different materials. Preliminary results revealed that annealed films belonging to  $Sm_yFe_xNi_{1-x}Sb_{12}$  exhibit a power factor of  $\sim 400 \mu\text{Wm}^{-1} \text{ K}^{-2}$  at 500 K, in good agreement with films of Co-based skutterudites [94] (figure 7(e)). Anyway, the most proper values of several factors, such as laser power, target-substrate distance, deposition duration and temperature, have to be optimized for every class of materials [94].



**Figure 7.** (a) SPS target of skutterudite  $\text{Sm}_y(\text{Fe}_x\text{Ni}_{1-x})_4\text{Sb}_{12}$  ( $x = 0.70$ ); (b) bottom-view of the PLD vacuum chamber showing the plume originated from the target by laser ablation during the deposition; (c) optical macro photograph of the  $\text{Sm}_y(\text{Fe}_x\text{Ni}_{1-x})_4\text{Sb}_{12}$  ( $x = 0.70$ ) thin films deposited on silica substrates; (d) top view high magnification LED-SEM images of film  $\text{Sm}_y(\text{Fe}_x\text{Ni}_{1-x})_4\text{Sb}_{12}$ , reproduced from [93]. [CC BY 4.0](#); (e) trend of the power factor as a function of temperature for films  $\text{Sm}_y(\text{Fe}_x\text{Ni}_{1-x})_4\text{Sb}_{12}$  ( $x = 0.63$ , red and  $0.70$ , blue) compared to other samples from the literature, reproduced from [93]. [CC BY 4.0](#).

*Advances in science and technology to meet challenges.* In the framework of the preparation of skutterudite and Heusler phases dense targets intended for the deposition of thin films, one of the most challenging issues deals with the reproducibility of the synthetic way. Regarding skutterudites, they hardly result to be perfectly monophasic, being often accompanied by a more or less large amount of additional phases; this can happen due to the precipitation of phases stable at high temperature, or to the not correct amount of filler ion with respect to the skutterudite composition, e.g. to the Fe/Ni ratio. The former is not an issue if films are deposited by PLD: one of the main advantages associated to this technique is in fact the stoichiometric transfer of material from the target to the film, which makes it ideal for the deposition of complex structures. This was recently verified in Sm-based skutterudite thin films, which resulted to be monophasic even if deriving from not perfectly monophasic targets [100]: in this respect, PLD ensures a very good control of the filler content in the film. On the contrary, the occurrence of extra phases caused by the wrong filler amount can only be avoided if the correlation between filler content and Fe/Ni ratio is precisely known, which is a not always easily available information.

With reference to Heusler phases containing high melting metals, their preparation by arc melting often suffers the not perfect incorporation of such elements, which leads to local inhomogeneities in the elemental distribution and in general to conditions of off-stoichiometry. Even the subsequent annealing treatment can provide not perfectly reproducible results due to issues related to synthesis still needing to be fixed.

A further point specifically related to the processing of Heusler phases regards the densification of the bulk material aimed at the preparation of dense targets (figure 7(a)). A fundamental requirement for PLD is in fact the availability of a dense target, from which material is ablated and deposited onto a substrate (figures 7(b)–(d)). To this end, the bulk material has to be finely ground, and powders have to be pressed either by spark plasma sintering, high pressure sintering, open die pressing, or another densification method. While the densification of filled skutterudites generally does not pose significant concerns [101], Heusler phases with thermoelectric properties often cannot be properly pressed, as they easily crush, turning out to be inadequate for film deposition.

*Concluding remarks.* The study of thermoelectric thin films is of particular relevance because of their reduced dimensionality, which helps to introduce new scattering centres able to depress  $k_{ph}$ . Within this framework, filled skutterudites and Heusler phases are interesting candidate materials, since their intrinsic thermoelectric properties can be improved in a relatively easy way by properly inserting doping and/or filling ions. Nevertheless, still open issues have to be faced by the materials science community. From the viewpoint of research challenges, efforts are directed toward the further reduction of  $k_{ph}$  in both classes of materials, being this parameter the only one which can be freely varied without negatively affecting electrical conductivity at the same time. This goal can be pursued, among other approaches, such as nanostructuring and introduction of vacancies, also by densifying bulk samples or synthesizing them under extremely high pressure. On the other hand, from the technological viewpoint, some issues still need to be fixed, such

as the ones related to a reproducible synthetic way for Heusler phases and to the identification of a synthetic procedure for filled skutterudites resulting in monophasic samples; last but not least, the densification of Heusler phases still remains an unresolved problem.

*Acknowledgments.* PM and GL acknowledge the partial financial support from the International Research Center for Green Electronics (IRCGE), Shibaura Institute of Technology. Prof Pietro Manfrinetti (University of Genova) is kindly acknowledged for his help in synthesizing bulk samples.

## 6. Transparent thermoelectric thin film materials for energy harvesting at low temperature

Francesca Di Benedetto, Gaetano Contento, Maria Federica De Riccardis, Raffaele Fucci, Barbara Palazzo, Antonella Rizzo

ENEA – Italian National Agency for New Technologies, Energy and the Sustainable Economic Development, SSPT-PROMAS-MATAS Brindisi Research Centre S.S. 7 - Km 706 72100 Brindisi (Italy)

Francesca Di Benedetto francesca.dibenedetto@enea.it, Gaetano Contento gaetano.contento@enea.it, Maria Federica De Riccardis federica.dericcardis@enea.it, Raffaele Fucci raffaele.fucci@enea.it, Barbara Palazzo barbara.palazzo@enea.it, Antonella Rizzo antonella.rizzo@enea.it

**Status.** Unlike conventional bulk thermoelectric, predominantly applied in high temperature regime, thin-film thermoelectrics find their main application in the low-temperature regime ( $<425$  K) [102] as a power source for micro- and nano-energy electronics, such as Internet of Thing (IoT) systems, wireless sensor network (WSN) for building energy management, medical and wearable devices. Emerging transparent thermoelectrics, with a wide bandgap ( $E_g$  above 3 eV), could disrupt the future of thin-film energy harvesting technology and pave the way for newly developed display screens, integrated solar cells, infrared photodetectors and smart windows. For example, by coupling thermoelectric materials to the display of a smartwatch or any other small gadget, the device could last longer between charges or not need to be charged at all due to the thermogenerated energy. In addition, the hybrid energy generator based on photothermal conversion could result in increased power output compared to photovoltaics alone [103].

The integration of a transparent TEG into glazing seems an intriguing possibility to address the future challenge of increasing energy demand. In fact, it would provide an opportunity to exploit a naturally existing temperature difference (which is about  $5$  °C– $20$  °C or even more depending on geographic location and period) between the outdoor and indoor environments (heated or cooled by energy-consuming air conditioning systems) of a building. In addition, the exploitation of this heat source improves environmental comfort without increasing heating/cooling consumption and allowing energy savings in modern construction. Finally, the large surface area of glazing could also make attractive the application of materials that would never achieve high performance.

To date, the development of fully transparent thermoelectric devices has been hindered by the lack of p-type inorganic thermoelectric materials with performance comparable to their n-type counterparts, which have been extensively studied even though they still demonstrate low performance. Recently, Yang *et al* [104] developed intrinsically transparent p-type thin films based on copper iodide (CuI) with a ZT figure of merit comparable ( $ZT = 0.21$  at 300 K) to that of the common bulk material of lead telluride (PbTe) and three

orders of magnitude higher than previous transparent p-type thermoelectrics. They estimated theoretically that a window of CuI-based thermoelectric elements with an area of about  $10$  m<sup>2</sup> could power a refrigerator (consuming about 1 kWh per day) all day long.

**Current and future challenges.** The integration of TEG into windows is particularly challenging because it requires balancing complex aspects. Materials must provide high optical transparency that can withstand multiple environmental exposure factors (such as UV, humidity, a wide range of temperatures) with minimal haze. In parallel, fabrication technologies must be environmentally and economically sustainable and easily scalable for wide-area mass production.

To make the technology feasible and widely used, it is more important to provide low-cost materials with acceptable performance than developing materials with high performance and high prices. For these reasons, the focus of recent research has been both on the development of sustainable materials made from nontoxic, earth-rich elements or obtained by simple synthetic routes, and on the evolution of low-temperature device fabrication procedures or solution-based printing processes.

Among inorganic materials, Zn-based oxides are inexpensive and abundant n-type compounds with excellent chemical stability in air and good thermal and electrical conductivities, which can be adjusted through doping, nanostructuring, and grain boundary engineering [105–108], although obtaining high ZT remains critical. As a well-matched p-type material, CuI obtained by reactive sputtering at room temperature shows higher thermoelectric performance ( $ZT = 0.22$  at 300 k) [109], compared with other p-type oxides such as  $\text{CuM}_2$  ( $M = \text{Al, Cr, Ga, In, Fe, B}$ ), although its stability is still problematic [104].

A suitable alternative to inorganic materials is conductive polymers (CP), due to their intrinsic low thermal conductivity and excellent processability with various scalable manufacturing approaches, e.g. coating, casting, and printing. They can be synthesized chemically or electrochemically with complete control over structure and thickness [110]. Among the commonly used CPs, PEDOT:PSS is an appropriate p-type material for use in smart windows due to its easy processability, high transparency, and good electrical conductivity [111, 112]. Unfortunately, fully organic transparent thermoelectric devices have not been reported because stable doping with n-type materials is still difficult to achieve. Therefore, PEDOT:PSS could be coupled with n-type transparent conductive inorganic oxides, such as ITO (In:  $\text{SnO}_2$ ), or with metal-organic composites based on CPs [113].

In terms of technologies, scalable high-throughput manufacturing has been dominated by solution-based printing processes, although the performance of printed materials is far inferior to those made with vacuum techniques. The recent implementation of PVD techniques with the commercial roll-to-roll process meets market needs for large-scale production [114].

**Advances in science and technology to meet challenges.** To improve the thermoelectric properties and optimize the performance of thin-film TE materials, several technological strategies are possible. In the case of Zn-based materials, different dopants have been studied and good ZTs (above 0.1 at room temperature) have been reported for aluminum-zinc oxide (AZO) films deposited by radio frequency (RF) and direct current (DC) pulsed magnetron sputtering at room temperature [105]. In our labs we have realized transparent AZO thin films (figure 8) by sputtering at 573 K with a two-fold increased electrical conductivity ( $791.3 \text{ S cm}^{-1}$ ) but a power factor (PF) of  $40.4 \mu\text{W mK}^{-2}$  and a  $ZT = 0.09$  due to the reduced Seebeck coefficient ( $-22.6 \mu\text{V K}^{-1}$ ) [115]. The incorporation of a structural defect can reduce the thermal conductivity of ZnO compounds through the creation of selective phonon scattering centers, but it has negative effects on crystal quality, electrical conductivity. Recently, double doping, i.e. the combination of dopants with a larger ionic radius (In, 0.080 nm) and smaller ionic radius (Ga, 0.062 nm) than the host atom (Zn, 0.074 nm), has resulted in a balanced control of the crystal structure and a better effect on all thermoelectric properties [108].

Regarding CuI thin films, Murmu *et al* [116] reported how a simple vacuum annealing process (at  $100 \text{ }^\circ\text{C}$ ) can increase the Seebeck coefficient due to a decrease in hole density and an energy filtering mechanism of charge carriers. Recently, Faustino *et al* [109] showed that the thermoelectric performance of CuI thin films can be improved by a subsequent doping process (vaporization or solid iodination), without affecting the optical transparency of the final films. I-rich (or VCu-rich) CuI thin films having a PF of  $37.4 (\mu\text{W mK}^{-2})$  and  $ZT = 0.22$  at room temperature have been realized by thermal evaporation and subsequent vapour doping. In agreement with the literature. These films exhibit a good optical transmittance (figure 8) but further efforts are needed to obtain stable layers under operating conditions. In addition, the low vapor pressure of  $\text{I}_2$  can easily activate desorption at low temperature, thus decreasing the  $[V_{\text{Cu}}]$  and electrical conductivity of the material. For these reasons, the use of suitable polymeric cap layers [117] has been optimized in our laboratories.

Finally, to improve the performance of CPs, which are normally p-type, it is possible to tune the electrical properties through doping or oxidation level [118–120], but this approach requires attention because, for example, in PEDOT it can induce low  $S$  due to the shift of the Fermi level toward the conduction band [121]. In parallel, the development of an



**Figure 8.** Optical transmittance of AZO (blue line) and CuI (red line) films deposited on glass substrate (dashed black line). Insert shows a photo of the analyzed samples.

n-type TE polymer could be achieved by incorporating nanometer-sized inorganic materials with excellent  $S$  values (e.g.  $\text{Bi}_2\text{Te}_3$  nanoparticles) into the organic matrix [122]. However, the homogeneous dispersion of TE fillers in the polymer matrix is critical to achieve a beneficial effect from the nanofiller/matrix interface.

**Concluding remarks.** Transparent thermoelectric materials have attracted much attention and understanding the key factors that influence their ultimate performance is a key step. However, many problems remain to be solved to transfer the readiness technologies to mass production and have widespread application of thermoelectric materials in thin-film form. A winning strategy to have more efficient devices with greater deployment potential could be to couple different methods of energy production, preferably from renewable sources, with those of energy harvesting, recovery, or saving.

**Acknowledgments.** We acknowledge the financial support received by the Ministry of the Economic Development (MiSE) through the collaboration contract ‘Exploitation of new active materials for the development of thermoelectric microgenerators’, Project 1.3 ‘Frontier materials for energy uses’, Three-year Implementation Plan 2019–2021 and partially funded by Three-year Implementation Plan 2022–2024.

## 7. Nanoscale thermoelectricity with III–V compound semiconductors

Valeria Demontis<sup>1</sup>, Domenic Prete<sup>1</sup>, Muhammad Isram<sup>2</sup>,  
Francesco Rossella<sup>2</sup>

<sup>1</sup>Scuola Normale Superiore and Istituto Nanoscienze—CNR, Piazza San Silvestro 12, 56127, Pisa, Italy

<sup>2</sup>Dipartimento di Scienze Fisiche Informatiche e Matematiche, Università di Modena e Reggio Emilia, via G. Campi 213/A, 41125, Modena, Italy

[valeria.demontis@sns.it; domenic.prete@sns.it; muhammad.isram@unimore.it; francesco.rossella@unimore.it]

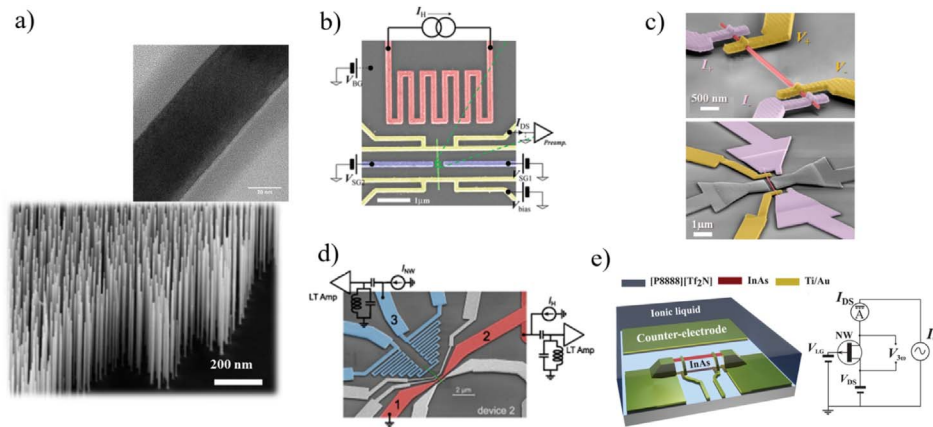
**Status.** Semiconductor nanostructures have been the subject of intense thermoelectricity research as they play a key role in demonstrating novel strategies for the optimization of the thermoelectric figure of merit  $ZT$ , a challenging task which took enormous advantages from the advent of nanosciences in the 1990s [123]. In this frame, semiconductor nanowires represent an ideal platform for investigating fundamental aspects of thermoelectric transport phenomena, allowing to separately address the parameters entering  $ZT$  [124, 125]. At a time, nanowires and nanowire heterostructures hold the promise for developing innovative device building blocks for high performance thermoelectric systems. In particular, III–V compound semiconductors represent an intriguing class of materials for nanowire engineering, allowing to combine excellent transport properties (e.g. large electron density and mobility and Seebeck coefficients) and fully controlled bottom-up epitaxial growth processes [126], leading to nanosystems and nanointerfaces of unprecedented crystalline and morphological quality (figure 9(a)). In the last two decades, countless applications of III–V semiconductor nanowires have been reported across a plethora of different fields including electronics [127], photonics [128], sensing [129, 130] and quantum technologies [131, 132]. Regarding thermoelectric applications, III–V semiconductor nanowires emerged as a formidable platform for investigating the basic physical mechanisms ruling thermoelectric energy conversion and harvesting at the nanoscale, and for developing new strategies towards the enhancement of thermoelectric device performances.

**Current and future challenges.** One of the main challenges that researchers succeeded to address in recent years has been the development of strategies and device architectures to probe the thermoelectric properties of materials at the level of an individual nanostructure. Starting from individual single-crystal nano-objects such as semiconductor nanowires, and resorting to state-of-the-art nanofabrication techniques, researchers were able to develop nanodevice architectures allowing to establish thermal gradients exceeding 1 K/100 nm over spatial scale of the micro meter—the characteristic length scale of a single InAs NW grown by chemical beam epitaxy [133]. Figure 9(b)) [134] and (d) [135] show two examples of thermoelectric nanodevices incorporating micro-

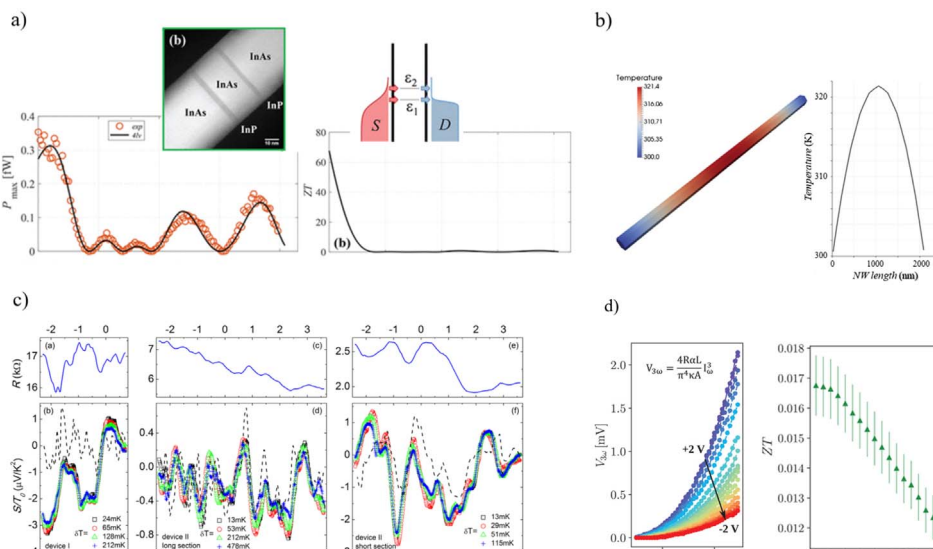
heaters and local thermometers. These systems are employed to characterise the electrical transport properties and Seebeck coefficient of nanowires and nanowire heterostructures by exploiting DC electrical measurements or advanced techniques such as the noise thermometry [1, 136, 137]. A reliable measurement of the thermal conductivity of individual nanowires has remained deceptive until the issue of the thermal leakages to the substrate [133] was fixed: to this purpose, device architectures implementing suspended nanowires have been developed. Resorting to these suspended nanowire device architectures, the thermal conductivity of individual nanowires is addressed by exploiting a self-heating technique referred to as the  $3\omega$  method: the nanostructure is fed with an AC current at frequency  $\omega$ , while the third harmonic of the voltage drop along the nanostructure is picked up (figure 9(c)) [138]. By using this approach it is possible to investigate experimentally one of the predicted main advantage of using artificially structured nanomaterials, i.e. the strong reduction of the thermal conductivity with respect to the counterpart bulk materials [133, 139]. A noteworthy step forward in nanowire thermoelectricity has been the development of an experimental platform allowing - simultaneously and in the same nanostructures - to measure all the electrical, thermal and thermoelectric parameters and to dynamically optimize  $ZT$ . This approach, schematically illustrated in figure 9(e)) [140], exploits the field effect induced by an electrolyte to modulate the electrical conductivity of a suspended nanowire [141] at room temperature: a crucial result, allowing to modulate also the Seebeck coefficient  $S$  and ultimately the figure of merit, that is not achievable resorting to conventional nano-FET architectures employing solid state gates.

**Advances in science and technology to meet challenges.**

The improvements in NWs epitaxial growth and nanofabrication techniques, together with the development of new device concepts, fostered the rapid advancement in semiconductor nanowire thermoelectricity in the last ten years. By using the  $3\omega$  method, thermal conductivity values of WZ InAs NWs in the interval 12–16 W mK<sup>-1</sup>—considerably reduced with respect to the bulk counterpart—were demonstrated [138], with  $ZT$  around 0.02 [140]. The strong electronic confinement occurring in low-dimensional systems, such as InAs/InP nanowire quantum dots, was also demonstrated as a remarkable tool to enhance, at low temperature, the thermopower and the electronic  $ZT$  (figure 10(a) [134]). By tuning the dot configuration, an electronic efficiency at maximum power of 47% of the Carnot efficiency was demonstrated, close to the Curzon-Ahlborn limit. The corresponding electronic  $ZT$  was  $\approx 35$ . Although these values neglect the phonon contribution to the thermal conductivity, they demonstrate the fundamental role of quantum confinement in optimizing the operation of thermoelectric engines. Low temperature investigations provide crucial insights on the impact of low dimensionality and quantum confinement on TE mechanisms, and contribute to the development of novel approaches for heat management



**Figure 9.** (a) SEM image of as grown InAs nanowire sample and HRTEM image of an individual InAs nanowire (inset); (b) false color SEM image of a nanowire based thermoelectric device equipped with a micro-heater (red), local thermometers/ohmic contacts (yellow) and side gates (purple). Reprinted with permission of [134]. Copyright (2019) American Chemical Society; (c) examples of a suspended nanowire device for thermal conductivity measure, exploiting the  $3\omega$  method. Adapted from [138], with permission from Springer Nature; (d) SEM image of a device for shot noise thermometry measurements. Reproduced from [137]. CC BY 4.0.; (e) pictorial view and equivalent circuit scheme of a nanowire device, embedded in an ionic liquid droplet, for the simultaneous measurement and modulation of the thermoelectric parameters. Reproduced from [140]. CC BY 4.0. and thermal transport measurements. The entire device is embedded in an ionic liquid droplet—represented by the blue color. We allow at most two figures (or 1 figure and 1 table) that are roughly the size of this box. If the figure is reproduced or adapted from another non-IOP publication, you must seek permission for re-use from the publisher.



**Figure 10.** (a) Generated power, thermoelectric figure of merit and efficiency at maximum power in units of the Carnot efficiency for a quantum dot-based heat engine operating at 30 K. Reprinted (adapted) with permission from [134]. Copyright (2019) American Chemical Society. (b) Finite element simulation of the temperature spatial distribution in an InAs nanowire thermally anchored at 300 K at both ends and fed with an AC current of  $\approx 50 \mu\text{A}$  in a  $3\omega$  experiment. Adapted from [138], with permission from Springer Nature. (c) Linear response resistance and normalized Seebeck coefficient as a function of back-gate voltage measured on various NWs device and different values of the thermal bias. Reproduced from [136]. © IOP Publishing Ltd. All rights reserved. (d) Modulation of the electronic transport properties and thermoelectric figure of merit exploiting ion gating in InAs NWs based thermoelectric devices. Reproduced from [140]. CC BY 4.0.

at the nanoscale, with potential applications in nanoelectronics and quantum sciences. In this frame, noise thermometry offers a unique sight on the impact of applied gate voltages and thermal gradients on the Seebeck coefficient of individual NWs (figure 10(c)) [136]. As the thermoelectric response of a semiconductor nanostructure is strongly dependent on the density of free carriers, the possibility to effectively tune the electrical properties by field effect is one of the biggest advantages of semiconductor nanowires for thermoelectric applications. In this frame, new approaches for

gating are emerging, which exploit ions in an electrolyte to induce charge accumulation in a semiconductor. This paradigm, called ionic-gating, can be implemented using different soft-matter systems and exploits the electrically driven formation of an electric double layer at the electrolyte/semiconductor interface to achieve outstanding gating performances when compared to conventional gate dielectrics, with an increase of the capacitive coupling of almost two orders of magnitudes [142]. Ionic gating is especially suited for high aspect ratio nanostructures, such as

nanowires, and is compatible with suspended nanowire device architectures, as the electrolyte embeds the nanowire and ensures a strong and conformal capacitive coupling. Recent studies demonstrated the simultaneous measurement of all thermoelectric parameters (including thermal conductivity) and the electrostatic control of ZT in suspended semiconductor NWs resorting to ionic gating, at temperatures of interest for real applications (figures 10(b), (d)).

*Concluding remarks.* The experimental studies on thermoelectric energy conversion and harvesting are taking enormous advantages from the developments of innovative semiconductor nanostructures. Among these, III–V semiconductor nanowires are emerging as an ideal class of nanomaterials in the race to achieve high performance

thermoelectric devices. On the one hand, progresses are expected from the increasing advances in the nanowire growth technology—enabling the realization of fully engineered crystal structures and morphologies with optimised thermoelectric parameters—combined with the development of visionary nanodevice architectures enabling novel thermal and electrical functionalities. On the other hand, novel routes for ZT improvement are rising from the exploration of hybrid platforms combining semiconductor nanowires and soft-matter systems of mobile ions to achieve ionic-gating of the semiconductor.

*Acknowledgments.* The authors acknowledge the financial support by the program PRIN 2017 for 717 the Project ‘Photonic Extreme Learning Machine’ (PELM), protocol number 20177PSCKT.



## 8. Challenges and advances in the fabrication and characterization of large temperature gradient cascade thermoelectric modules

Alberto Ferrario<sup>1</sup>, Alvise Miozzo<sup>2</sup>, Stefano Boldrini<sup>3</sup>

CNR – ICMATE, Corso Stati Uniti 4, 35127 Padova, Italy

<sup>1</sup>alberto.ferrario@cnr.it,

<sup>2</sup>alvise.miozzo@cnr.it,

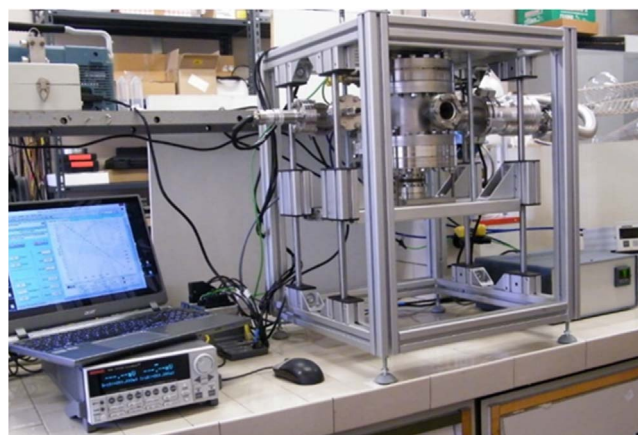
<sup>3</sup>stefano.boldrini@cnr.it

**Status.** In the nearly two centuries of thermoelectric (TE) modules history, the only real hindrance to the large scale diffusion of this technology for electrical generation was its limited efficiency: generally, in real world thermoelectric generators (TEGs) applications, less than 5% thermal energy is converted into electric power. Aside material improvements, the other way to increase efficiency is to deploy larger thermal gradients. Unfortunately, with some recent possible exceptions [143], high temperature TE materials did not prove the possibility to achieve significantly higher conversion efficiencies, since each material could possess an important thermoelectric figure of merit only within a specific temperature range. The traditional way to overcome this issue is the use of multiple materials, each working at or near its optimal temperature [144]. Despite higher technological barriers, this idea has been followed with two main approaches: segmented (or functionally graded) legs and cascade modules. In the former, two or more materials are integrated in a single leg, while in the latter two or more TE modules are arranged thermally—and generally electrically- in series [145]. This configuration is regarded as more efficient than segmenting and simpler from the construction point of view, but it is considered problematic in its implementation [146].

Whilst the panorama of low temperature (up to about 500 K) TEG has been somehow frozen for decades on calcogenides, intermediate range of temperature, despite several material families with interesting performances [147], still lack of commercial grade TEG.

This deficiency is of course motivated by more relevant technological issues (the need for expensive brazing alloys, chemical diffusion at interfaces, gap in thermal expansion between n and p legs, just to mention a few), but it is mainly caused by the lack of improvement in conversion efficiency of intermediate temperature materials with respect to low temperature materials. It is generally worthless to employ a high temperature source if a comparable output power could be produced at lower temperature. This can be clearly overcome by cascade generator configuration.

**Current and future challenges.** The quest for a cascade TEG configuration passes through the availability of reliable intermediate temperature TEG, but it is not limited to this. Several issues in TEG design should be faced. Working temperatures of different stages should not only be optimized, but they have to meet materials limitation in all possible



**Figure 11.** Test station for the complete characterization of TE module at intermediate temperature up to 900 K.

operating conditions, to avoid failures or degradations due to overheating. Device testing is also crucial to assess performance and reliability of TEG. Despite improvements for low temperature range [148], to the best of our knowledge no round-robin or assessed test procedure have been developed for intermediate temperature test. Even the maximum power point tracking and operating conditions of cascade modules have been barely explored. While efficiency improvement is crucial to lower the energy final cost (€/Wh), device cost plays a fundamental role for the installed power cost (€/W). For this reason, the widespread use of TEG requires low materials and fabrication costs. In this direction innovative material sintering routes, like Cold Sintering Process (CSP) [149] or Ultrafast High-temperature Sintering (UHS) [150], and the study of novel brazing alloys and procedures could be the keys to TEG cost reduction.

Among all technical challenges, the design of a device requires an adequate modelling. Since in most cases no analytical solution can be found, numerical procedures must be used. Discretization techniques such as Finite Element [151] or Finite Volumes Methods [152] provide an efficient design tool. In particular, the first one can be employed for the evaluation of every step of device realisation, from sintering operations to the final assembly in its operating conditions, taking into account all involved flux contributions.

An important issue in the implementation of a large temperature gradient TEG is also the control of the operating point of each module of a cascade device. This could be achieved, on the one hand, with a correct design assisted by numerical simulation, and, on the other hand, with a smart electronic control of the load to optimize the output power.

**Advances in science and technology to meet challenges.** In the last years, in our group several intermediate TE materials were studied and functionally characterized [153], like Mg<sub>2</sub>Si [154], higher manganese silicides, Ca<sub>3</sub>Co<sub>4</sub>O<sub>9</sub>, SnSe [155], TiNiSn (see section 2.2), Yb-Co<sub>4</sub>Sb<sub>12</sub>, Co<sub>2</sub>(Zr, Hf)Sn [156] and others.

Testing of intermediate TEG is crucial, both to assess their performance and in the view of an integration with lower

temperature stages. We developed a test station (figure 11) able to perform test (both electrical and heat flux measurements) on large TEG, with hot side temperature up to 600 °C [157]. This will allow to explore multistage generators under various boundary conditions (constant temperatures, constant heat flux) and environmental conditions (applied pressure, atmosphere).

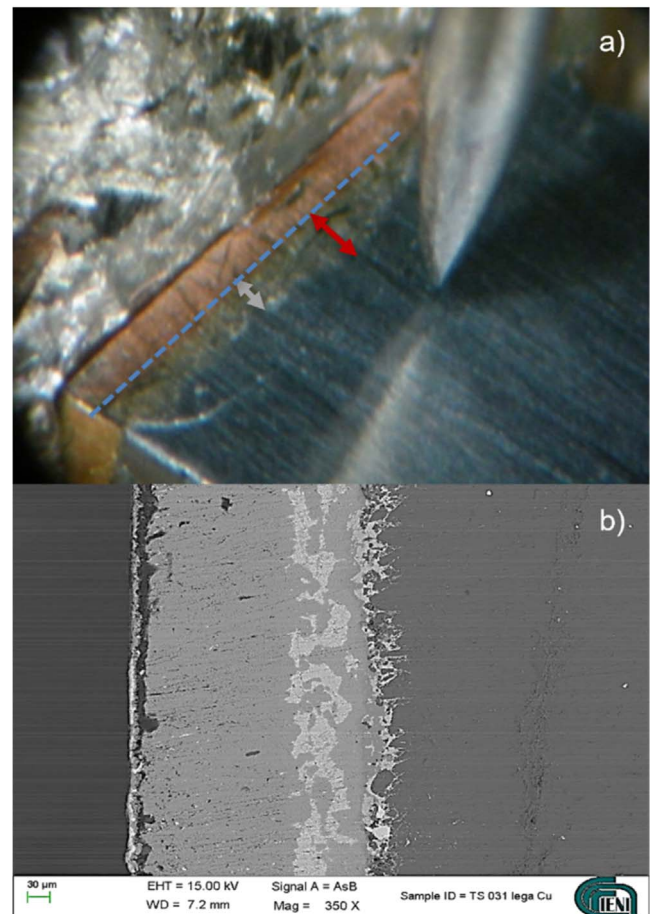
The study of low-cost materials and synthesis, together with low energy processing and sintering techniques, as the aforementioned CSP and UHS, will contribute to pave the road to a more convenient, diffuse and environmental friendly thermoelectric technology.

A key point to the realization of a cascade device is the feasibility of assembly procedures. In this perspective, it is possible to take advantages of the developed test station to braze multiple TE couple and simple TE module on both hot and cold side. The choice of a proper brazing alloy, and module configuration of legs and insulating materials, is still an open issue in order to obtain reliable mechanical coupling, thus avoiding stresses under thermal cycling.

Chemical interdiffusion and the presence of different layers between TE materials and electrodes can lead to a poor electrical contact resistance. To guarantee optimal conversion efficiency, this parasitic resistance must be as low as possible, in the order of  $10^{-5}$  to  $10^{-6}$   $\Omega$  cm<sup>2</sup>. Nowadays, scanning probe measurement techniques can be employed to access the Ohmic or Schottky properties of metal-semiconductor interfaces [158], to optimize brazing materials and procedures. These techniques also allow for highlighting interdiffusions areas and cracks (figure 12).

Fast numerical procedures, already implemented for a single module [159], could help to investigate the properties of segmented or cascade configuration. 1D discretization of energy balance for thermoelectric materials (Domenicali's equation), with constitutive relation for thermal flux [152, 160], can lead to a basic evaluation of a thermoelectric device performances in classical boundary conditions, still taking into account temperature-dependent properties. Suitable code can be developed, for example in Matlab® or Python, to evaluate multi-stage TEG modules considering different currents of each stage of the device.

*Concluding remarks.* Despite its huge potentiality, the diffusion of thermoelectricity for power generation will require the TEG efficiency increase and the device cost reduction.



**Figure 12.** (a) Scanning probe electrical measurement used for the evaluation of the electrical contact resistance. This technique also allows for the detection of interdiffusion layers. (b) SEM image of silver interdiffusion in Mg<sub>2</sub>Si material after brazing.

These objectives could be achieved through TEG in a cascade configuration, as a result of material and processing cost reduction, and improving the device and systems design routes with suitable numerical tools. Regardless of the challenges, dedicated fabrication and characterization techniques have proven to be effective in the realization of TE cascade modules.

A holistic approach over these aspects could be a necessary complement to fundamental research in order to promote the transition of this technology from niche applications to a significant role in power generation.

## 9. Nanostructured silicon devices for thermoelectric applications

Giovanni Pennelli\*, Elisabetta Dimaggio\*\*

Dipartimento di Ingegneria dell'Informazione      Università  
di Pisa      Via Caruso 16, I-56122 PISA

\*[giovanni.pennelli@unipi.it](mailto:giovanni.pennelli@unipi.it)

\*\*[elisabetta.dimaggio@unipi.it](mailto:elisabetta.dimaggio@unipi.it)

**Status.** Direct thermal to electrical energy conversion with compact, low-cost and reliable devices, based on thermoelectric phenomena, offers interesting perspectives in the fields of energy recovery/energy harvesting; energy scavenging for the supply of small, wireless, electronics, such as sensor nodes, through hot surfaces; heat pumping/cooling and micro-cooling for localized temperature control [161–166]. Despite these very interesting applications, the use of thermoelectric devices is still strongly limited by the materials available for their fabrication: very few semiconductors show high Seebeck coefficient and electrical conductivity, and simultaneously have a low thermal conductivity, and unfortunately most of these semiconductors are based on tellurium, which is a rare and poisoning element. The selection of materials for the fabrication of devices should not be driven only by the criterion of optimal thermoelectric parameters, but at first by its abundance and sustainability, and then on the basis of fundamental technological aspects, as for example the ease of doping both  $n$  and  $p$  type, the possibility to make good ohmic electrical contacts, the possibility of making lithography/etching and other technological steps necessary for the on-chip integration, fundamental in particular for scavenging applications and for the direct supply of electronic circuit.

In all these aspects, silicon is in our vision the winner material in front of many others [166–168]. Earth's crust is made principally of silicon compounds: silicon comes from sand. From the technological point of view, silicon is at the top of a world wide network of fabrication industries (silicon-foundries), which support the strong and evenly increasing market of electronic devices: we can dare to say that silicon is the best known material from all the physical, chemical and technological aspects.

From the point of view of thermoelectric parameters, silicon shows a very high Seebeck coefficient and electrical conductivity, which can be tailored by an accurate calibration of the doping concentration [166]. The main drawback is its high thermal conductivity ( $148 \text{ W (m K)}^{-1}$ ) which is comparable to that of aluminium. However, over a decade of experimental and theoretical studies [169–171] have largely demonstrated that the thermal conductivity can decrease well below  $10 \text{ W (m K)}^{-1}$  when the phonon transport, mainly responsible of the thermal conductivity, is confined in nanostructures, such as nanowires, narrower than 100 nm.

Hence, in addition to its abundance, biocompatibility and technological feasibility, silicon, when nanostructured, is an excellent thermoelectric material: a combination that can be

disruptive for large scale applications of thermoelectric devices [172].

**Current and future challenges.** The strong reduction of thermal conductivity in silicon nanostructures has been measured from many research group, both in nanowires [168, 169] and in very thin nanomembranes [170]. The thermal conductivity suppression increases with the roughness of the surfaces [170, 171]: this confirms that the phonon scattering on the nanowire walls, which is strongly affected by the surface status, plays a fundamental role. Even if this is a well assessed fact, further theoretical and experimental activity is still required in order to establish clear 'phonon engineering' strategies relating technological steps for the modification (roughening) of the surfaces and thermal conductivity reduction.

As the Seebeck coefficient  $S$  decreases with doping concentration, and the electrical conductivity  $\sigma$  increases, the optimum doping concentration must be found as a trade-off to maximize the power factor  $S^2\sigma$ . To this end, doping concentrations higher than  $10^{19} \text{ cm}^{-3}$ , either  $n$  or  $p$ , must be considered [166].

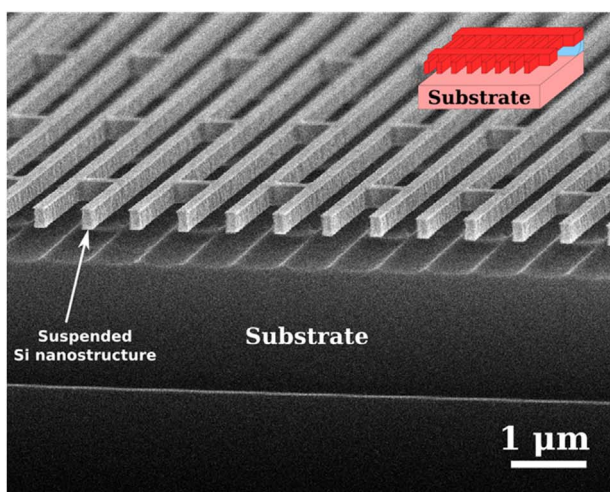
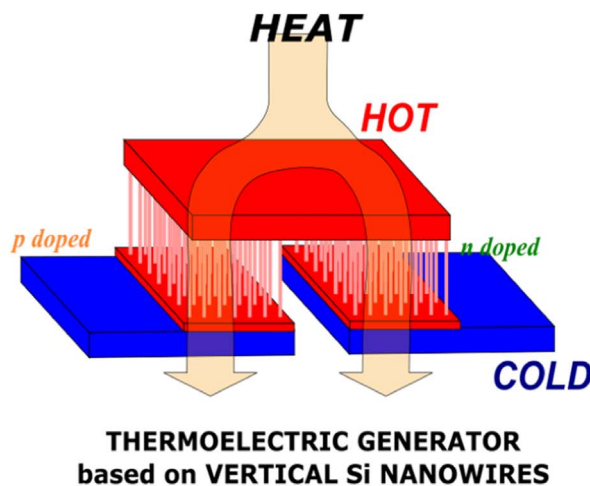
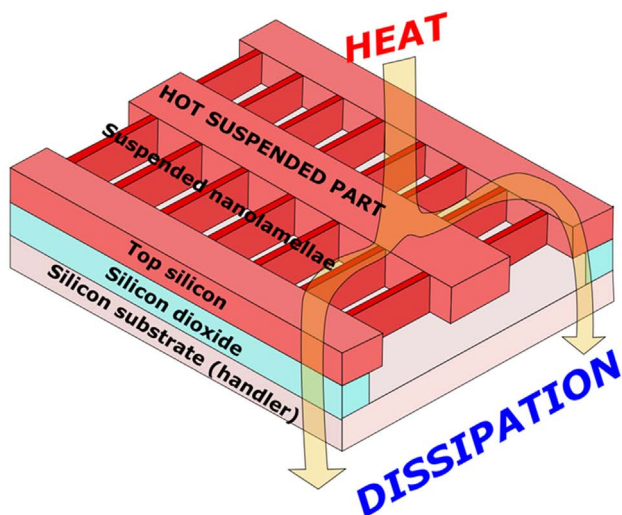
Theoretical studies showed that  $S$  increases in nanowires narrower than 5 nm. However, in so narrow structures the electrical transport, as well as the thermal transport, would be strongly penalized by the surface scattering. A possible via for the increasing of the power factor, yet maintaining a good electrical conductivity, is the energy filtering of electrons through a succession of very thin potential barriers [173].

The principal advantage in the use of nanostructured silicon remains the reduction of the thermal conductivity. A width narrower than 100 nm is sufficient for a strong reduction of the phonon conduction; instead, for heavily doped silicon, the electrical conductivity begins to decrease in nanowires narrower than 40 nm. Therefore, the parameters useful for thermoelectric devices based on nanostructured silicon are: width between 40 and 100 nm (the 'thermoelectric range'), doping concentrations higher than  $10^{19} \text{ cm}^{-3}$ .

The main point for the use of nanostructured silicon for thermoelectric devices is to go beyond the experimental devices developed for the measurement of the thermal and electrical transport, which are typically based on one (or very few) nanowires. The technological challenge to reach practical applications is related with the development of techniques that allow the fabrication of large collections of silicon nanowires, or of thin silicon nanomembranes; these collections must be doped, interconnected in a suitable way, and the design of the device must be optimized to allow the maximum temperature difference between the hot and the cold part.

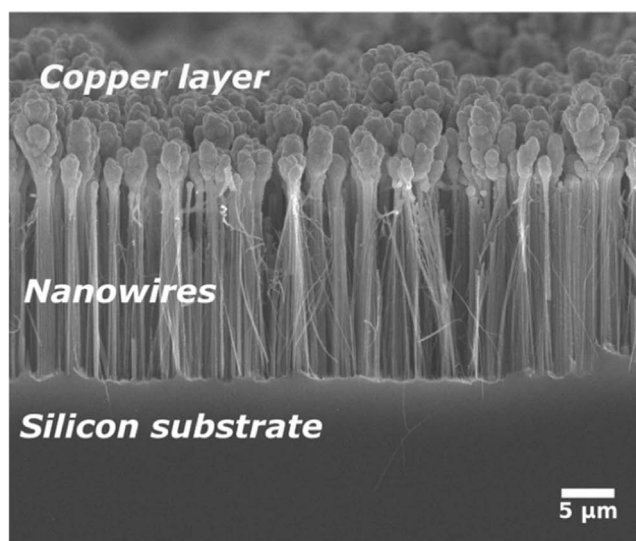
**Advances in science and technology to meet challenges.**

Large collections of silicon nanowires and/or of nanostructures can be fabricated by means of top-down processes based on high resolution lithography and etching [174, 175]; doping and metal interconnections can be defined by standard IC processing.



**Figure 13.** Suspended nanostructures, bridging large silicon platforms acting as heat collector/heat dissipator. The heat paths must be accurately designed to allow the maximum temperature drop between the ends of the nanostructures. On the top: a pictorial sketch of a thermoelectric device. On the bottom: a SEM image of fabricated suspended Si nanostructured.

The main issue of the lithography/etching approach is that it relies on surface fabrication (typical of IC technology), hence this strategy is suitable for the fabrication of large collections of nanostructures parallel to the surface of a silicon substrate. This implies that they need to be suspended (insulated), to avoid the parallel conduction of heat through the substrate itself. A possible via is to fabricate parallel nanostructures bridging suspended Si platforms (figure 13), achieved by MEMS techniques and used as heat collectors [176, 177]. Even if e-beam lithography has been used for the fabrication of prototypes, the ‘thermoelectric range’ is well within the capabilities of advanced optical lithography, so that these devices are fully compatible with standard MEMS/CMOS technologies. The total surface of these MEMS-NEMS thermoelectric generators is anyway quite small (few  $\text{mm}^2$ ), hence their main target of application is the conversion of small quantity of energy (scavenging). They can be combined, in a multi-chip single-packaging approach, for the



**Figure 14.** Thermoelectric generator based on forests of vertical silicon nanowires (perpendicular to a silicon substrate). On the top: a pictorial sketch of a device, based on two forests, *p* and *n* doped, connected through the top copper layer. On the bottom: a SEM image of a silicon nanowire forest, contacted on the top through an electrodeposited copper layer.

direct powering of small electronic circuits, such as sensor nodes, exploiting any available heat surface.

Large scale energy harvesting requires thermoelectric devices with large surfaces, comparable to those of photovoltaic. To this end, cheap (and hence lithography-free) and reliable nanostructuring processes are needed. We developed Si-based thermoelectric generators made of large collections of vertical silicon nanowires: more than  $10^7$  nanowires, narrower than 80 nm and taller several hundred of micrometers, can be simultaneously fabricated by a Metal Assisted Etching process (MACE) [178–180], see figure 14: it consists in soaking a silicon substrate (wafer) in a diluted solution of HF and Silver Nitrate. Electrical and thermal contact can be fabricated by copper electrodeposition [179]. The nanowire diameter has a spread because the etching process is random, but the process parameters (temperature, reagent concentration and time) can be tailored so that the average value and

dispersion make most of the nanowires within the ‘thermoelectric range’. The MACE process requires low doped silicon, but nanowire forests can be doped after their fabrication by standard diffusion techniques [180].

Thermoelectric generators based on nanowire forests have been fabricated and tested: this process has reached its maturity as laboratory testing, and it is ready for the industrialization.

*Concluding remarks.* When nanostructured, silicon shows excellent thermoelectric parameters, in addition to its abundancy (bringing to low-costs devices), biocompatibility and technological readiness. The use of silicon for direct conversion of heat into electrical power can bring important break-throughs for a large number of thermoelectric applications, which currently are limited due to the lack of sustainable and low-cost materials. Of course, even starting

from the strong technological base of silicon, a large amount of experimental and technological work is still required to bring the thermoelectric silicon to the level of practical applications. Well assessed MEMS/NEMS technologies can be exploited for the production of thermoelectric devices made of suspended Si platforms bridged by silicon nanostructures. The path to commercial device requires the development of techniques for the connection of these suspended (and very fragile) Si platforms to the cold and hot heat sources.

The exploitation of a cheap fabrication process (MACE) for making large numbers of vertical, high aspect ratio, silicon nanowires (silicon nanowire forests), which can then be doped and connected by copper electrodeposition, has been demonstrated on a laboratory scale, and it is ready for being implemented in an industrial pilot line.

## 10. Solution processable organic thermoelectric materials and devices

Marcello Franzini<sup>1</sup>, Simone Galliano<sup>2</sup>, Claudia Barolo<sup>1</sup>, Saeed Mardi<sup>3,4</sup>, Andrea Reale<sup>3</sup>

<sup>1</sup>Department of Chemistry, NIS Interdepartmental Centre and INSTM Reference Centre, Università degli Studi di Torino, Via Gioacchino Quarello 15A, Torino 10135, Italy; marcello.franzini@unito.it (M.F.); claudia.barolo@unito.it (C.B.)

<sup>2</sup>Department of Agricultural, Forest and Food Science, INSTM Reference Centre, Università degli Studi di Torino, Largo Paolo Braccini 2, Grugliasco 10095, Italy; simone.galliano@unito.it

<sup>3</sup>CHOSE - Centre for Hybrid and Organic Solar Energy and Department of Electronic Engineering, University of Rome Tor Vergata, 00133 Rome, Italy; reale@uniroma2.it

<sup>4</sup>Laboratory of Organic Electronics (LOE) Department of Science and Technology, University of Linköping, Bredgatan 34, Norrköping 581 83, Sweden; saeed.mardi@liu.se

**Status.** Numerous TE materials with a ZT of >1 have been reported in the past decade. Nevertheless, many high-performance inorganic TE materials work at high temperatures whose are typically expensive, brittle, and heavy and contain toxic elements such as Pb, Bi, and Te.

Even though the temperature range of most industrial waste heat sources is between 500 K to 900 K, most of the waste heat is exhausted at temperatures below 400 K [181]. However, there are not many suitable options to recover heat below 400 K, and as such only Bi<sub>2</sub>Te<sub>3</sub> has been shown to be a promising candidate. Organic TE (OTE) materials have newly been received a great interest among the researchers because of several advantages, such as, mechanical flexibility, low material cost, light weight, low toxicity and increased sustainability (organic materials are synthesized and not extracted from the earth and the final device might end to be potentially biodegradable or recyclable), which make them promising candidates for a new generation of near-room-temperature TE materials.

Despite the benefits of organic TE materials, their limited TE performances have affected their practical applications, especially regarding *n*-type semiconductors. However, in the last decade, significant progresses have been reported in developing high-TE-performance organic materials and their ZT has been significantly improved. Up to now, the highest reported ZT value among organic materials is 0.75, which was reported by Fan *et al* in 2018 [182]. Moreover, there are many reports which showed remarkably high-power factors (more than 1000  $\mu\text{W mK}^{-2}$ ) [183]. This trend shows the improving of the TE performance of organic materials and they are getting close their inorganic counterpart. Moreover, the advantages in material cost and scalability make them competitive in various applications [184].

**Current and future challenges.** One of the most important challenges in the field of OTE materials is the manufacturing of the device for everyday applications. Although there is a

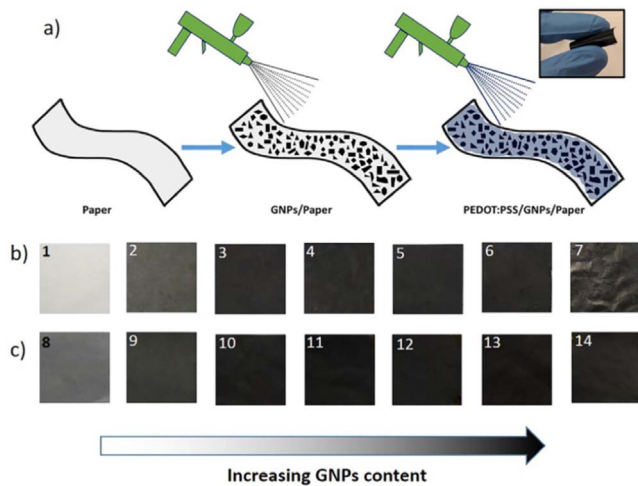
huge progress in the ZT and power factor, these materials require the overcome of practical technological issues for real applications, such as suitable thickness control for 3D device design and scalable and economical fabrication methods. An example of these efforts can be found in [185, 186] (see figure 15). Another important challenge in OTE is to obtain *n* type materials to realize p-n modules. Most of *n* type materials exhibit poor air stability, low electrical conductivity and poor *n*-doping yield. Besides, tremendous progresses have been made and their ZT has been boosted. Promising routes can be found in printable *n*-type mixed ion-electron conductor [187], in the design of new *n*-type conjugated polymers, more efficient *n*-dopants, and doping engineering [188]. Using novel *n*-type dopants which enhance the electrical conductivity without disturbing the morphology of the host polymer is another strategy [189].

Concerning organic semiconductors, the improvement in the crystallinity and charge carrier mobility could alter the slope of the density of states (DOS) near the Fermi level, and thus it is possible to improve Seebeck coefficient and the charge carrier mobility simultaneously. The increase of the charge carrier concentration by doping process and the improvement of the morphology and structure of polymer for increasing the mobility affects the power factor. Regarding to thermal properties, polymers do not conduct heat properly, with thermal conductivity usually less than 0.5  $\text{W m}^{-1} \text{K}^{-1}$ . Heat carriers in conductive polymers include both phonons and charge carriers. However, the electronic part of thermal conductivity is much smaller according to the Wiedemann–Franz law, and is proportional to the electrical conductivity. Therefore, the phononic contribution to thermal conduction is much larger and the thermal conduction in polymers is generally recognized by phonons. Unlike the metals, the improvement of in electrical conductivity would therefore not lead to an enhancement in the thermal conductivity. Given the importance of thermal conductivity on ZT value, the thermal properties of organic materials are desirable for TE applications. It should be noted that from practical points of view, the measure of thermal conductivity is challenging and difficult especially in thin films, due to heat conduction through the substrate, radiation loss, and thermal contact resistance [190], however the power factor value already provides enough insight on the TE properties of polymers.

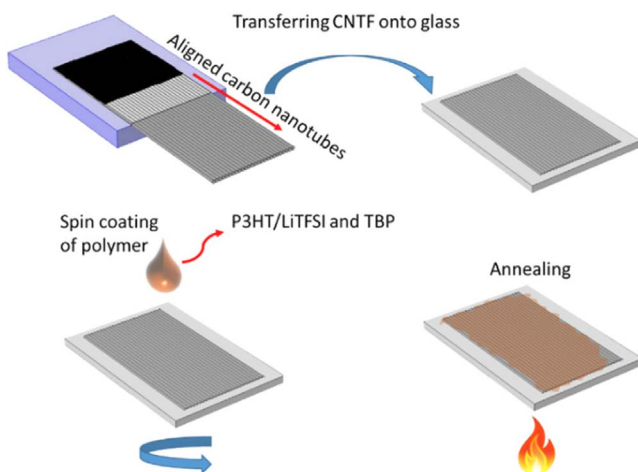
### *Advances in science and technology to meet challenges.*

The integration of polymers with low dimensional fillers is a facile and efficient approach to improve the TE properties of polymers. The fillers are usually carbon-based materials or inorganic-based materials. The most common fillers are carbon nanotubes [191] (see figure 16), graphene sheets [185, 186], Bi<sub>2</sub>Te<sub>3</sub> nanowires [192], SnSe [193], and tellurium nanowires [194].

Due to the interdependence of the Seebeck coefficient and electrical conductivity, the increasing of the electrical conductivity would decrease the Seebeck coefficient. However, in the composite there are two phase-separated parts filler-rich and polymer-rich [195]. So, the electrical



**Figure 15.** (a) Sample preparation process for PEDOT:PSS/GNPs/paper composite: biopolymer/GNP inks sprayed on paper substrates, and conducting polymer solution sprayed on top of them. On the top right, there is the photograph of the most conductive composite bent. Photographs of (b) GNPs/paper samples (with the indexes of 1–7) and (c) PEDOT:PSS/GNPs/paper samples (with the indexes of 8–14) with different GNP contents. Reproduced from [186]. © The Author(s). Published by IOP Publishing Ltd. [CC BY 4.0](#).



**Figure 16.** Sample Preparation Process for P3HT/CNTF Composites. Reproduced from [191]. [CC BY 4.0](#).

conductivity of the composites could be decoupled from the Seebeck coefficient to enable a simultaneous increase of both parameters. Another benefit of the polymer composite is the minor variation in thermal conductivity when the electrical conductivity increases. The phenomenon behind the low thermal conductivity of the composite is the existence of the interfaces between fillers and polymer. These interfaces can increase the phonon scattering rate, so the phonon transport would suppress and it ensures the low thermal conductivity of composite.

Carbon nanotubes (CNTs) are one of the fillers which are drawn a lot of interest for TE applications especially the composite of CNTs and organic materials exhibit high

electrical conductivity, without significantly increasing the thermal conductivity. CNTs possess several advantages including: (1) depending on the structure CNTs can have different band gaps, (2) due to one-dimensional structure quantum confinement effects,  $S$  and  $\sigma$  could improve simultaneously, and (3) due to their mechanical properties the lightweight and flexible TE devices could be developed. The reason for low thermal conductivity of the composite is the existence of the interfaces between fillers and polymer, which suppresses phonon transport [196]. There are several reports about the correlation thermal and electrical properties and they confirmed that loading of CNTs in organic materials leads to an enhancement of electrical conductivity, without the significant growth of the thermal conductivity [197]. Simultaneous improvement of the Seebeck coefficient and electrical conductivity was also reported [195, 198]. Using organic and inorganic conductive fillers is a powerful tool for the design [199] of composites of polymers as an efficient approach to decouple the TE parameters for increasing the ZT values [200].

**Concluding remarks.** Organic thermoelectric materials allow a facile, scalable, and reproducible method to fabricate efficient printable TE devices using both chemical and physical doping strategies. TE device can be manufactured using spray coating, blade coating or other printing process, enabling to produce thick, lightweight, flexible, and wearable devices. Interestingly, compositing the organic semiconductor and the conductive filler can lead to a simultaneous increase in the Seebeck coefficient and electrical conductivity.

The morphological characterization shows that despite common approaches, including for instance the physical blending of CNTs and P3HT into a solvent, the deposition of the polymer can leave the aligned morphology of CNT unaltered. This can be exploited for improving the electrical properties of the composite.

A promising direction to further improve the TE properties of both  $p$ - and  $n$ -type materials, is the investigation of different additives, treatments and doping methods. For example, to keep the morphology intact, the postprocessing approaches such as the introduction of the dopant from the vapor phase or immersion in the dopant solution could also be used as alternative to improve the electrical properties of the organic semiconductor.

These organic composites also show bending stability at different angles and remarkable environmental stability at ambient conditions, confirming their suitability for applications in portable and flexible devices.

**Acknowledgments.** AR acknowledges the partial financial support from the Department of Electronic Engineering of the University of Rome Tor Vergata under the project ‘AIDED - Progetto di Ricerca Dipartimentale’. MF acknowledges the support of Martur Italy srl.

## 11. Towards an effective thermoelectric hybridization of photovoltaics

Bruno Lorenzi<sup>1</sup>, Dario Narducci<sup>2</sup>

Department of Materials Science—University of Milano Bicocca Via R. Cozzi 55, 20125 – Milano, Italy  
[<sup>1</sup>bruno.lorenzi@unimib.it, <sup>2</sup>dario.narducci@unimib.it]

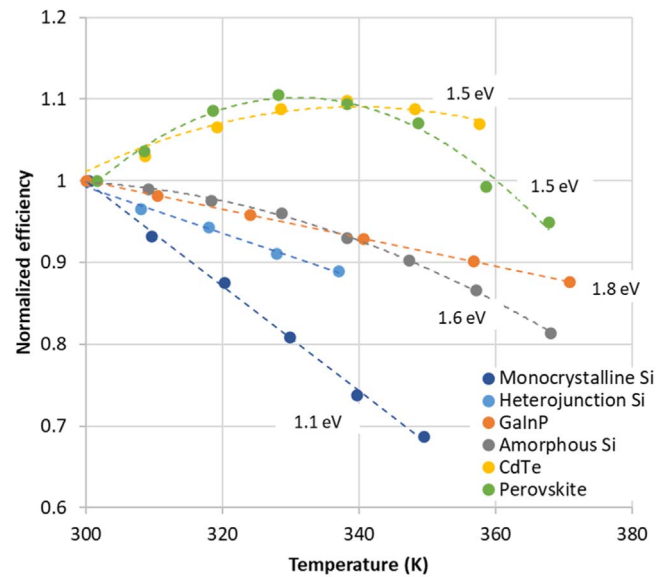
**Status.** Paradoxically enough, solar cells are more efficient at converting solar power into heat than into electricity. The physics of the photovoltaic (PV) effect limits the efficiency of single-junction PV panels to a maximum of  $\approx 30\%$ . Of the remaining 70%, the vast majority is lost as heat. In addition, Silicon-based solar cells, which dominate the PV industry, are extremely sensitive to temperature, with Si-based PV panels losing up to 15%–20% of their room temperature efficiency under normal operating conditions [201]. For this reason, heat recovery strategies have a great potential in the field of solar harvesting. Among the solution proposed, thermoelectric hybridization is very promising. In this approach, a thermoelectric generator (TEG) is implemented to harvest the heat generated within the solar panel to produce additional electrical power. This in turn enhances the overall conversion efficiency of the system.

Two main strategies have been proposed for the thermoelectric hybridization of PV. The first, referred to as *optical coupling*, makes use of a beam splitter to direct the visible part of the solar light towards the solar cell, while the infrared part is addressed towards the TEG part. The second approach consists instead of the direct *thermal coupling* between the PV and TEG devices, and normally sees a TEG placed at the back side of the solar cell. In recent years it has been widely demonstrated how thermal coupling is the most efficient approach, as it can access the whole spectrum of heat losses occurring in the PV section, instead of only their infrared part [202, 203]. However, over the last decade the opinion on the effectiveness of the thermoelectric hybridization of solar cells has been rather swaying. Some studies reported very high efficiency gains [204, 205] while others casted doubts on the possibility of increase the efficiency of solar cells by hybridization [206, 207]. We report our contributions to clarify the key elements that set the convenience of thermally coupled hybridization, also discussing the main challenges and the recent advances in the field.

**Current and future challenges.** The overall efficiency of hybrid thermoelectric-photovoltaic (HTEPV) devices can be written as

$$\eta_{h tepv}(T) = \eta_{pv}(T) + \eta_{ot}(T) \eta_{teg}(T), \quad (2)$$

where  $\eta_{pv}(T)$  and  $\eta_{teg}(T)$ , are respectively the PV and TEG efficiencies, while  $\eta_{ot}(T)$  is the so-called opto-thermal efficiency, namely the efficiency with which the system converts solar power into heat flowing through the TEG. Note that all these efficiencies are functions of temperature. To this extent the biggest challenge when trying to combine PV and



**Figure 17.** Normalized efficiency of various type of solar cells versus temperature. The value of the energy gap of the absorbing material is reported next to the traces. All the data were measured by the authors except for the case of heterojunction silicon solar cell extrapolated from [210].

TEG devices consists in the opposite behaviour of their efficiency versus temperature. While the efficiency of a TEG increases by increasing the working temperature of its hot side (considering the cold side set at room temperature) a solar cell displays the opposite trend. In general, the temperature sensitivity of PVs is a well-known and substantiated problem, and for the case of hybrid systems it is a key parameter determining its profitability. The physics of heat losses in solar cell has been only recently fully analysed [208, 209], showing that the energy gap of the absorbing material plays a fundamental role in the temperature sensitivity of solar cells. It could be shown how the efficiency of wide gap-solar cells is much less sensitive to temperature compared to small or mid-gap solar cells. This behaviour is displayed in figure 17 where the normalized efficiency of single-crystalline silicon solar cells is compared to that of various wide-gap solar cells. The plot also reports the peculiar cases of amorphous silicon (a-Si), Cadmium Telluride (CdTe), and perovskite solar cells (PSCs), which exhibit a non-linear behaviour, leading in some cases to an efficiency increase with temperature. Another interesting behaviour is found in heterojunction silicon (HJ-Si) solar cells for which the presence of several a-Si layers mitigates the temperature sensitivity of Si-based PV [210]. In all these systems, but especially in the cases of HJ-Si, perovskites, and their combination in tandem devices, are the most promising candidates for an effective thermoelectric hybridization of PV.

Recently the energetic and economic profitability of perovskite-based hybrid devices was demonstrated by several research groups [211–215]. The effectiveness is remarkable especially for optically concentrated systems for which the higher solar input increases the recoverable heat load while decreasing the temperature sensitivity of  $\eta_{pv}$ . Optical



concentrations up to 5 suns seem the most profitable option since they do not require extreme temperatures and/or extensive maintenance, and can be implemented without tracking systems. In these cases, a 3%–4% efficiency enhancement has been demonstrated.

*Advances in science and technology to meet challenges.*

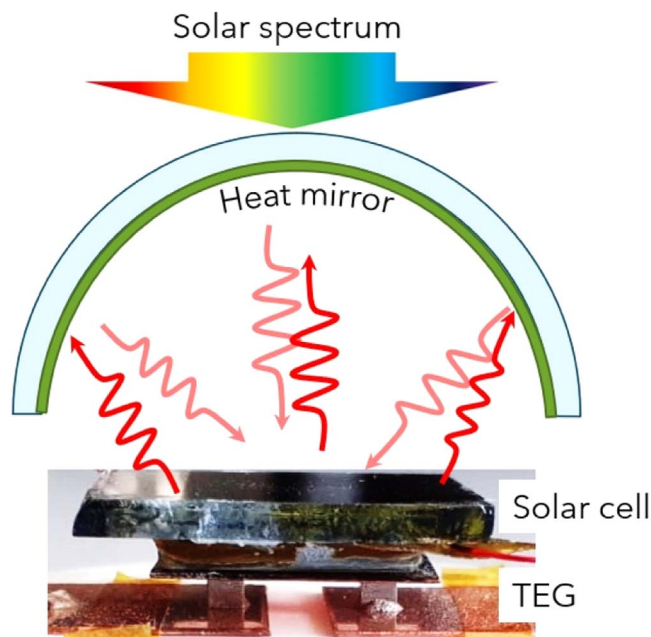
Even if the effectiveness of HTEPV systems has been demonstrated, advances are still needed to make them a valuable commercial solution:

*Stability:* as PSCs are the best candidates for hybridization with thermoelectrics, their stability up to 350 K remains a key issue. The effort being deployed promises stabilized PV cells to become available in the next few years [216].

*Optimized TEG thermal resistance:* optimal working temperatures for hybrid systems implementing PSCs fall near 340 K. Luckily, this is the same range of temperatures where commercial TEGs based on  $\text{Bi}_2\text{Te}_3$  are more efficient. However, as showed by several scholars, the thermal resistances of commercial TEGs are much smaller than those needed in HTEPV devices [217, 218]. Better matching requires TEGs with a smaller density of legs. Even though such low filling factors do not display any technological hurdle, still TEGs of this type are not yet commercially available.

*Encapsulation:* maximal HTEPV efficiency gain requires the minimization of heat exchanges with the environment. Ideally, the heat generated in the solar cell should flow entirely by conduction through the TEG. In real situations, instead, convective and radiative heat dissipation, especially from the solar cell top surface, occur. Thus, HTEPV encapsulation within e.g. evacuated pipes is required. In addition, strategies to reduce radiative heat losses are also necessary. A possible solution is to implement Heat Mirrors (HMs), reflecting the radiative emission of the solar cell back to the system (figure 18). To be effective a HM should display high transparency for the solar spectrum and high reflectance in the infrared range where most of the emission takes place [219]. Transparent Conductive Oxides natively report good HM properties. Nevertheless, material optimization and validation of the effective efficiency enhancement are required with reference to the specific system characteristics.

*Heat dissipation:* as a rule of thumb, realistic thermoelectric hybridizations can bring to a maximum of 5% efficiency enhancement. This means that the hybridization of a solar cell with 25% efficiency, can lead to a maximum total efficiency of 30%. For this reason, in HTEPV devices a large amount of heat ( $\approx 600\text{--}700 \text{ W/m}^2$ ) must be dissipated at the TEG cold side. In this perspective, proper heat dissipation strategies must be implemented. The easiest solution is to use a fluid. As a result, with proper engineering the warm water exiting the systems can be



**Figure 18.** Schematic of a HTEPV system implementing a HM able to reflect radiative heat losses towards the system.

employed for sanitary/domestic uses, enabling solar tri-generation.

*Concluding remarks.* Thermoelectric hybridization of solar cells is a viable solution that can turn the problem of heat generation in solar cell into an opportunity of efficiency gain. Unfortunately, hybridization of common silicon solar cells with commercial TEG do not promise any significant improvement. PV materials with low temperature sensitivity, such as wide-gap solar cells, must be chosen to be hybridized with thermoelectrics. In addition, TEG with higher thermal resistance than those commercially available must be fabricated. As mentioned, the thermoelectric hybridization of perovskite solar cells has been demonstrated to be energetically and economically feasible, when properly engineered. This can be a possible seed for a near future commercialization of HTEPV systems. Additional optimization remains possible, including the implementation of suitable heat mirrors. Furthermore, effective heat dissipation systems must be engineered and economically evaluated. Testing of such components must be planned for the next few years, to make the hybridization strategies ready when the stability of perovskite solar cells will be mature enough to make them commercially available.

*Acknowledgments.* This project has received funding from the European Union's Horizon 2020 research and innovation program under the Marie Skłodowska–Curie grant no. 745304.

## 12. Advances and challenges in low-dimensional halide perovskite thermoelectrics

Vanira Trifiletti<sup>1</sup>, Silvia Milita<sup>2</sup>

<sup>1</sup>Department of Materials Science and Solar Energy Research Center (MIB- SOLAR), University of Milano-Bicocca, Via Cozzi 55, I-20125 Milan, Italy; vanira.trifiletti@unimib.it.

<sup>2</sup>Institute for Microelectronics and Microsystems (CNR- IMM), Via Piero Gobetti 101, 40129 Bologna, Italy; milita@bo.imm.cnr.it.

**Status.** The 3D halide perovskites have been successfully used in photovoltaics, lasers and light-emitting diodes thanks to their versatility and excellent optoelectronic properties [220]. Since their thermal conductivity is extremely low, they have been investigated also as thermoelectric materials. A ZT of 2 has been predicted, but the maximum demonstrated value is one order of magnitude lower [221]. This ZT value is that one reached by commercial thermoelectric materials at 650 °C [222]. Since the thermoelectric industry is nowadays seeking new materials operating at temperatures minor than 150 °C, hybrid perovskites are attracting increasing attention. The thermoelectric technology could compete with other heat engines, but to do so the ZT should be at least doubled. This is hard to reach employing conventional materials, where the factors defining ZT (Seebeck coefficient, electrical and thermal conductivities) are interdependent. Taking advantage of the nanoscale phenomena following the charge confinement in 2D quantum-well, 1D quantum-wire or 0D quantum dot structures, the variables on which ZT depends can be decoupled [223]. The thermal conductivity is reduced by the phonons scattering in the low-dimensional lattice. The Seebeck coefficient, or thermopower, is increased and reaches the highest value when the energy levels are discrete (figure 19(a)) [224]. Additionally, engineering perovskites with high stability (in air, under light and moisture exposure) is of significant importance for thermoelectrics. A possible solution is low-dimensional perovskites that have been shown to exhibit enhanced stability and lower ion migration than their 3D counterparts [221, 225, 226]. Another market requirement is that tons of self-assembly low dimensional thermoelectric materials should be easily produced. Halide perovskite can be straightforwardly sensitised at low temperatures on rigid or flexible substrates to meet the market demand. Moreover, bulk materials with 2D, 1D or 0D characters can be produced (figure 19(b)) [221, 227], even if few reports on one-dimensional thin-film have been published (they have been mostly synthesised as large single crystals) [228]. It has to be mentioned that all the compounds not having ABX<sub>3</sub> stoichiometry (where A and B are the organic or inorganic cations, and X is the halide) should be named perovskite derivatives, and often the charge is partially confined so they are called quasi-low dimensional materials [228, 229]. For the sake of brevity, here, we will imply this statement. The largest ZT value reported for halide

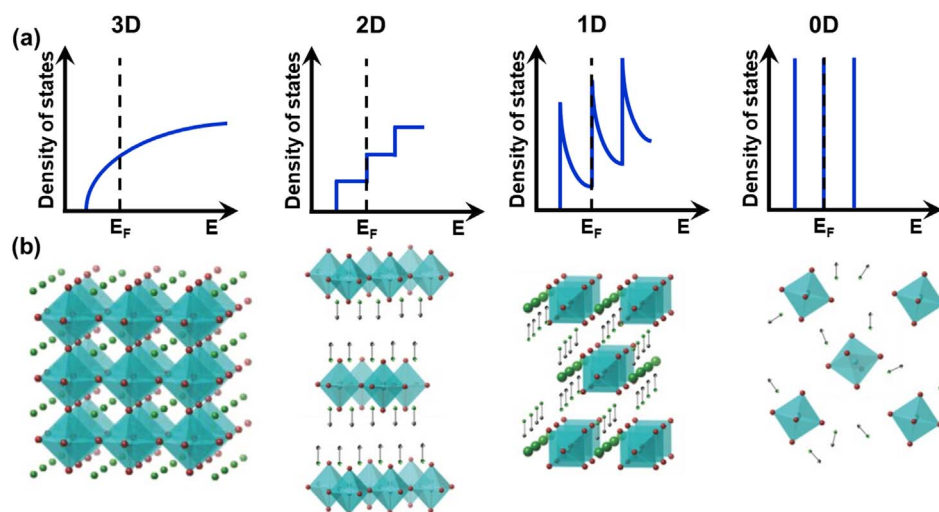
perovskites is about 0.1 (320–430 K), but the investigation for thermoelectric applications has just begun [230].

**Current and future challenges.** It has been proven that in CsPbCl<sub>3</sub> the thermal conductivity is reduced as the dimensionality moves from 3D to 0D [222, 231]. An impressive Seebeck coefficient of +2.6 mV K<sup>-1</sup> has been reported in the 0D (CH<sub>3</sub>NH<sub>3</sub>)<sub>3</sub>Bi<sub>2</sub>I<sub>9</sub>, confirming the possibility to increase the power factor with the dimensionality reduction. On the other hand, the charge confinement impacts one of the main factors, critical for thermoelectrics: the charge mobility is dramatically reduced. Therefore, low electrical conductivity is the first concern of researchers working in the thermoelectric sector [221].

- The 0D perovskite structure is composed of metal halide clusters which are so isolated by the organic or inorganic cations to enable the 0D properties. The most common structure assumed is the vacancy ordered one, with chemical formula A<sub>3</sub>B<sub>2</sub>X<sub>9</sub>, where B is the metal, X is the halide and A stands for the organic or inorganic cation. Bismuth is the preferred choice for B, considering the good chemical stability of the Bi-based perovskite compounds. Although, their filmability seems to be challenging because they have straightforward self-assembly in large crystals [221]. Studies on single crystals and pellets have reported Seebeck values of the order of mV for K but have also pointed out that the high exciton binding energy (about 300 mV) can be a serious obstacle to the generation of free charges [221].
- 1D halide perovskites suffer even more filmability issues: most of the publications on the topic concern the synthesis and characterization of large crystals, appearing as long needles, introducing limitations in the instruments that could be used for the thermoelectric investigation [228]. Moreover, among the low-dimensional perovskite family, the 1D structure synthesised until now appears to have a higher moisture sensibility compared with the 0D and 2D arrangements [228, 231].
- The 2D compounds self-assemble in layered structures, where the metal halide clusters are placed in planes spaced by the A cations' counterparts. Interestingly, the electrical properties can be enhanced, not only by doping, in a similar manner that the 3D halide perovskite, but also by altering the orientation of the inorganic layer within the material, since the electrical conductivity perpendicular and parallel to the layers can differ by many orders of magnitude [231, 232]. Despite these excellent properties, the use of 2D-perovskites as a thermoelectric material is in its infancy. Besides the self-assembly of layered perovskite management, the defects control is under intensive investigation [221, 231].

**Advances in science and technology to meet challenges.**

The preliminary results on the power factor and thermal conductivity are exciting, but the charge density has to be enhanced to push the power factor up. Extrinsic doping has



**Figure 19.** (a) A depiction of the density of states as a function of energy for materials with dimensionality corresponding to 3D, 2D, 1D and 0D. (b) Schematic representation of perovskite structures with dimensionalities 3D, 2D, 1D, and 0D; [227] John Wiley & Sons. [© 2015 WILEY-VCH Verlag GmbH & Co. KGaA, Weinheim].

been proven effective in increasing the electrical conductivity in the 3D halide perovskite [221]. Lately, some attempt has been reported also in low dimensional compounds: for example, Bi(xt)<sub>3</sub> (bismuth tri-ethylxanthate) has proven to be an effective dopant for (CH<sub>3</sub>NH<sub>3</sub>)<sub>3</sub>Bi<sub>2</sub>I<sub>9</sub> thin films, enhancing the carrier concentration of five orders of magnitude [232, 233]. These results have been reported for photovoltaic applications, so no information on how sulphur doping could enhance the thermoelectric properties are available in the literature. The 0D halide perovskite's high resistivity could be further reduced by improving the thin-film quality: the layer should be compact with a smooth surface. Lately, a two-step deposition method has been suggested as a possible way to do so: a compact BiI<sub>3</sub> layer has been thermally evaporated and it has been converted into (CH<sub>3</sub>NH<sub>3</sub>)<sub>3</sub>Bi<sub>2</sub>I<sub>9</sub> by dipping it in a 10 mg ml<sup>-1</sup> methylammonium iodide solution in isopropyl alcohol [234]. On the other hand, 1D compounds show good conductivity, but the nanowires randomly align along the layer giving poor uniformity and films hard to be implemented in a real device [235]. Deposition methods, designed on purpose, such as antisolvent vapour-assisted crystallization, have been proposed to produce an aligned array [236]. Finally, one of the biggest challenges in the preparation of quasi-2D perovskite films is the achievement of a phase pure sample, since the prepared films often consist of multiple phases, especially for compounds with a high number of layers [228]. Additionally, the orientation of the layered structures parallel to the substrate, which is crucial for thin film-based thermoelectric systems, where the lateral transport is the most relevant, has to be obtained. We have to underline that all these mentioned features are strongly

interconnected with each other: the layers' number, for instance, which guides the quantum confinement impacts on the energy bandgap (which has an inverse dependence with layers' number) and the Seebeck coefficient, and it is also related to the orientation of the 2D layered structure and their in-depth distribution [237]. Additive engineering could be applied to reduce surface defectivity and increase material stability, and it could aid in controlling the crystallization process, so assisting the layers' self-assembly [238].

**Concluding remarks.** The research on low-dimensional halide perovskite for thermoelectrics is still in its infancy, but the preliminary results indicate that they could be revolutionary also in thermoelectricity. A high Seebeck coefficient can be delivered, the low thermal conductivity is an intrinsic property, and more and more efforts are being made to address the power factor's limit. The deposition of smooth and compact layers is more challenging than in 3D perovskite because the crystallization kinetics change with dimensionality: this factor should be investigated further. The synthesis processes should also be engineered to control the charge transport, by regulating the ambipolar character typical of halide perovskites. Finally, the concentration and mobility of charge carriers must be improved, both drawing inspiration from the strategies adopted in 3D halide perovskites and manipulating their arrangement on the substrate.

**Acknowledgments.** VT was supported by the 'European Union's Horizon 2020 research and innovation programme under the Marie Skłodowska-Curie grant agreement, Grant Number 798271'.

### 13. Thermoelectrics for hybrid solid-state power generators

Alessandro Bellucci\* and Daniele M. Trucchi\*\*

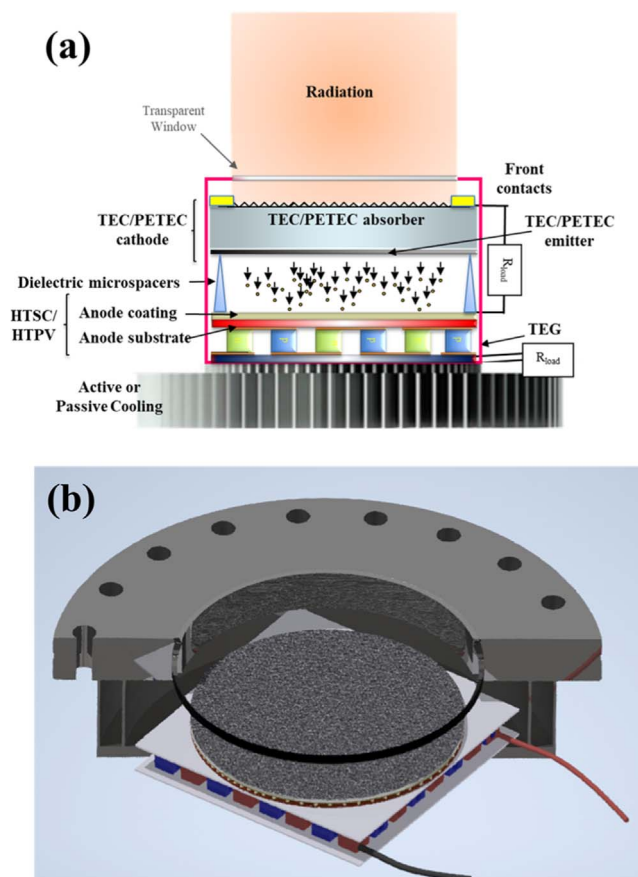
Istituto di Struttura della Materia (ISM-CNR), DiaTHEMA Lab, Montelibretti Unit

\*alessandro.bellucci@cnr.it, \*\*danielemaria.trucchi@cnr.it

**Status.** The use of thermoelectric generators (TEGs) for electric power production has been limited by the low thermal-to-electrical conversion efficiency ( $\eta$ ) with respect to other technologies, such as Rankine or Stirling engines, as well as the difficulty of working at relatively high operating temperatures which reduce the possible applicative scenarios [239]. However, the integration of TEGs into hybrid solutions connected to the use of exhaust thermal fluxes can represent the proper opportunity for widening the diffusion of this technology in the sector of power generation.

One of the most appealing energy fields for the application of hybrid devices is the conversion of solar radiation. Conversely to the concept of Solar Thermoelectric Generator (STEG) [240], in which TEGs are directly irradiated by the concentrated sunlight and need a very high operating temperature ( $>1000$  °C) for guaranteeing competitive values of solar-to-electrical conversion efficiency, or of recent TEGs coupled with a solar absorber layer and a starch-polyacrylamide hydrogel for combined electricity and clean water production [239, 241], hybrid solid-state power generators make use of TEGs to convert energy fluxes otherwise lost. Recently, the combination of TEGs with thermionic converters (TECs)[242] and photovoltaic (PV) modules [243, 244] has been reported for the fabrication of completely solid-state generators with performance higher than those of the single converters operating independently in terms of  $\eta$  and output power density. In particular, the verified technical feasibility of the Solar Thermionic-Thermoelectric Generator (ST<sup>2</sup>G) opens up the path towards the fabrication of even more attractive structures in terms of hybridization, since TEGs can be coupled in a versatile way to more efficient solid-state concepts, such as Photon-Enhanced Thermionic Emission converters (PETECs) [245], high-temperature solar cells (HTSCs) [246], or hybrid thermionic-high temperature photovoltaic (HTPV) cells [247–249]. Figure 20 shows the typical sketch representing the possible hybrid solid-state power generators in different configurations.

Generally, TECs have a very simple structure (i.e. two parallel plane electrodes, a hot cathode and a colder anode separated by a vacuum gap, with a thermally stable coating on their surfaces for optimizing the performance) and are relatively cheap. Their efficiency reduces negligibly if the anode operates at a temperature higher than room temperature up to a given value depending on the anode physical properties [250]. Therefore, the use of TEGs as secondary conversion stages fits perfectly with the TEC architecture. Since for hybrid converters based on TECs the nature of the conversion source is thermal, a full optimization of their



**Figure 20.** (a) Sketch of a hybrid thermionic-based energy converter illuminated by radiation (i.e. radiation emitted by a hot body according to the Planck's law). The impinging photons stimulate the thermionic emission from the cathode by thermalization or photogeneration. Electrons are collected by the anode, which is constituted by a metal, a HTSC, a HTPV, a TEG, or a combination of them. (b) Design of a compact vacuum enclosure as a prototype for the hybrid solid-state power generator.

integration in the final system will allow the advancement of the hybrid devices in several power generation applications.

**Current and future challenges.** The essential concept for the hybridization of TEGs with thermionic-based converters or PV cells relies on the opportunity of exploiting together the single devices operating at different temperature ranges without reducing significantly the efficiency of the single converters. Generally, in hybrid solar devices TEGs convert the exhaust heat coming from the thermalization of the absorbed sunlight, which is typically a concentrated radiation for the applications of the hybrid converters. The exhaust heat is detrimental to the efficiency of PV cells and needs to be removed by passive/active cooling systems. Therefore, the role of TEGs is to exploit the thermal gradient between the PV cell and the rejection temperature. Also in TECs the heat has to be removed to improve the performance of the converter but this technology presents an important advantage: TECs can operate with anode temperatures much higher than room temperature without affecting  $\eta$ , thus offering an additional heat source to be converted.

However, since commercial TEGs are currently based on  $\text{Bi}_2\text{Te}_3$  with a limited maximum operating temperature ( $\sim 280^\circ\text{C}$ ), the development of materials with higher operating temperatures is mandatory for a full exploitation of the concept since the anode temperature can be higher than  $500^\circ\text{C}$ .

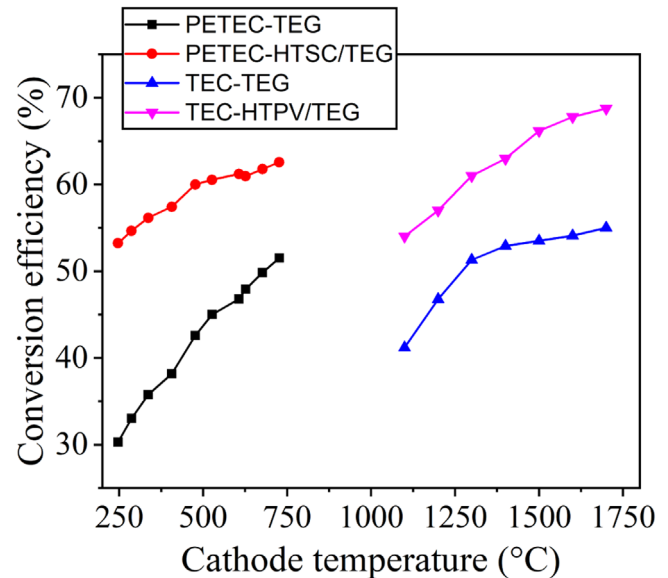
Finally, the minimization of thermal losses is one of the most important aspects for improving the performance of hybrid power generators. One of the advantages of hybrid devices with TECs is the operation under vacuum, which is the most cost-effective solution for TECs to maximize  $\eta$ : even if vacuum constraint can be considered a technological issue, it represents an important aspect for optimizing the thermal management of the involved energy fluxes minimizing the heat convection transfer. In a recent work on  $\text{ST}^2\text{G}$  [251], the use of a conversion prototype designed to reduce the limitations which were previously experimentally identified, allowed to explicitly evaluate the different contributions of heat losses, as well as the single converter performances. The most challenging research activities must be performed on vacuum TECs, which did not reach a significant technological maturity yet, whereas TEGs are mature enough to convert into electric energy the energy flux transported by the anode. The main challenges for TEGs are the development of higher performance materials (the commercial materials do not exceed 7%–8% efficiency which is reduced down to 3%–4% once TEGs are integrated into practical thermal systems) and new solutions for the optimization of the (non-ideal) thermal matching induced by the contact thermal resistance, which is a common problem for medium-high temperature hybrid solid-state converters [252].

#### Advances in science and technology to meet challenges.

The first necessary advance for TEGs in hybrid generators is the development of new and high-performance materials for increasing further both maximum operating temperature and  $\eta$ . Despite different experimental approaches demonstrated significant results, such as the measured  $ZT$  maximum values  $>2.0$  at  $650^\circ\text{C}$  of  $\text{SnSe}$  [253], more effective and faster general procedure for predicting the thermoelectric performance of new materials with the desired composition is emerging, e.g. using artificial intelligence methods with deep or machine learning algorithms [254].

A possible alternative is to change the paradigm of the classical thermoelectric architecture, by proposing thin-film structures [255, 256] able to convert thermal radial fluxes or Y-type structures [257]. In this context, it is important to notice the recent demonstration of the coupling effect between thermoelectric carriers and triboelectric charges, which can significantly increase the TEG performance of the same thermoelectric material [258]. However, these solutions are still far to be implemented in practical devices.

Beyond the research on materials and architectures to optimize the conversion performance, one of the most important efforts in developing hybrid converters is the engineering activity deriving from the matching of the involved devices. The main factors significantly affecting



**Figure 21.** Upper limit for conversion efficiencies of hybrid solid-state energy converters in the range from 200 to  $1700^\circ\text{C}$  of PETEC/TEC cathode temperature, derived from a simulation performed by matching all the involved energy fluxes. The maximum operating temperature of the anode was fixed to  $300^\circ\text{C}$  when the PV structures are considered, and  $300^\circ\text{C}$  and  $500^\circ\text{C}$  for PETEC-TEG and TEC-TEG, respectively. We recall that the PETECs need an input radiation flux to work properly instead of a simpler thermal source as occurred for TECs.

the overall performance of TEGs in hybrid devices are the thermal and electrical contact resistance, the thermal matching between active couples and electrically insulating layers, and, to a lesser extent, the thermal emittance and the geometrical factors (i.e. number of elements, size, segmentation). A lack of optimization of these parameters could induce parasitic losses in the device and, consequently, an efficiency reduction that results uncorrelated with the materials' thermoelectric behavior [259]. Also, heat losses due to the not perfect coupling between the different thermally-coupled elements (i.e. a high parasitic thermal resistance) significantly affect the efficiency of the overall system, definitively reducing the performance of TEGs.

Once these advances will be carried out, TEGs will be used in novel hybrid power generators which present outstanding calculated values of conversion efficiencies in a wide range of operating temperatures. Figure 21 shows the upper limited values of conversion efficiency from solar and thermal radiation in electricity as a function of the cathode (TEC or PETEC) temperature. These values derives from a simulation performed under ideal conditions by matching all the involved energy fluxes for different hybrid solutions. An optimistic  $ZT = 2$  is assumed for the TEG. Very high values can be ideally achieved, as previously shown for PETEC with a secondary thermal cycle [260]. A conversion efficiency of 63% at  $700^\circ\text{C}$  and 68% at  $1700^\circ\text{C}$  can be achieved for the hybrid PETEC-HTSC/TEG and TEC-HTPV/TEG solutions, respectively, which are extremely competitive results in the context of solid-state thermal-to-electrical devices for a large range of operative temperatures.

*Concluding remarks.* The possibility of using TEGs in hybrid solid-state power generator devices represents a very challenging opportunity for renewing the research and development in thermoelectric devices applied in this field. TEGs can be used to convert a heat flux that intrinsically derives from the practical operations of primary conversion stages, such as thermionic-based converters and PV cells for all-solid-state converters. In particular, the architecture of TECs can provide large energy fluxes to be converted by TEGs, maintaining unaltered the TEC efficiency despite the high residual thermal energy. The requirements for thermoelectric materials, established by the combination with TECs, are higher maximum operating temperatures and a higher overall conversion efficiency for the resulting TEGs, coming from a more accurate engineering of the thermal management.

*Acknowledgments.* The authors thank Dr Gianfranco Sabbatella of IONVAC Process srl for providing the




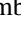


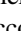




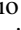
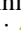



Computer-Aided Design of the generic hybrid solid-state power generators.

This research was funded by the European Union's Horizon 2020 research and innovation program, Future Emerging Technologies (FET) Innovation Launchpad (ILP) action, under the project 'TECSAS—Thermionic Energy Conversion & Storage Applied to Sunlight: Taking Concentrating Solar Power to the next level', Grant Agreement No. 101034922. website: [www.tecsas-project.eu](http://www.tecsas-project.eu); <https://cordis.europa.eu/project/id/101034922>. The accessed dates for the links are 20 January 2022. The sole responsibility for the content of this publication lies with the authors.

*Data availability statement*

No new data were created or analysed in this study.

## ORCID iDs

Cristina Artini  <https://orcid.org/0000-0001-9699-7973>  
 Zhen Li  <https://orcid.org/0000-0001-8411-7537>  
 Claudio Melis  <https://orcid.org/0000-0002-5768-8403>  
 Luciano Colombo  <https://orcid.org/0000-0001-5335-4652>  
 Eleonora Isotta  <https://orcid.org/0000-0002-5864-463X>  
 Ketan Lohani  <https://orcid.org/0000-0003-1059-6744>  
 Alberto Castellero  <https://orcid.org/0000-0001-8290-7543>  
 Marcello Baricco  <https://orcid.org/0000-0002-2856-9894>  
 Marcella Pani  <https://orcid.org/0000-0002-4711-1504>  
 Giovanna Latronico  <https://orcid.org/0000-0002-9959-9302>  
 Paolo Mele  <https://orcid.org/0000-0002-9291-7646>  
 Francesco Rossella  <https://orcid.org/0000-0002-0601-4927>  
 Alberto Ferrario  <https://orcid.org/0000-0002-0994-4919>  
 Stefano Boldrini  <https://orcid.org/0000-0002-2241-9748>  
 Dario Narducci  <https://orcid.org/0000-0002-3307-1070>  
 Vanira Trifiletti  <https://orcid.org/0000-0003-4066-3426>

## References

- [1] Beretta D *et al* 2019 Thermoelectrics: from history, a window to the future *Mater. Sci. Eng. R* **138** 100501
- [2] Neophytou N 2020 *Theory and Simulation Methods for Electronic and Phononic Transport in Thermoelectric Materials* ed Springer Cham (Berlin: Springer Briefs in Physics) (<https://doi.org/10.1007/978-3-030-38681-8>)
- [3] Neophytou N *et al* 2020 Hierarchically nanostructured thermoelectric materials: challenges and opportunities for improved power factors *Invited Colloquium: Eur. Phys. J. B* **93** 213
- [4] Kokalj A 1999 XCrySDen—a new program for displaying crystalline structures and electron densities *J. Mol. Graph. Modelling* **17** 176
- [5] Graziosi P, Kumarasinghe C and Neophytou N 2019 Impact of the scattering physics on the power factor of complex thermoelectric materials *J. Appl. Phys.* **126** 155701
- [6] Graziosi P, Kumarasinghe C and Neophytou N 2020 Material descriptors for the discovery of efficient thermoelectrics *ACS Appl. Energy Mater.* **3** 5913–26
- [7] Poncé S, Margine E R and Giustino F 2018 Towards predictive many-body calculations of phonon limited carrier mobilities in semiconductors *Phys. Rev. B* **97** 121201(R)
- [8] Parker D and Singh D J 2020 High-temperature thermoelectric performance of heavily doped PbSe *Phys. Rev. B* **82** 035204
- [9] Chen W *et al* 2016 Understanding thermoelectric properties from high-throughput calculations: trends, insights, and comparisons with experiment *J. Mater. Chem. C* **4** 4414–26
- [10] Li X, Zhang Z, Xi J, Singh D J, Sheng Y, Yang J and Zhang W 2021 TransOpt. A code to solve electrical transport properties of semiconductors in constant electron–phonon coupling approximation *Comput. Mater. Sci.* **186** 110074
- [11] Zhou J-J, Park J, Lu I-T, Maliyov I, Tong X and Bernardi M 2021 Perturbo: a software package for *ab initio* electron–phonon interactions, charge transport and ultrafast dynamics *Comput. Phys. Commun.* **264** 107970
- [12] Ganose A M, Park J, Faghaninia A, Woods-Robinson R, Persson K A and Jain A 2021 Efficient calculation of carrier scattering rates from first principles *Nat. Commun.* **12** 2222
- [13] Mandia A K, Muralidharan B, Choi J-H, Lee S-C and Bhattacharjee S 2021 AMMCR: *Ab initio* model for mobility and conductivity calculation by using Rode Algorithm *Comput. Phys. Commun.* **259** 107697
- [14] Rudderham C and Maassen J 2020 Analysis of simple scattering models on the thermoelectric performance of analytical electron dispersions *J. Appl. Phys.* **127** 065105
- [15] Graziosi P, Li Z and Neophytou N 2023 *Comput. Phys. Comm.* **287** 108670
- [16] Fischetti M V and Laux S E 1996 Band structure, deformation potentials, and carrier mobility in strained Si, Ge, and SiGe alloys *J. Appl. Phys.* **80** 2234
- [17] Lundstrom M 2000 *Fundamentals of Carrier Transport* (Cambridge: Cambridge University Press)
- [18] Graziosi P and Neophytou N 2020 Ultra-high thermoelectric power factors in narrow gap materials with asymmetric bands *J. Phys. Chem. C* **124** 18462–73
- [19] Graziosi P, Li Z and Neophytou N 2022 Bipolar conduction asymmetries lead to ultra-high thermoelectric power factor *Appl. Phys. Lett.* **120** 072102
- [20] Li Z, Graziosi P and Neophytou N 2021 Deformation potential extraction and computationally efficient mobility calculations in silicon from first principles *Phys. Rev. B* **104** 195201
- [21] Ogata M and Fukuyama H 2019 *J. Phys. Soc. Jpn.* **88** 074703
- [22] Matsuura H, Ogata M, Mori T and Bauer E 2021 *Phys. Rev. B* **104** 214421
- [23] Hinterleitner B *et al* 2019 *Nature* **576** 85
- [24] Hicks L D and Dresselhaus M S 1993 Thermoelectric figure of merit of a one-dimensional conductor *Phys. Rev. B* **47** 16631
- [25] Hicks L D and Dresselhaus M S 1993 Effect of quantum-well structures on the thermoelectric figure of merit *Phys. Rev. B* **47** 12727
- [26] Rowe D M 2018 *CRC Handbook of Thermoelectrics* (Boca Raton, FL: CRC press)
- [27] Fugallo G and Colombo L 2018 Calculating lattice thermal conductivity: a synopsis *Phys. Scr.* **93** 043002
- [28] Peierls R 1929 Zur kinetischen theorie der wärmeleitung in kristallen *Ann. Phys.* **395** 1055–101
- [29] Fugallo G, Cepellotti A, Paulatto L, Lazzeri M, Marzari N and Mauri F 2014 Thermal conductivity of graphene and graphite: collective excitations and mean free paths *Nano Lett.* **14** 6109–14
- [30] Cepellotti A, Fugallo G, Paulatto L, Lazzeri M, Mauri F and Marzari N 2015 Phonon hydrodynamics in two-dimensional materials *Nat. Commun.* **6** 1–7
- [31] Sellan D P, Landry E S, Turney J, McGaughey A J and Amon C H 2010 Size effects in molecular dynamics thermal conductivity predictions *Phys. Rev. B* **81** 214305
- [32] Melis C, Dettori R, Vandermeulen S and Colombo L 2014 Calculating thermal conductivity in a transient conduction regime: theory and implementation *Eur. Phys. J. B* **87** 1–9
- [33] Schelling P K, Phillpot S R and Keblinski P 2002 Comparison of atomic-level simulation methods for computing thermal conductivity *Phys. Rev. B* **65** 144306
- [34] Sæther S, Falck M, Zhang Z, Lervik A and He J 2021 Thermal transport in polyethylene: the effect of force fields and crystallinity *Macromolecules* **54** 6563–74
- [35] Xu K, Gabourie A J, Hashemi A, Fan Z, Wei N, Farimani A B, Komsa H-P, Krashennikov A V, Pop E and Ala-Nissila T 2019 Thermal transport in mos 2 from molecular dynamics using different empirical potentials *Phys. Rev. B* **99** 054303
- [36] Simoncelli M, Marzari N and Mauri F 2019 Unified theory of thermal transport in crystals and glasses *Nat. Phys.* **15** 809–13
- [37] Behler J 2016 Perspective: machine learning potentials for atomistic simulations *J. Chem. Phys.* **145** 170901
- [38] Ouyang Y, Yu C, Yan G and Chen J 2021 Machine learning approach for the prediction and optimization of thermal transport properties *Front. Phys.* **16** 1–16

- [39] Crossno J *et al* Observation of the dirac fluid and the breakdown of the Wiedemann–Franz law in graphene *Science* **351** 1058–61 (2016)
- [40] Mason S, Wesenberg D, Hojem A, Manno M, Leighton C and Zink B 2020 Violation of the Wiedemann–Franz law through reduction of thermal conductivity in gold thin films *Phys. Rev. Mater.* **4** 065003
- [41] Ciftci Y O and Mahanti S D 2016 Electronic structure and thermoelectric properties of half-Heusler compounds with eight electron valence count—kscx ( $x = c$  and  $ge$ ) *J. Appl. Phys.* **119** 145703
- [42] Slack G A 1979 The thermal conductivity of nonmetallic crystals *Journal of Physics C: Solid State Physics* **34** 1–71
- [43] Baláz P *et al* 2021 Thermoelectric Cu–S-based materials synthesized via a scalable mechanochemical process *ACS Sustain. Chem. Eng.* **9** 2003–16
- [44] Lohani K *et al* 2021 Experimental and Ab Initio Study of  $Cu_2SnS_3$  (CTS) polymorphs for thermoelectric applications *J. Phys. Chem. C* **125** 178–88
- [45] Scragg J J S, Choubrac L, Lafond A, Ericson T and Platzer-Björkman C 2014 A low-temperature order-disorder transition in  $Cu_2ZnSnS_4$  thin films *Appl. Phys. Lett.* **104** 041911
- [46] Rey G, Redinger A, Weiss T P and Guennou M 2014 The band gap of  $Cu_2ZnSnSe_4$ : effect of order-disorder *Appl. Phys. Lett.* **105** 112106
- [47] Isotta E, Mukherjee B, Fanciulli C, Pugno N M and Scardi P 2020 Order–disorder transition in kesterite  $Cu_2ZnSnS_4$ : thermopower enhancement via electronic band structure modification *J. Phys. Chem. C* **124** 7091–6
- [48] Isotta E *et al* 2020 Origin of a simultaneous suppression of thermal conductivity and increase of electrical conductivity and Seebeck coefficient in disordered cubic  $Cu_2ZnSnS_4$  *Phys. Rev. Appl.* **14** 064073
- [49] Mukherjee B, Isotta E, Fanciulli C, Ataollahi N and Scardi P 2021 Topological Anderson insulator in cation-disordered  $Cu_2ZnSnS_4$  *Nanomaterials* **11** 2595
- [50] Pal K, Anand S and Waghmare U V 2015 Thermoelectric properties of materials with nontrivial electronic topology *J. Mater. Chem. C* **3** 12130–9
- [51] Lohani K, Nautiyal H, Ataollahi N, Maji K, Guilmeau E and Scardi P Effects of grain size on the thermoelectric properties of  $Cu_2SnS_3$ : an experimental and first-principles study *ACS Appl. Energy Mater.* **4** 12604–12
- [52] Hendricks T, Caillat T and Mori T 2022 Keynote review of latest advances in thermoelectric generation materials, devices, and technologies 2022 *Energies* **15** 7307
- [53] Liu Z, Gao W, Oshima H, Nagase K, Lee C H and Mori T 2022 Maximizing the performance of n-type  $Mg_3Bi_2$  based materials for room-temperature power generation and thermoelectric cooling *Nat. Commun.* **13** 1–9
- [54] Ying P *et al* 2021 Towards tellurium-free thermoelectric modules for power generation from low-grade heat *Nat. Commun.* **12** 1–6
- [55] Liu Z *et al* 2021 Demonstration of ultrahigh thermoelectric efficiency of  $\sim 7.3\%$  in  $Mg_3Sb_2/MgAgSb$  module for low-temperature energy harvesting *Joule* **5** 1196–208
- [56] Syafiq U *et al* 2022 Facile and low-cost fabrication of Cu/Zn/Sn-based ternary and quaternary chalcogenides thermoelectric generators *ACS Appl. Energy Mater.* **5** 5909–18
- [57] Isotta E *et al* 2022 Towards low cost and sustainable thin film thermoelectric devices based on quaternary chalcogenides *Adv. Funct. Mater.* **32** 2202157
- [58] Ishibe T *et al* 2021 Carrier and phonon transport control by domain engineering for high-performance transparent thin film thermoelectric generator *Appl. Phys. Lett.* **118** 151601
- [59] Ohkubo I *et al* 2022 Miniaturized in-plane  $\pi$ -type thermoelectric device composed of a II–IV semiconductor thin film prepared by microfabrication *Mater. Today Energy* **28** 101075
- [60] Wen D L, Deng H T, Liu X, Li G K, Zhang X R and Zhang X S 2020 Wearable multi-sensing double-chain thermoelectric generator *Microsyst. Nanoeng.* **6** 1–13
- [61] Yang F, Zheng S, Wang H, Chu W and Dong Y 2017 A thin film thermoelectric device fabricated by a self-aligned shadow mask method *J. Micromech. Microeng.* **27** 055005
- [62] Freer R *et al* 2022 Key properties of inorganic thermoelectric materials—tables (version 1) *J. Phys.: Energy* **4** 022002
- [63] Schiering G *et al* 2015 Concepts for medium-high to high temperature thermoelectric heat-to-electricity conversion: a review of selected materials and basic considerations of module design *Transl. Mater. Res.* **2** 025001
- [64] Radousky H B and Liang H 2012 Energy harvesting: an integrated view of materials, devices and applications *Nanotechnology* **23** 502001
- [65] Artini C, Castellero A, Baricco M, Buscaglia M T and Carlini R 2018 Structure, microstructure and microhardness of rapidly solidified  $Sm_x(Fe_xNi_{1-x})_4Sb_{12}$  ( $x = 0.45, 0.50, 0.70, 1$ ) thermoelectric compounds *Solid State Sci.* **79** 71–8
- [66] Salvador J R *et al* 2014 Conversion efficiency of skutterudite-based thermoelectric modules *Phys. Chem. Chem. Phys.* **16** 12510–20
- [67] Bartholomé K *et al* 2014 Thermoelectric modules based on half-Heusler materials produced in large quantities *J. Electron. Mater.* **43** 1775–81
- [68] Nolas G, Slack G A, Morelli D T, Tritt T M and Ehrlich A C 1996 The effect of rare-earth filling on the lattice thermal conductivity of skutterudites *J. Appl. Phys.* **79** 4002–8
- [69] Shi X *et al* 2011 Multiple-filled skutterudites: High thermoelectric figure of merit through separately optimizing electrical and thermal transports *J. Am. Chem. Soc.* **133** 7837–46
- [70] Hooshmand Zaferani S, Ghomashchi R and Vashaee D 2019 Strategies for engineering phonon transport in Heusler thermoelectric compounds *Renew. Sustain. Energy Rev.* **112** 158–69
- [71] Legrain F, Carrete J, Van Roekeghem A, Madsen G K H and Mingo N 2018 Materials screening for the discovery of new half-Heuslers: machine learning versus ab initio methods *J. Phys. Chem. B* **122** 625–32
- [72] Rogl G *et al* 2019 High-ZT half-Heusler thermoelectrics,  $Ti_{0.5}Zr_{0.5}NiSn$  and  $Ti_{0.5}Zr_{0.5}NiSn_{0.98}Sb_{0.02}$ : physical properties at low temperatures *Acta Mater.* **166** 466–83
- [73] Dasmahapatra A, Daga L E, Karttunen A J, Maschio L and Casassa S 2020 Key role of defects in thermoelectric performance of  $TiMSn$  ( $M = Ni, Pd,$  and  $Pt$ ) half-Heusler alloys *J. Phys. Chem. C* **124** 14997–5006
- [74] Berche A and Jund P 2018 Fully *ab initio* determination of the thermoelectric properties of half-Heusler  $NiTiSn$ : crucial role of interstitial Ni defects *Materials* **11** 868
- [75] Geng Y H, Ochi S and Guo J Q 2007 Solidification contraction-free synthesis for the  $Yb_{0.15}Co_4Sb_{12}$  bulk material *Appl. Phys. Lett.* **91** 022106
- [76] Aversano F *et al* 2020 Role of secondary phases and thermal cycling on thermoelectric properties of  $TiNiSn$  half-Heusler alloy prepared by different processing routes *Intermetallics* **127** 106988
- [77] Tang Y, Chen S-W and Snyder G J 2015 Temperature dependent solubility of Yb in  $Yb-CoSb_3$  skutterudite and its effect on preparation, optimization and lifetime of thermoelectrics *J. Mater.* **1** 75–84
- [78] Aversano F *et al* 2019 Effect of rapid solidification on the synthesis and thermoelectric properties of Yb-filled  $Co_4Sb_{12}$  skutterudite *J. Alloys Compd.* **796** 33–41
- [79] Aversano F *et al* 2018 Thermoelectric properties of  $TiNiSn$  half-Heusler alloy obtained by rapid solidification and sintering *J. Mater. Eng. Perform.* **27** 6306–13



- [80] Rogl G, Zehetbauer M J and Rogl P F 2019 The effect of severe plastic deformation on thermoelectric performance of skutterudites, half-Heuslers and bi-tellurides *Mater. Trans.* **60** 2071–85
- [81] El-Desouky A, Carter M, Andre M A, Bardet P M and LeBlanc S 2016 Rapid processing and assembly of semiconductor thermoelectric materials for energy conversion devices *Mater. Lett.* **185** 598–602
- [82] Uher C 2005 Skutterudite-based thermoelectrics *Thermoelectrics Handbook—Macro to Nano* ed D M Rowe 1st edn (Boca Raton, USA: Taylor and Francis) ch 34 pp 1–17
- [83] Graf T, Felser C and Parkin S S P 2011 Simple rules for the understanding of Heusler compounds *Prog. Solid State Chem.* **39** 1–50
- [84] Sootsman J R, Young Chung D and Kanatzidis M G 2009 New and old concepts in thermoelectric materials *Angew. Chem. Int. Ed.* **48** 9616–38
- [85] Kong L, Jia X, Zhang Y, Sun B, Liu B, Liu H, Wang C, Liu B, Chen J and Ma H 2018 N-type  $\text{Ba}_{0.3}\text{Ni}_{0.15}\text{Co}_{3.85}\text{Sb}_{12}$  skutterudite: high pressure processing technique and thermoelectric properties *J. Alloys Compd.* **734** 36–42
- [86] Artini C, Zanichchi G, Costa G A, Carnasciali M M, Fanciulli C and Carlini R 2016 Correlations between structural and electronic properties in the filled skutterudite  $\text{Sm}_y(\text{Fe}_x\text{Ni}_{1-x})_4\text{Sb}_{12}$  *Inorg. Chem.* **55** 2574–83
- [87] Duan F, Zhang L, Dong J, Sakamoto J, Xu B, Li X and Tian Y 2015 Thermoelectric properties of Sn substituted p-type Nd filled skutterudites *J. Alloys Compd.* **639** 68–73
- [88] Artini C, Carlini R, Gigli L and Fanciulli C 2020 Compositional optimization and structural properties of the filled skutterudite  $\text{Sm}_y(\text{Fe}_x\text{Ni}_{1-x})_4\text{Sb}_{11.5}\text{Sn}_{0.5}$  *Metals* **10** 692
- [89] Pani M, Pallecchi I, Bernini C, Ardoino N and Marrè D 2018 Synthesis and structural characterization of Sb-doped  $\text{TiFe}_2\text{Sn}$  Heusler compounds *J. Mater. Eng. Perform.* **27** 6314–21
- [90] Pallecchi I, Pani M, Ricci F, Lemal S, Bilc D I, Ghosez P, Bernini C, Ardoino N, Lamura G and Marrè D 2018 Thermoelectric properties of chemically substituted full-Heusler  $\text{Fe}_2\text{TiSn}_{1-x}\text{Sb}_x$  ( $x = 0, 0.1, \text{ and } 0.2$ ) compounds *Phys. Rev. Mater.* **2** 075403
- [91] Burton M, Howells J, Atoyo J and Carmie M 2022 Printed thermoelectrics *Adv. Mater.* **34** 2108183
- [92] Nandihalli N, Liu C-J and Mori T 2020 Polymer based thermoelectric nanocomposite materials and devices: fabrication and characteristics *Nano Energy* **78** 105186
- [93] Latronico G *et al* 2021 Investigation on the power factor of skutterudite  $\text{Sm}_y(\text{Fe}_x\text{Ni}_{1-x})_4\text{Sb}_{12}$  thin films: effects of deposition and annealing temperature *Materials* **14** 5773
- [94] Artini C, Carlini R, Spotorno R, Failamani F, Mori T and Mele P 2019 Structural properties and thermoelectric performance of the double filled skutterudite  $(\text{Sm}, \text{Gd})_y(\text{Fe}_x\text{Ni}_{1-x})_4\text{Sb}_{12}$  *Materials* **12** 2451
- [95] Karthikeyan N, Sivaprasad G, Jaiganesh G, Anbarasu V, Partha Pratim J and Sivakumar K 2017 Thermoelectric properties of Se and Zn/Cd/Sn double substituted  $\text{Co}_4\text{Sb}_{12}$  skutterudite compounds *Phys. Chem. Chem. Phys.* **19** 28116–26
- [96] Phuangyod A, Hayashi J, Kawamura Y, Artini C, Latronico G, Carlini R, Saini S, Mele P and Sekine C 2020 Low temperature thermoelectric properties of p-type and n-type filled skutterudite compounds  $\text{Sm}_y(\text{Fe}_{1-x}\text{Ni}_x)_4\text{Sb}_{12}$  prepared under high pressure *Jpn. J. Appl. Phys.* **59** 061004
- [97] Rogl G *et al* 2012 Effect of HPT processing on the structure, thermoelectric and mechanical properties of  $\text{Sr}_{0.07}\text{Ba}_{0.07}\text{Yb}_{0.07}\text{Co}_4\text{Sb}_{12}$  *J. Alloys Compd.* **537** 183–9
- [98] Hooshmand Zaferani S, Ghomaschchi R and Vashaee D 2019 Strategies for engineering phonon transport in Heusler thermoelectric compounds *Renew. Sust. Energy Rev.* **112** 158–69
- [99] Hinterleitner B *et al* 2019 Thermoelectric performance of a metastable thin-film Heusler alloy *Nature* **576** 85
- [100] Latronico G *et al* 2023 Effect of the annealing treatment on the structural and transport properties of thermoelectric  $\text{Sm}_y(\text{Fe}_x\text{Ni}_{1-x})_4\text{Sb}_{12}$  thin films *Nanotechnology* **34** 115705
- [101] Artini C, Cingolani A, Anselmi Tamburini U, Valenza F, Latronico G and Mele P 2021 Effect of the sintering pressure on structure and microstructure of the filled skutterudite  $\text{Sm}_y(\text{Fe}_x\text{Ni}_{1-x})_4\text{Sb}_{12}$  *Mater. Res. Bull.* **139** 111261
- [102] Klochko N P *et al* 2018 Semitransparent p-CuI and n-ZnO thin films prepared by low temperature solution growth for thermoelectric conversion of near-infrared solar light *Sol. Energy* **171** 704–15
- [103] Kim Y J *et al* 2019 High-performance monolithic photovoltaic–thermoelectric hybrid power generator using an exothermic reactive interlayer *ACS Appl. Energy Mater.* **2** 2381–6
- [104] Yang C *et al* 2017 Transparent flexible thermoelectric material based on non-toxic earth-abundant p-type copper iodide thin film *Nat. Commun.* **8** 16076 1–7
- [105] Loureiro J *et al* 2014 Transparent aluminium zinc oxide thin films with enhanced thermoelectric properties *J. Mater. Chem. A* **2** 6649–55
- [106] Althaf R and Ashok A M 2020 Realization of high thermoelectric power factor in Ta-doped ZnO by grain boundary engineering *J. Appl. Phys.* **128** 165110 1–13
- [107] Nguyen N H T *et al* 2016 Thermoelectric properties of indium and gallium dually doped ZnO thin films *ACS Appl. Mater. Interfaces* **8** 33916–23
- [108] Felizco J C, Uenuma M, Ishikawa Y and Uraoka Y 2020 Optimizing the thermoelectric performance of InGaZnO thin films depending on crystallinity via hydrogen incorporation *Appl. Surf. Sci.* **527** 146791
- [109] Faustino B M M *et al* 2018 CuI p-type thin films for highly transparent thermoelectric p-n modules *Sci. Rep.* **8** 6867
- [110] Tamburri E, Orlanducci S, Toschi F, Terranova M L and Passeri D 2009 Growth mechanisms, morphology, and electroactivity of PEDOT layers produced by electrochemical routes in aqueous medium *Synth. Met.* **159** 406–14
- [111] Fan Z, Du D, Yao H and Ouyang J 2017 Higher PEDOT molecular weight giving rise to higher thermoelectric property of PEDOT:PSS: a comparative study of clevis p and clevis ph1000 *ACS Appl. Mater. Interfaces* **9** 11732–8
- [112] Xia Y and Ouyang J 2012 Significant different conductivities of the two grades of poly(3,4-thylenedioxythiophene): poly(styrenesulfonate), clevis p and clevis ph1000 arising from different molecular weights *ACS Appl. Mater. Interfaces* **4** 4131–40
- [113] Wang S *et al* 2016 Thermoelectric properties of solution processed n-doped ladder-type conducting polymers *Adv. Mater.* **28** 10764–71
- [114] Morgan K A *et al* 2019 High-throughput physical vapour deposition flexible thermoelectric generators *Sci. Rep.* **9** 1–9
- [115] Di Benedetto F *et al* Rapporto di avanzamento dell'attività scientifica: sviluppo ed ottimizzazione di materiali termoelettrici e procedure di deposizione: Report RdS/PTR2021/212
- [116] Murmu P P *et al* 2021 Effect of native defects on thermoelectric properties of copper iodide films *Emergent Mater.* **4** 761–8
- [117] Di Benedetto F *et al* Rapporto di avanzamento scientifico: studio e messa a punto di materiali termoelettrici e delle procedure di deposizione su microchip Report RdS/PTR2020/264
- [118] Kim G-H, Shao L, Zhang K and Pipe K P 2018 Engineered doping of organic semiconductors for enhanced thermoelectric efficiency *Nat. Mater.* **12** 719–23

- [119] Mazaheripour A *et al* 2018 Tailoring the seebeck coefficient of PEDOT:PSS by controlling ion stoichiometry in ionic liquid additives *Chem. Mater.* **30** 4816–22
- [120] Bubnova O *et al* 2011 Optimization of the thermoelectric figure of merit in the conducting polymer poly(3,4-ethylenedioxythiophene) *Nat. Mater.* **10** 429–33
- [121] Poehler T O and Katz H E 2012 Prospects for polymer-based thermoelectrics: state of the art and theoretical analysis *Energy Environ. Sci.* **5** 8110–5
- [122] Sahu A *et al* 2017 Bottom-up design of de novo thermoelectric hybrid materials using chalcogenide resurfacing *J. Mater. Chem. A* **5** 3346–57
- [123] Dresselhaus M S, Chen G, Tang M Y, Yang R G, Lee H, Wang D Z, Ren Z F, Fleurial J -P and Gogna P 2007 New directions for low-dimensional thermoelectric materials *Adv. Mater.* **19** 1043–53
- [124] Chen R, Lee J and Li D 2019 Thermoelectrics of nanowires *Chem. Rev.* **119** 9260–302
- [125] Caballero-Calero O and Martín-González M 2016 Thermoelectric nanowires: a brief prospective *Scr. Mater.* **111** 54–7
- [126] Demontis V, Zannier V, Sorba L and Rossella F 2021 Surface nano-patterning for the bottom-up growth of III–V semiconductor nanowire ordered arrays *Nanomaterials*. **11** 2079
- [127] Thelander C *et al* 2006 Nanowire-based one-dimensional electronics *Mater. Today* **9** 28–35
- [128] Zagaglia L, Demontis V, Rossella F and Floris F 2021 Semiconductor nanowire arrays for optical sensing *Nanotechnology* **32** 335502
- [129] Demontis V, Rocci M, Donarelli M, Maiti R, Zannier V, Beltram F, Sorba L, Roddaro S, Rossella F and Baratto C 2019 Conductometric sensing with individual InAs nanowires *Sensors* **19** 2994
- [130] Cornia S, Rossella F, Demontis V, Zannier V, Beltram F, Sorba L, Affronte M and Ghirri A 2019 Microwave-assisted tunneling in hard-wall InAs/InP nanowire quantum dots *Sci. Rep.* **19523**
- [131] Frolov S M, Plissard S R, Nadj-Perge S, Kouwenhoven L P and Bakkers E P A M 2013 Quantum computing based on semiconductor nanowires *MRS Bull.* **38** 809–15
- [132] Sadre Momtaz Z *et al* 2020 Orbital tuning of tunnel coupling in InAs/InP nanowire quantum dots *Nano Lett.* **20** 1693
- [133] Rossella F, Pennelli G and Roddaro S 2018 Chapter six—measurement of the thermoelectric properties of individual nanostructures, part of volume: nanowires for energy applications edited by Sudha Mokkaapati, Chennupati Jagadish *Semicond. Semimet.* **98** 409–44
- [134] Prete D, Erdman P A, Demontis V, Zannier V, Ercolani D, Sorba L, Beltram F, Rossella F, Taddei F and Roddaro S 2019 Thermoelectric conversion at 30 K in InAs/InP nanowire quantum dots *Nano Lett.* **19** 3033–9
- [135] Denisov A O, Tikhonov E S, Piatrusha S U, Khrapach I N, Rossella F, Rocci M, Sorba L, Roddaro S and Khrapai V S 2020 Strategy for accurate thermal biasing at the nanoscale *Nanotechnology* **31** 324004
- [136] Tikhonov E S, Shovkun D V, Ercolani D, Rossella F, Rocci M, Sorba L, Roddaro S and Khrapai V S 2016 Noise thermometry applied to thermoelectric measurements in InAs nanowires *Semicond. Sci. Technol.* **31** 104001
- [137] Tikhonov E S, Shovkun D V, Ercolani D, Rossella F, Rocci M, Sorba L, Roddaro S and Khrapai V S 2016 Local noise in a diffusive conductor *Sci. Rep.* **6** 30621
- [138] Rocci M, Demontis V, Prete D, Ercolani D, Sorba L, Beltram F, Pennelli G, Roddaro S and Rossella F 2018 Suspended InAs nanowire-based devices for thermal conductivity measurement using the  $3\omega$  method *J. Mater. Eng. Perform.* **27** 6299–305
- [139] He J, Kanatzidis M G and Dravid V P 2013 *Mater. Today* **16** 166–76
- [140] Prete D, Dimaggio E, Demontis V, Zannier V, Rodriguez Douton M-J, Guazzelli L, Beltram F, Sorba L, Pennelli G and Rossella F 2021 Electrostatic control of the thermoelectric figure of merit in ion-gated nanotransistors *Adv. Funct. Mat.* **31** 2104175
- [141] Prete D *et al* 2021 Impact of electrostatic doping on carrier concentration and mobility in InAs nanowires *Nanotechnology* **32** 145204
- [142] Lieb J, Demontis V, Prete D, Ercolani D, Zannier V, Sorba L, Ono S, Beltram F, Sacepe B and Rossella F 2019 Ionic liquid gating of InAs nanowire-based field effect transistors *Adv. Funct. Mater.* **29** 1804378
- [143] Zhou C *et al* Polycrystalline SnSe with a thermoelectric figure of merit greater than the single crystal *Nat. Mater.* **20** 102021
- [144] Hendricks T, Caillat T and Mori T 2022 Keynote review of latest advances in thermoelectric generation materials, devices, and technologies 2022 *Energies* **15**
- [145] Harman T C 1958 Multiple stage thermoelectric generation of power *J. Appl. Phys.* **29** 10
- [146] Snyder G J 2005 Thermoelectric power generation: efficiency and compatibility *Thermoelectrics Handbook: Macro to Nano* 2006, pp 9–19
- [147] (<http://thermoelectrics.matsci.northwestern.edu/thermoelectrics/index.html>)
- [148] Ziolkowski P, Blaschkewitz P, Ryu B, Park S and Müller E 2022 International round robin test of thermoelectric generator modules *Materials* **15** 5
- [149] Guo H, Baker A, Guo J and Randall C A 2016 Cold sintering process: a novel technique for low-temperature ceramic processing of ferroelectrics *J. Am. Ceram. Soc.* **99** 11
- [150] Wang C *et al* 2020 A general method to synthesize and sinter bulk ceramics in seconds *Science* **368** 6490
- [151] Pérez-Aparicio J L, Taylor R L and Gavela D 2007 Finite element analysis of nonlinear fully coupled thermoelectric materials *Comput. Mech.* **40** 1
- [152] Hogan T P and Shih T 2005 *Thermoelectrics Handbook: Macro to Nano* (Boca Raton, FL: CRC Press) pp 12–1
- [153] Boldrini S, Famengo A, Montagner F, Battiston S, Fiameni S, Fabrizio M and Barison S 2013 Test rig for high-temperature thermopower and electrical conductivity measurements *J. Electron. Mater.* **42** 7
- [154] Sakamoto T, Famengo A, Barison S, Battiston S, Boldrini S, Ferrario A, Fiameni S, Iida T, Takanashi Y and Fabrizio M 2016 Structural, compositional and functional properties of Sb-doped Mg<sub>2</sub>Si synthesized in Al<sub>2</sub>O<sub>3</sub>-crucibles *RSC Adv.* **6** 81037–45
- [155] Fanciulli C, Coduri M, Boldrini S, Abedi H, Tomasi C, Famengo A, Ferrario A, Fabrizio M and Passaretti F 2017 Structural texture induced in SnSe thermoelectric compound via open die pressing *J. Nanosci. Nanotechnol.* **17** 3
- [156] Difalco A, Aversano F, Boldrini S, Ferrario A, Baricco M and Castellero A 2020 Synthesis and characterization of thermoelectric Co<sub>2</sub>XSn (X = Zr, Hf) heusler alloys *Metals* **10** 5
- [157] Boldrini S, Ferrario A, Bison P, Miozzo A, Montagner F and Fabrizio M 2016 IR thermography for the assessment of the thermal conductivity of thermoelectric modules at intermediate temperature *Proc. SPIE, Thermosense: Thermal Infrared Applications* 38 vol 986198610J
- [158] Ferrario A, Battiston S, Boldrini S, Sakamoto T, Miorin E, Famengo A, Miozzo A, Fiameni S, Iida T and Fabrizio M 2015 Mechanical and electrical characterization of low-resistivity contact materials for Mg<sub>2</sub>Si *Mater. Today Proc.* **2** 2
- [159] Ferrario A, Boldrini S, Miozzo A and Fabrizio M 2019 Temperature dependent iterative model of thermoelectric

- generator including thermal losses in passive elements *Appl. Therm. Eng.* **150** 620–7
- [160] Mahan G D 1991 Inhomogeneous thermoelectrics *J. Appl. Phys.* **70** 8
- [161] Akinaga H 2021 Recent advances and future prospects in energy harvesting technologies *J. Appl. Phys.* **59** 110201
- [162] Tarancon A 2019 Powering the IoT revolution with heat *Nat. Electron.* **2** 270–1
- [163] Petsagkourakis I *et al* 2018 Thermoelectric materials and applications for energy harvesting power generation *Sci. Tech. Adv. Mater.* **19** 836–62
- [164] Yanagisawa R *et al* 2020 Nanostructured planar-type uni-leg Si thermoelectric generators *Appl. Phys. Express* **13** 095001
- [165] Koike S *et al* 2020 Design of a planar-type uni-leg SiGe thermoelectric generator *Jpn. J. Appl. Phys.* **59** 074003
- [166] Pennelli G, Dimaggio E and Masci A 2021 Silicon nanowires: a breakthrough for thermoelectric applications *Materials* **14** 5305
- [167] Pennelli G 2015 Top-down fabrication of silicon nanowire devices for thermoelectric applications: properties and perspectives *Eur. Phys. J. B* **88** 121
- [168] Elyamny S, Dimaggio E, Magagna S, Narducci D and Pennelli G 2020 High power thermoelectric generator based on vertical silicon nanowire *Nano Lett.* **20** 4748–53
- [169] Pennelli G, Elyamny S and Dimaggio E 2018 Thermal conductivity of silicon nanowire forests *Nanotechnology* **29** 505402
- [170] Pennelli G, Dimaggio E and Macucci M 2018 Thermal conductivity reduction in rough silicon nanomembranes *IEEE Trans. Nanotechnol.* **17** 500–5
- [171] Lim J, Hippalgaonkar K, Andrews C S, Majumdar A and Yang P 2012 Quantifying surface roughness effects on phonon transport in silicon nanowires *Nano Lett.* **12** 2475–82
- [172] Dimaggio E and Pennelli G 2018 Potentialities of silicon nanowire forests for thermoelectric generation *Nanotechnology* **29** 135401
- [173] Neophytou N, Foster S, Vargiamidis V, Pennelli G and Narducci D 2019 Nanostructured potential well/barrier engineering for realizing unprecedentedly large thermoelectric power factors *Mater. Today Phys.* **11** 100159
- [174] Pennelli G, Totaro M, Piotto M and Bruschi P 2013 Seebeck coefficient of nanowires interconnected into large area networks *Nano Lett.* **13** 2592–7
- [175] Pennelli G and Macucci M 2016 High-power thermoelectric generators based on nanostructured silicon *Semicond. Sci. Technol.* **31** 054001
- [176] Pennelli G, Dimaggio E and Macucci M 2017 Fabrication techniques for thermoelectric devices based on nanostructured silicon *J. Nanosci. Nanotechnol.* **17** 1627–33
- [177] Davila D, Tarancon A, Calaza C, Salleras M, Fernandez-Regulez M, SanPaulo A and Fonseca L 2012 Monolithically integrated thermoelectric energy harvester based on silicon nanowire arrays for powering micro/nanodevices *Nano Energy* **1** 812
- [178] Dimaggio E, Narducci D and Pennelli G 2018 Fabrication of silicon nanowire forests for thermoelectric applications by metal-assisted chemical etching *J. Mater. Eng. Perform.* **27** 6279–85
- [179] Dimaggio E and Pennelli G 2016 Reliable fabrication of metal contacts on silicon nanowire forests *Nano Lett.* **16** 4348–54
- [180] Elyamny S, Dimaggio E and Pennelli G 2020 Seebeck coefficient of silicon nanowire forests doped by thermal diffusion *Beilstein J. Nanotechnol.* **11** 1707–13
- [181] Toshima N 2017 Recent progress of organic and hybrid thermoelectric materials *Synth. Met.* **225** 3–21m
- [182] Fan Z, Du D, Guan X and Ouyang J 2018 Polymer films with ultrahigh thermoelectric properties arising from significant seebeck coefficient enhancement by ion accumulation on surface *Nano Energy* **51** 481–8
- [183] Cho C, Wallace K L, Tzeng P, Hsu J, Yu C and Grunlan J C 2016 Outstanding low temperature thermoelectric power factor from completely organic thin films enabled by multidimensional conjugated nanomaterials *Adv. Energy Mater.* **6** 1502168
- [184] Xu S, Shi X-L, Dargusch M, Di C, Zou J and Chen Z-G 2021 Conducting polymer-based flexible thermoelectric materials and devices: from mechanisms to applications *Prog. Mater. Sci.* **121** 100840
- [185] Mardi S, Ambrogioni M R and Reale A 2020 Developing printable thermoelectric materials based on graphene nanoplatelet/ethyl cellulose nanocomposites *Mater. Res. Express* **7** 085101
- [186] Mardi S, Cataldi P, Athanassiou A and Reale A 2022 3D cellulose fiber networks modified by PEDOT:PSS/graphene nanoplatelets for thermoelectric applications *Appl. Phys. Lett.* **120** 033102
- [187] Yang C-Y *et al* 2021 A high-conductivity n-type polymeric ink for printed electronics *Nat. Commun.* **12** 2354
- [188] Meng B, Liu J and Wang L 2021 Recent development of n-type thermoelectric materials based on conjugated polymers, *Nano Mater. Sci.* **3** 113–23
- [189] Tripathi A, Lee Y, Lee S and Woo H Y 2022 Recent advances in n-type organic thermoelectric materials, dopants, and doping strategies *J. Mater. Chem. C* **10** 6114–40
- [190] Weathers A, Khan Z U, Brooke R, Evans D, Pettes M T, Andreasen J W, Crispin X and Shi L 2015 Significant electronic thermal transport in the conducting polymer poly(3, 4-ethylenedioxythiophene) *Adv. Mater.* **27** 2101–6
- [191] Mardi S, Yusupov K, Martinez P M, Zakhidov A, Vomiero A and Reale A 2021 Enhanced thermoelectric properties of poly(3-hexylthiophene) through the incorporation of aligned carbon nanotube forest and chemical treatments *American Chemical Society – ACS Omega* **6** 1073–82
- [192] He M, Ge J, Lin Z, Feng X, Wang X, Lu H, Yang Y and Qiu F 2012 Thermopower enhancement in conducting polymer nanocomposites via carrier energy scattering at the organic–inorganic semiconductor interface *Energy Environ. Sci.* **5** 8351–8
- [193] Ju H and Kim J 2016 Chemically exfoliated SnSe nanosheets and their SnSe/poly(3, 4-ethylenedioxythiophene): poly(styrenesulfonate) composite films for polymer based thermoelectric applications *ACS Nano* **10** 5730–9
- [194] Liang Z, Boland M J, Butrouna K, Strachan D R and Graham K R 2017 Increased power factors of organic–inorganic nanocomposite thermoelectric materials and the role of energy filtering *J. Mater. Chem. A* **5** 15891–900
- [195] Tonga M, Wei L, Wilusz E, Korugic-Karasz L, Karasz F E and Lahti P M 2018 Solution-fabrication dependent thermoelectric behavior of iodine-doped regioregular and regiorandom P3HT/carbon nanotube composites *Synth. Met.* **239** 51–8
- [196] Hong C T, Kang Y H, Ryu J, Cho S Y and Jang K-S 2015 Spray-printed CNT/P3HT organic thermoelectric films and power generators *J. Mater. Chem. A* **3** 21428–33
- [197] Bounioux C, Díaz-Chao P, Campoy-Quiles M, Martín-González M S, Goni A R, Yerushalmi-Rozen R and Müller C 2013 Thermoelectric composites of poly(3-hexylthiophene) and carbon nanotubes with a large power factor *Energy Environ. Sci.* **6** 918–25
- [198] Mardi S, Pea M, Notargiacomo A, Nia N Y, Carlo A D and Reale A 2020 The molecular weight dependence of thermoelectric properties of poly(3-hexylthiophene) *Materials* **13** 1404

- [199] Nandihalli N, Liu C-J and Mori T 2020 Polymer based thermoelectric nanocomposite materials and devices: Fabrication and characteristics *Nano Energy* **78** 105186
- [200] Wang H and Yu C 2019 Organic thermoelectrics: materials preparation, performance optimization, and device integration *Joule* **3** 53–80
- [201] Berthod C *et al* 2019 Temperature sensitivity of multicrystalline silicon solar cells *IEEE J. Photovolt.* **9** 927–64
- [202] Lorenzi B, Acciarri M and Narducci D 2018 Experimental determination of power losses and heat generation in solar cells for photovoltaic-thermal applications *J. Mater. Eng. Perform.* **27** 6291–8
- [203] Contento G, Lorenzi B, Rizzo A and Narducci D 2017 Efficiency enhancement of a-Si and CZTS solar cells using different thermoelectric hybridization strategies *Energy* **131** 230–8
- [204] Park K-T *et al* 2013 Lossless hybridization between photovoltaic and thermoelectric devices *Sci. Rep.* **3** 422–7
- [205] Zhang M *et al* 2013 Efficient, low-cost solar thermoelectric cogenerators comprising evacuated tubular solar collectors and thermoelectric modules *Appl. Energy* **109** 51–9
- [206] Beerl O, Rotem O, Hazan E, Katz E A, Braun A and Gelbstein Y 2015 Hybrid photovoltaic-thermoelectric system for concentrated solar energy conversion: experimental realization and modeling *J. Appl. Phys.* **118** 115104
- [207] Bjørk R and Nielsen K K 2015 The performance of a combined solar photovoltaic (PV) and thermoelectric generator (TEG) system *Sol. Energy* **120** 187–94
- [208] Dupré O, Vaillon R and Green M A 2016 A full thermal model for photovoltaic devices *Sol. Energy* **140** 73–82
- [209] Dupré O, Vaillon R and Green M A 2015 Physics of the temperature coefficients of solar cells *Sol. Energy Mater. Sol. Cells* **140** 92–100
- [210] Peter Seif J *et al* 2014 Amorphous silicon oxide window layers for high-efficiency silicon heterojunction solar cells *J. Appl. Phys.* **115** 024502
- [211] Xu L *et al* 2018 Efficient perovskite photovoltaic-thermoelectric hybrid device *Adv. Energy Mater.* **8** 1702937
- [212] Zhou Y *et al* 2019 Perovskite solar cell-thermoelectric tandem system with a high efficiency of over 23 *Mater. Today Energy* **12** 363–70
- [213] Zhang J, Xuan Y and Yang L 2016 A novel choice for the photovoltaic-thermoelectric hybrid system: the perovskite solar cell *Int. J. Energy Res.* **40** 1400–9
- [214] Narducci D and Lorenzi B 2021 Economic convenience of hybrid thermoelectric-photovoltaic solar harvesters *ACS Appl. Energy Mater.* **4** 4029–37
- [215] Lorenzi B, Mariani P, Reale A, di Carlo A, Chen G and Narducci D 2021 Practical development of efficient thermoelectric—photovoltaic hybrid systems based on wide-gap solar cells *Appl. Energy* **300** 117343
- [216] Wang R, Mujahid M, Duan Y, Wang Z K, Xue J and Yang Y 2019 A review of perovskites solar cell stability *Adv. Funct. Mater.* **29** 1808843
- [217] Narducci D and Lorenzi B 2016 Challenges and perspectives in tandem thermoelectric–photovoltaic solar energy conversion *IEEE Trans. Nanotechnol.* **15** 348–55
- [218] Zhang J and Xuan Y 2016 Investigation on the effect of thermal resistances on a highly concentrated photovoltaic-thermoelectric hybrid system *Energy Convers. Manage.* **129** 1–10
- [219] Lorenzi B and Chen G 2018 Theoretical efficiency of hybrid solar thermoelectric-photovoltaic generators theoretical efficiency of hybrid solar thermoelectric-photovoltaic generators *J. Appl. Phys.* **124** 024501
- [220] Tian H 2020 *Perovskite Materials, Devices and Integration* (Rijeka: IntechOpen) 190
- [221] Trifiletti V, Asker C, Tseberlidis G, Riva S, Zhao K, Tang W, Binetti S and Fenwick O 2021 Quasi-zero dimensional halide perovskite derivatives: synthesis, status, and opportunity *Front. Electron.* **2**
- [222] Zhao L-D, Lo S-H, Zhang Y, Sun H, Tan G, Uher C, Wolverton C, Dravid V P and Kanatzidis M G 2014 ‘Ultralow thermal conductivity and high thermoelectric figure of merit in SnSe crystals *Nature* **508** 373–7
- [223] Hinterleitner B *et al* 2019 Thermoelectric performance of a metastable thin-film Heusler alloy *Nature* **576** 85–90
- [224] Goldsmid H J 2016 *Introduction to Thermoelectricity* vol 2016 (Berlin, Heidelberg: Springer)
- [225] Smith I C, Hoke E T, Solis-Ibarra D, McGehee M D and Karunadasa H I 2014 A layered hybrid perovskite solar-cell absorber with enhanced moisture stability *Angew. Chem. Int. Ed.* **53** 11232–5
- [226] Zhou T, Xu Z, Wang R, Dong X, Fu Q and Liu Y 2022 Crystal growth regulation of 2D/3D perovskite films for solar cells with both high efficiency and stability *Adv. Mater.* **34** 2200705
- [227] González-Carrero S, Galian R E and Pérez-Prieto J 2015 Organometal halide perovskites: bulk low-dimension materials and nanoparticles *Part. Part. Syst. Charact.* **32** 709–20
- [228] Hu S, Ren Z, Djurišić A B and Rogach A L 2021 Metal halide perovskites as emerging thermoelectric materials *ACS Energy Lett.* **6** 3882–905
- [229] Akkerman Q A and Manna L 2020 What defines a halide perovskite? *ACS Energy Lett.* **5** 604–10
- [230] Haque M A, Kee S, Villalva D R, Ong W L and Baran D 2020 Halide perovskites: thermal transport and prospects for thermoelectricity *Adv. Sci. (Weinh)* **7** 1903389
- [231] Zhou Y, Wang J, Luo D, Hu D, Min Y and Xue Q 2022 Recent progress of halide perovskites for thermoelectric application *Nano Energy* **94** 106949
- [232] Vigneshwaran M *et al* 2016 Facile synthesis and characterization of sulfur doped low bandgap bismuth based perovskites by soluble precursor route *Chem. Mater.* **28** 6436–40
- [233] Li J, Liu X, Xu J, Chen J, Zhao C, Salma Maneno M, Zhang B and Yao J 2019 Fabrication of sulfur-incorporated bismuth-based perovskite solar cells via a vapor-assisted solution process *Sol. RRL* **3** 1900218
- [234] Trifiletti V, Luong S, Tseberlidis G, Riva S, Galindez E S S, Gillin W P, Binetti S and Fenwick O 2021 Two-step synthesis of bismuth-based hybrid halide perovskite thin-films *Materials* **14** 7827
- [235] Hong K, Le Q V, Kim S Y and Jang H W 2018 Low-dimensional halide perovskites: review and issues *J. Mater. Chem. C* **6** 2189–209
- [236] Kumar G S, Sumukam R R, Rajaboina R K, Savu R N, Srinivas M and Banavoth M 2022 Perovskite nanowires for next-generation optoelectronic devices: Lab to Fab *ACS Appl. Energy Mater.* **5** 1342–77
- [237] Li X, Hoffman J M and Kanatzidis M G 2021 The 2D halide perovskite rulebook: how the spacer influences everything from the structure to optoelectronic device efficiency *Chem. Rev.* **121** 2230–91
- [238] Li Y, Dailey M, Lohr P J and Printz A D 2021 Performance and stability improvements in metal halide perovskite with intralayer incorporation of organic additives *J. Mater. Chem. A* **9** 16281–338
- [239] Bellucci A, Girolami M and Trucchi D M 2021 Thermionic and thermoelectric energy conversion *Ultra-High Temperature Thermal Energy Storage, Transfer and Conversion* ed A Datas (Business Centre, Royston Road, Duxford, CB22 4QH, United Kingdom: Woodhead Publishing Series in Energy: Elsevier Ltd) 1st edn pp 253–84

- [240] Baranowski L L, Snyder G J and Toberer E S 2012 Concentrated solar thermoelectric generators *Energy Environ. Sci.* **5** 9055
- [241] Mu X *et al* 2022 A robust starch–polyacrylamide hydrogel with scavenging energy harvesting capacity for efficient solar thermoelectricity–freshwater cogeneration *Energy Environ. Sci.* **15** 3388–99
- [242] Trucchi D M *et al* 2018 Solar thermionic-thermoelectric generator (ST<sup>2</sup>G): concept, materials engineering, and prototype demonstration *Adv. Energy Mater.* **8** 1802310
- [243] Lorenzi B and Chen G 2018 Theoretical efficiency of hybrid solar thermoelectric-photovoltaic generators *J. Appl. Phys.* **124** (2) 024501
- [244] Narducci D and Lorenzi B 2021 Economic convenience of hybrid thermoelectric-photovoltaic solar harvesters *ACS Appl. Energy Mater.* **4** 4029–37
- [245] Schwede J W *et al* 2010 Photon-enhanced thermionic emission for solar concentrator systems *Nat. Mater.* **9** 762–7
- [246] Yang Y, Yang W, Tang W and Sun C 2013 High-temperature solar cell for concentrated solar-power hybrid systems *Appl. Phys. Lett.* **103** 083902
- [247] Bellucci A *et al* 2020 Photovoltaic anodes for enhanced thermionic energy conversion *ACS Energy Lett.* **5** 1364–70
- [248] Bellucci A, García-Linares P, Martí A, Trucchi D M and Datas A 2022 A three-terminal hybrid thermionic-photovoltaic energy converter *Adv. Energy Mater.* **12**
- [249] Bellucci A, Linares P G, Villa J, Martí A, Datas A and Trucchi D M 2022 Hybrid thermionic-photovoltaic converter with an In<sub>0.53</sub>Ga<sub>0.47</sub>As anode *Sol. Energy Mater. Sol. Cells* **238** 111588
- [250] Bellucci A *et al* 2021 Novel concepts and nanostructured materials for thermionic-based solar and thermal energy converters *Nanotechnology* **32** 024002
- [251] Bellucci A, Girolami M, Mastellone M, Serpente V and Trucchi D M 2021 Upgrade and present limitations of solar thermionic-thermoelectric technology up to 1000 K *Sol. Energy Mater. Sol. Cells* **223** 110982
- [252] Zeneli M *et al* 2020 Performance evaluation and optimization of the cooling system of a hybrid thermionic-photovoltaic converter *Energy Convers. Manage.* **210** 112717
- [253] Zhao L D *et al* 2014 Ultralow thermal conductivity and high thermoelectric figure of merit in SnSe crystals *Nature* **508** 373–7
- [254] Jaafreh R, Yoo Seong K, Kim J-G and Hamad K 2022 A deep learning perspective into the figure-of-merit of thermoelectric materials *Mater. Lett.* **319** 132299
- [255] Cappelli E *et al* 2014 Nano-crystalline Ag–PbTe thermoelectric thin films by a multi-target PLD system *Appl. Surf. Sci.* **336** 283–89
- [256] Bellucci A *et al* 2017 ZnSb-based thin films prepared by ns-PLD for thermoelectric applications *Appl. Surf. Sci.* **418** 589–93
- [257] Nguyen Huu T, Nguyen Van T and Takahito O 2018 Flexible thermoelectric power generator with Y-type structure using electrochemical deposition process *Appl. Energy* **210** 467–76
- [258] Kim S-W *et al* 2023 Boosted output voltage of BiSbTe-based thermoelectric generators via coupled effect between thermoelectric carriers and triboelectric charges *Adv. Energy Mater.* **13** 2202987
- [259] Zebarjadi M, Esfarjani K, Dresselhaus M S, Ren Z F and Chen G 2012 Perspectives on thermoelectrics: from fundamentals to device applications *Energy Environ. Sci.* **5** 5147–62
- [260] Segev G, Rosenwaks Y and Kribus A 2015 Limit of efficiency for photon-enhanced thermionic emission versus photovoltaic and thermal conversion *Sol. Energy Mater. Sol. Cells* **140** 464–76